

**CZECH TECHNICAL UNIVERSITY
IN PRAGUE**

**FACULTY OF
MECHANICAL ENGINEERING**



DIPLOMA THESIS

Hill Climbing Algorithm For Fuel
Consumption Optimization Of HEV

2021

**ANURAG
KAR**

Thesis Supervisors:

Ing. Milan Cvetkovic, Ricardo Prague

Ing. Josef Morkus, CSc., CTU Prague



MASTER'S THESIS ASSIGNMENT

I. Personal and study details

Student's name: **Kar Anurag** Personal ID number: **483093**
Faculty / Institute: **Faculty of Mechanical Engineering**
Department / Institute: **Department of Automotive, Combustion Engine and Railway Engineering**
Study program: **Master of Automotive Engineering**
Branch of study: **Advanced Powertrains**

II. Master's thesis details

Master's thesis title in English:

Hill Climbing Algorithm for Fuel Consumption Optimization of HEV vehicles

Master's thesis title in Czech:

Algoritmus pro optimalizaci spotřeby paliva HEV pro jízdu vozidla v kopcích

Guidelines:

Research of available state of the art algorithms for fuel consumption optimization for HEV
Develop power distribution algorithm for HEV controller to optimize fuel consumption of HEV during hill climbing and descending
Implement the algorithm in Matlab. Integrate an algorithm into Ricardo Ignite Software HEV model
Validate developed algorithm in Ricardo Ignite Software on a set of predefined scenarios.
Compare fuel consumption with default rule-based Hybrid Controller

Bibliography / sources:

Dušan Teodorovič - Bee Colony Optimization (BCO) Innovations in Swarm Intelligence. Volume 248
Fritzon Peter - Principal of object oriented Modeling and Simulation with Modelica
James Larmin, John Lory - Electric Vehicle Technology explained
Mehrdad Ehsani, Yimin Gao, Stefano Longo - Modern Electric, hybrid electric and fuel cell vehicles

Name and workplace of master's thesis supervisor:

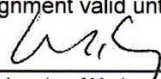
Ing. Josef Morkus, CSc., Department of Automotive, Combustion Engine and Railway Engineering, FME

Name and workplace of second master's thesis supervisor or consultant:

Ing. Milan Cvetkovic, Ricardo Prague

Date of master's thesis assignment: **30.10.2020** Deadline for master's thesis submission: **06.01.2021**

Assignment valid until: _____


Ing. Josef Morkus, CSc.
Supervisor's signature


doc. Ing. Oldřich Vitek, Ph.D.
Head of department's signature


prof. Ing. Michael Valášek, DrSc.
Dean's signature

III. Assignment receipt

The student acknowledges that the master's thesis is an individual work. The student must produce his thesis without the assistance of others, with the exception of provided consultations. Within the master's thesis, the author must state the names of consultants and include a list of references.

Date of assignment receipt

Student's signature

Declaration

I declare that I have worked out this thesis independently assuming that the results of thesis can also be used at the discretion of the supervisor of thesis as its co-author. I also agree with the potential publication of the results of thesis or of its substantial part, provided I will be listed as the co-author.

Anurag Kar

Acknowledgements

I would firstly like to thank to Ricardo Prague for lending their collaboration for the conduct my diploma thesis. I express my sincere gratitude to Ing. Milan Cvetkovic, who constantly guided and motivated me throughout the thesis and helped me with all tasks involving Ricardo software. I am forever thankful for his philosophy of the finite element method – if the model is accurate, it should provide valid results even with 2 elements, irrespective of the element size, which was instrumental in the validation of the Matlab model.

I am greatly thankful to my thesis supervisor, Ing. Josef Morkus for his consistent suggestions, advice, guidance and support and most importantly showing the right direction whenever I was in dilemma. He persistently motivated and encouraged me to find answers to the problems encountered.

I also thank my colleagues from TU Belgrade, Marko Stokić and Nemanja Mijovic who dedicated several online meeting sessions spanning entire nights for the construction and validation of the custom bee algorithm.

I am grateful to be a student of the Czech Technical University in Prague and nourished by the excellence of the professors and the extraordinary teaching methodologies which in many ways shaped this diploma thesis and enriched me with an everlasting perspective to look at things.

The best teachers are those who show you where to look, but don't tell you what to see.

-Alexander Trenfor

Abstract

This diploma thesis provides an overview of various hybrid vehicle drive modes and control strategies implemented to minimize fuel consumption. A novel control strategy for a hill climb and descent journey of a parallel hybrid vehicle using eHorizon road slope information is proposed that uses particle swarm optimization, a meta-heuristic based optimization algorithm to optimize power distribution between hybrid vehicle drive units during a hill climb event. A black box vehicle model is developed in Matlab as an abstract function operating on simple input-output logic. The control strategy is tested over different scenarios of terrain profiles with various velocity profiles and battery state of charge parameters. The optimum results of fuel consumption for each scenario were compared with that of a rule-based controller in Ricardo Ignite software, which demonstrate the optimality and predictive ability of the new control strategy over a rule-based controller.

Keywords

hybrid vehicle, drive modes, control strategy, fuel consumption, eHorizon, slope, particle swarm optimization, meta-heuristic, optimization, power distribution, hill climb, black box, Matlab, abstract, terrain, state of charge, parameters, optimum, rule-based controller, Ricardo Ignite, predictive

Contents

- Abbreviations1
- Nomenclature2
- 1 Introduction.....4
 - 1.1 Outline of the thesis.....5
- 2 Problems with HEVs6
 - 2.1 Architectures.....6
 - 2.1.1 Series HEV7
 - 2.1.2 Parallel HEV7
 - 2.1.3 Series Parallel HEV8
 - 2.2 Degree of Hybridization8
 - 2.3 P2 Parallel Hybrid Architecture9
 - 2.4 Hybrid vehicle modes of operation10
 - 2.4.1 Regenerative Braking Strategies11
- 3 Review of HEV Control Strategies12
 - 3.1 Rule-Based v/s Optimization Based14
 - 3.1.1 Rule-Based Control Strategies14
 - 3.1.2 Optimization Based Control Strategies14
 - 3.2 Adaptive and Predictive Control Strategy15
 - 3.3 eHorizon.....15
 - 3.4 Meta-heuristics16
 - 3.5 Particle Swarm Optimization.....17
- 4 Vehicle Model.....18
 - 4.1 Vehicle Specifications.....18
 - 4.2 Engine18
 - 4.3 Electric motor generator20
 - 4.4 Battery21
 - 4.4.1 Battery Electric Model22
 - 4.4.2 Battery SoC Model and Losses23
 - 4.5 Transmission25
 - 4.6 Longitudinal Vehicle Dynamics.....25
 - 4.7 IGNITE Vehicle Models.....28
 - 4.7.1 IGNITE Model with default rule-based controller28
 - 4.7.2 IGNITE Model with Novel Control Strategy.....28
- 5 Description of Control Algorithm.....29

5.1	Terrain Scenarios	29
5.2	Drive Cycles.....	29
5.3	Black Box Vehicle Model	31
5.3.1	Traction power	33
5.3.2	Shift Strategy	35
5.3.3	Optimal hybrid operating mode and motor control strategy.....	40
5.3.4	Engine control strategy.....	40
5.3.5	Battery	41
5.4	Control Algorithm for Various Scenarios.....	41
5.4.1	Working Principle of Artificial Bee Colony Power Algorithm for EV / Boost.....	42
5.4.2	ABC for Generation.....	46
5.4.3	Optimal ABC parameters	46
5.5	Working of Ignite Rule-Based Parallel Hybrid Controller.....	50
5.5.1	Demand Split Strategy	50
5.5.2	Generation Strategy.....	51
5.5.3	Regeneration Strategy	51
6	Results and Discussion.....	52
6.1	MATLAB Model with novel control strategy	57
6.2	Validation of MATLAB vehicle model with IGNITE	58
6.3	Comparison of results of new control strategy with Rule-Based controller in IGNITE	58
7	Conclusion	61
7.1	Possible continuation of the thesis	62
8	Bibliography.....	63
9	List of Figures.....	66
10	List of Tables.....	67
11	Appendix	68
11.1	2020 Ioniq Hybrid Engine BSFC Map	68
11.2	Engine Fuel Consumption Map extended till engine friction torque	68
11.3	2011 Hyundai Sonata Hybrid Combined Motor Inverter Map.....	69
11.4	Battery specifications of 2020 Hyundai Ioniq and 2011 Sonata Hybrid	69
11.5	Original Battery Test Results of 2011 Hyundai Sonata Hybrid	69
11.6	2011 Hyundai Sonata Hybrid Battery Characteristics	70
11.7	Design speeds and road grade data for motorways in the Czech Republic	71
11.8	Ignite Model with New Controller	72
11.9	Summary of Results with new Control Strategy	73
12	Attachments	77

Abbreviations

ABC	Artificial Bee Colony
ADASIS	Advanced Driver Assistance Systems Interface Specifications
BA	Bee Algorithm
BCO	Bee Colony Optimization
BEV	Battery Electric Vehicle
BMS	Battery Management System
CESO	Catch Energy Saving Opportunities
DC	Direct Current
ECMS	Equivalent Consumption Minimization Strategy
ECU	Engine Control Unit
EM	Electric Machine
EMS	Energy Management System
ESS	Energy Storage System
EV	Electric Vehicle
GA	Genetic Algorithm
GDi	Gasoline Direct Injection
GHG	Green House Gas
GIS	Geographic Information System
GPS	Global Positioning System
HD	High Definition
HEV	Hybrid Electric Vehicle
ICE	Internal Combustion Engine
IMPERIUM	Implementation of Powertrain Control for Economic and Clean Real driving emISSION and fuel ConsUMption
LB	Learning Based
MCU	Motor Control Unit
MHEV	Mild Hybrid Electric Vehicle
mHEV	Micro Hybrid Electric Vehicle
OB	Optimization Based
PHEV	Plug-in Hybrid Electric Vehicle
P-HEV	Parallel Hybrid Electric Vehicle
PMSM	Permanent Magnet Synchronous Motor
P-RBS	Parallel Regenerative Braking Strategy
PSO	Particle Swarm Optimization
RB	Rule Based
RBS	Regenerative Braking Strategy
S-HEV	Series Hybrid Electric Vehicle
SP-HEV	Series Parallel Hybrid Electric Vehicle
S-RBS	Series Regenerative Braking Strategy
TCU	Transmission Control Unit

Nomenclature

a	Acceleration	[m/s ²]
C_{max}	Maximum battery capacity	[Ah]
C_{roll}	Rolling resistance coefficient	[-]
C_x	Aerodynamic drag coefficient	[-]
$F_{BrakeMech}$	Mechanical brake force	[N]
$F_{BrakeRegen}$	Regenerative braking force	[N]
F_{Aero}	Aerodynamic drag	[N]
F_{Brake}	Total braking force on the wheels	[N]
F_{Roll}	Rolling resistance	[N]
F_{Slope}	Gradient resistance	[N]
F_{Trac}	Tractive force on the wheels	[N]
G	Discrete gearbox gear	[-]
g	Acceleration due to gravity	[m/s ²]
I_{eff}	Battery effective internal current	[A]
I_{term}	Battery terminal current	[A]
m	Vehicle mass	[kg]
\dot{m}_{eq}	Equivalent fuel consumption	[g/s]
\dot{m}_f	Engine fuel mass flow rate	[g/s]
n_e	Engine speed	[rpm]
$n_{gbxInput}$	Rotational speed of gearbox input shaft	[rpm]
n_{mg}	Motor generator shaft rotational speed	[rpm]
n_w	Wheel rotational speed	[rpm]
P_{mgElec}	Motor generator electrical power	[W]
P_{mgMech}	Motor generator mechanical power	[W]
P_{batt}	Battery electric power	[W]
P_{Coul}	Battery coulombic loss power	[W]
P_e	Engine power	[W]
P_{elec}	Net battery electric power	[W]
P_{fuel}	Energy content of fuel mass flow	[-]
P_{Joul}	Battery joule loss power	[W]
P_{Req}	Power required at gearbox input shaft	[W]
P_{Trac}	Traction power at the wheels	[W]
Q_{LHV}	Lower heating value of fuel	[J/g]
r_{dyn}	Dynamic tyre radius	[m]
r_{FD}	Final drive ratio	[-]
r_G	Gear ratio at gear G	[-]
R_{int}	Battery internal resistance	[Ω]
S_x	Vehicle frontal area	[m ²]
SoC	Battery state of charge	[-]
T_e	Engine torque	[Nm]

T_{fric}	Engine friction torque	[Nm]
T_{Gen}	Generator torque	[Nm]
T_{ind}	Engine indicated torque	[Nm]
T_{mg}	Motor generator torque	[Nm]
T_{Motor}	Motor torque	[Nm]
T_{Req}	Torque required at gearbox input shaft	[Nm]
t_{seg}	Segment traversal time	[s]
T_{Trac}	Traction torque at the wheels	[Nm]
v	Vehicle velocity	[m/s]
V_{nom}	Battery nominal voltage	[V]
V_{OC}	Battery open circuit voltage	[V]
V_{term}	Battery terminal voltage	[V]
x	Vehicle longitudinal position	[m]
α	Road slope	[rad]
$\eta_{Coulomb}$	Battery coulombic efficiency	[-]
η_{drive}	Overall driveline efficiency	[-]
η_e	Engine efficiency	[-]
η_{FD}	Final drive efficiency	[-]
η_G	Gearbox efficiency at gear G	[-]
η_{Gen}	Generator efficiency	[-]
η_{Motor}	Motor efficiency	[-]
ρ	Ambient air density	[kg/m ³]
ω_e	Engine speed	[rad/s]
$\omega_{gbxInput}$	Rotational speed of gearbox input shaft	[rad/s]
ω_w	Wheel rotational speed	[rad/s]

1 Introduction

The use of fossil fuels has led to an increase in global greenhouse gas (GHG) emissions leading to global warming. The transport sector accounts for 30.8% of total energy consumption of which road transport accounts for 85% and 24.6% of GHG emissions. Road transport also accounts for 71.7% of the total GHG emissions from transport sector in the European Union for 2017, with cars contributing 60.6%, light duty trucks 11.9%, heavy duty trucks and buses 26.3% and motorcycles 1.2%.[1]

While growing environmental concerns have led to stricter emission legislations, thus pushing manufacturers and researchers towards electrification of vehicles. While pure electric vehicles continue to struggle with issues regarding range, price, battery weight and charging networks, hybrid vehicles seem to be an intermediate choice between the transition from conventional combustion engine propelled vehicles to pure electric vehicles [2]. Hybrid vehicles have two or more energy converters and energy storage system (ESS), available on board for vehicle propulsion. One aspect of hybrid vehicle design is development of energy management strategies which share power among the multiple sources of energy to meet several objectives such as minimizing consumption, emission reduction and drivability enhancements.

Besides electrification, autonomous and connected vehicles are other dimensions towards which the future of automobiles is heading [3]. Increasing demand and research in these fields make available various tools and information which expand the scope of fulfilling these objectives. One such tool is electronic horizon or eHorizon which provides connected vehicles digital maps including information about the road ahead much beyond the visual range of the driver and on-board sensors [4]. Based on the available information, the future course of the vehicle can be predicted for improved safety, efficiency and comfort.

This diploma thesis deals with the development of an optimal control algorithm for a parallel hybrid electric vehicle during a hill climb journey with minimum fuel consumption as the goal. The reason behind this topology selection was its simple architecture, fewer components and fewer energy conversions which makes it robust for the application of the discussed optimization algorithm. The main idea is to design a control strategy for a HEV travelling across a hilly terrain using road slope information which minimizes fuel consumption for the trip, while using particle swarm optimization to optimize the power distribution between the engine and the electric motor for hill climb section of a trip and additionally for generation of the battery

from the engine. The effectiveness of the new control strategy will be compared against a generic rule-based controller from the Ignite powertrain library. It also investigates the possibility to use a predictive optimisation strategy aimed at reducing fuel consumption of a HEV by using eHorizon road slope information and explores the real-time optimization capabilities of bee algorithm.

1.1 Outline of the thesis

The next chapter deals with a brief overview of classification of hybrid vehicles based on topology and degree of hybridization. The various modes of a parallel hybrid electric vehicle and the associated control strategies are discussed.

Chapter 3 briefly describes the types of control strategies associated with energy management of a hybrid vehicle. In this, the concepts of eHorizon and particle swarm optimization are also introduced.

Chapter 4 describes the vehicle models created in Ricardo Ignite and Matlab along with detailed mathematical models of critical vehicle components.

In Chapter 5, the novel control strategy along with its implementation as Matlab programs are described. This includes the application of an artificial bee colony algorithm for optimal power distribution between the engine and the electric motor during a hill climb event. The control strategy is applied to four hypothetical scenarios of hilly terrains, each with its unique velocity trajectory.

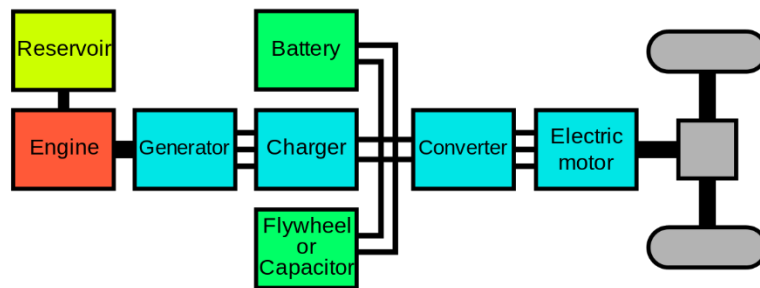
In Chapter, the results of fuel consumption of the new control algorithm are discussed and compared with a rule-based controller in Ignite.

2 Problems with HEVs

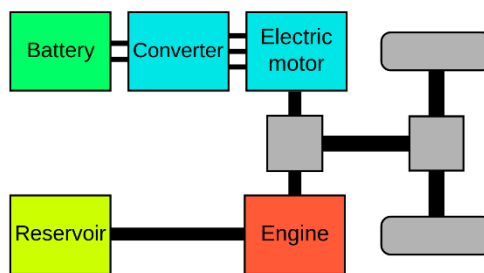
A hybrid electric vehicle or HEV is a hybrid vehicle in which at least one energy converter for vehicle propulsion is an electric drive (electric machine) and has an electric energy source (battery, supercapacitor) to drive the electric machine. A vehicle powertrain consists of parts essential to drive the vehicle – engine, motor generator, transmission, differential, shafts and wheels.

2.1 Architectures

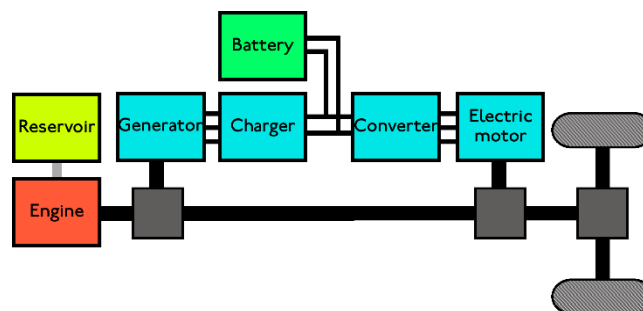
In order to optimize the energy expenditure of a HEV, it is necessary to understand the operating modes and architecture of various HEV topologies and the degree of complexity involved. Depending on the structural arrangement of the driveline mainly the engine and the electric machine (EM), HEV topologies can be broadly classified into the following:



(a) Serial Hybrid Electric Vehicle



(b) Parallel Hybrid Electric Vehicle



(c) Series-Parallel Hybrid Electric Vehicle

Figure 1 Topology of various HEV architectures [5]

2.1.1 Series HEV

Series-HEV (S-HEV) is similar to an electric vehicle or EV with two DC sources – an internal combustion engine (ICE) – generator group and an Energy Storage System or ESS, usually a battery pack with a bidirectional DC/DC converter for charging and discharging. Since the ICE is mechanically decoupled from the wheels, it is possible to perpetually operate the engine at its most efficient region of fuel consumption and/or emissions, which is the main advantage of such topology. Depending on the traction power demand, excess energy is stored in the ESS or energy is provided by the ESS to compensate for the deficit power. S-HEV provides high performance at low speeds and frequent start stops, but the main disadvantage is energy losses during multiple conversions and inability to perform efficiently at high speeds, since the driving is always electric.

2.1.2 Parallel HEV

In Parallel-HEV (P-HEV), not to be confused with PHEV (Plug-in HEV), the ICE and electric machine (EM) are mechanically coupled such that their combined torque and transmitted to the wheels via a conventional drive train consisting of gearbox, final drive and differential. The energy losses are lower compared to S-HEV, because of the mechanical connection. In contrast to S-HEVs, P-HEVs usually consist of a larger combustion engine and a small but efficient motor generator unit, since the drive is predominantly by the engine with electric drive being secondary.

Depending on the size of the EM and ESS, P-HEV can operate in EV only mode, though only for short duration and at low speeds, engine only mode which is suitable for high speeds, e.g., highway driving and P-HEV mode, where EM is used in boost mode, which assists the ICE for better drivability and performance.

P-HEVs can be further classified as P0, P1, P2, P3, P4 based on the position where the EM is torque coupled relative to ICE and Transmission in the drivetrain as shown in Figure 2. Based on the size of the electric machine (EM) and battery, P2 and P3 parallel hybrids can also feature full electric drive for short distances.

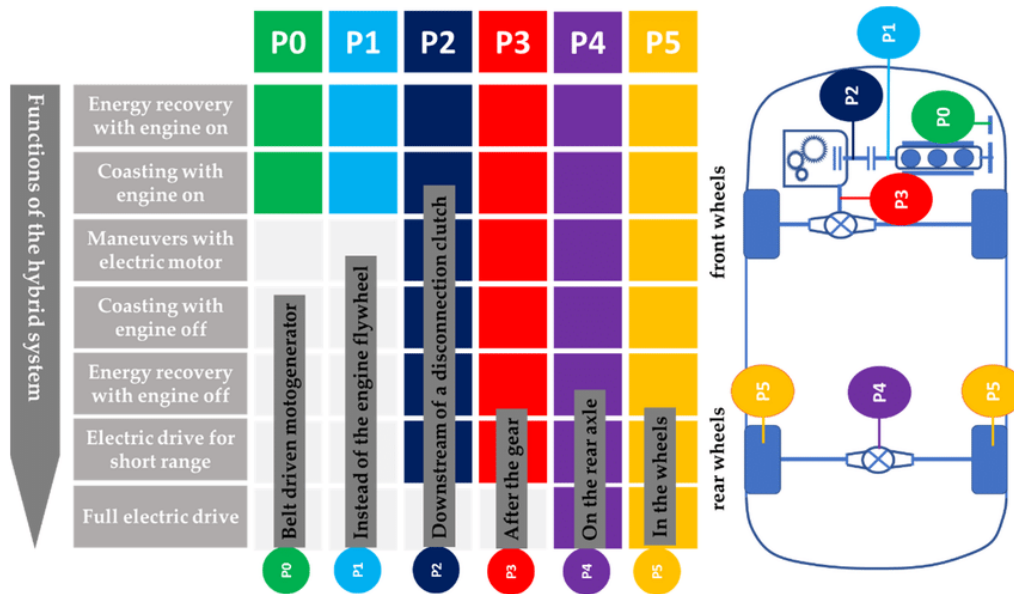


Figure 2 Topology and features of Parallel HEV configurations based on position of electric machine [6]

2.1.3 Series Parallel HEV

Series-Parallel HEV (SP-HEV), also known as power split HEV, is a combination of the advantages of series and parallel HEV. It enables use of downsized electrical components compared to S-HEV and downsized ICE compared to P-HEV. A major addition is the use of a power-split (usually a planetary gear system) device which splits the ICE power to drive the wheels and charge the ESS. The main disadvantages include packaging challenges and control complexity because of additional degrees of freedom of operation for the individual components.

2.2 Degree of Hybridization

Based on the extent of the degree to which electric energy is used, hybrid vehicles can be classified as micro (mHEV), mild (MHEV), full (HEV), plug-in (PHEV), battery electric vehicle (BEV) with range extender engine which charges the battery when discharged or low on charge and finally BEV with pure electric drive only. Due to relatively small size of battery and electric machine on the mHEV and MHEV, it is not beneficial to design control strategies because of low potential for improvement. Full Hybrids and above, on the other hand have enough share electric operation and demand for optimal control strategies, to fully exploit the benefits of hybridization.

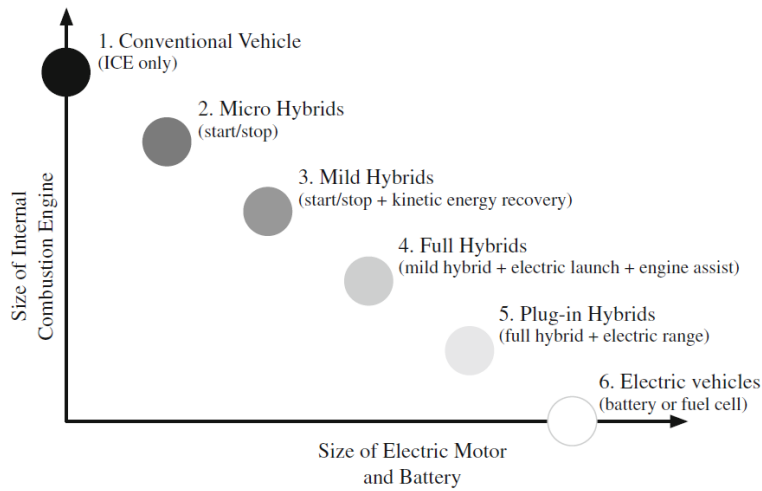


Figure 3 Various hybridization degrees with increasing electrification [7]

2.3 P2 Parallel Hybrid Architecture

P2 and power-split hybrids are the most common hybrid types available on the market because of the large potential for likely reduction of fuel consumption of about 30 % [8]. This is slightly higher for P2 because of fewer energy conversions. While power-split hybrids allow more operational flexibility over P2, though at the cost of increased complexity. Moreover, with a direct coupling of the motor to the transmission input shaft, means the engine and the motor always rotate at the same speed when coupled, resulting in a simple model. So, the P2 architecture was selected for this study. Notable HEVs with the P2 architecture include Hyundai Sonata, Ioniq, Volkswagen Jetta, Kia Niro. Because of the recency of the available data and the vehicle itself, the vehicle model used in this study is based on the 2020 Hyundai Ioniq Hybrid [9].

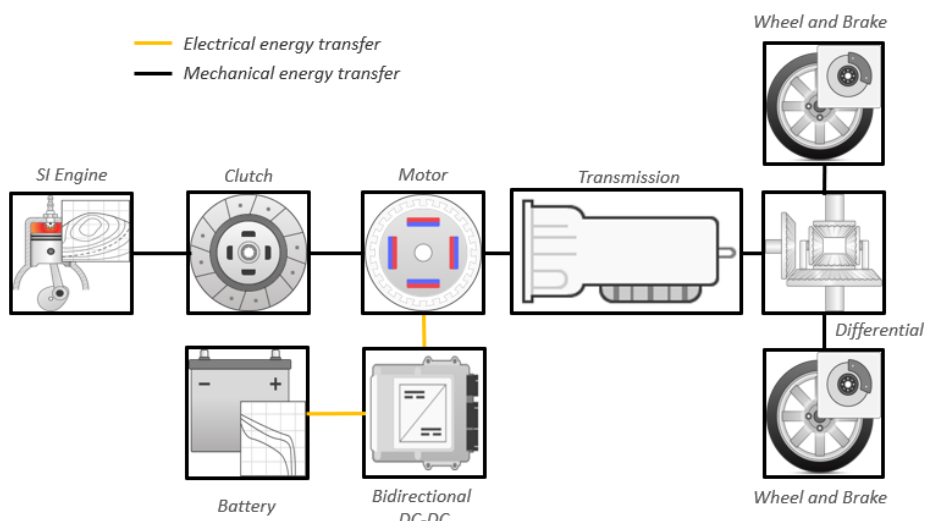


Figure 4 Topology of a P2 Parallel Hybrid Electric Vehicle [10]

Figure 4 shows the vehicle model with a P2 parallel hybrid topology. The internal combustion engine and electric machine are sources of mechanical power as torque, with the former converting chemical energy of the fuel and the latter electric potential energy of the battery. Both sources are connected to the gearbox which transmits the torque to the front wheels via the final drive and differential. The transmission clutch required to shift gears is located within the transmission housing in the figure. The Clutch also called as engine clutch or eClutch separates the engine from the rest of the powertrain during electric drive and regenerative braking. This avoids engine braking during regenerative braking and allows the engine to run in idle or switched off.

2.4 Hybrid vehicle modes of operation

Unlike conventional vehicles, HEVs, due to their diverse and dynamic powertrain, can work in multiple modes of operation, depending on the topology and parameters. The choice is usually made by software logic in the Hybrid Vehicle Controller, sometimes referred to as Energy Management System (Figure 6). Depending on the state of the engine and electric motor, a hybrid drive train has several modes of operation:

- 1) **Pure electric** (electric only or EV mode): The ICE is switched OFF and the battery provides the full traction power via the EM.
- 2) **Pure ICE** (Engine-only): The EM is electrically switched off and the ICE provides the full traction power.
- 3) **Hybrid or Electric Assist**: Both the ICE and EM simultaneously provide the requested torque in parallel to the rest of the driveline.
- 4) **Battery charging**: The ICE propels the vehicle while simultaneously charging the battery via the EM working as generator.
- 5) **Regenerative braking**: The kinetic energy of the vehicle during braking (or potential energy during downhill motion) can be used to rotate the electric motor which would act in generator mode to produce electricity which simultaneously slows the vehicle and charges the battery.
- 6) **Stationary charging**: The vehicle is at standstill and the ICE powers the generator to charge the battery.
- 7) **Hybrid regeneration**: During braking, a part of the kinetic energy is dissipated by friction brakes and a part is recuperated by regeneration braking

2.4.1 Regenerative Braking Strategies

Regenerative braking converts the kinetic energy of vehicle to electric energy by braking through the electric motor acting as generator. This electric energy can be stored in the battery to be used later to drive the vehicle. The amount of recuperated energy depends on the type of regenerative braking strategy applied, which defines brake force blending between the mechanical brakes and the generator. According to the amount of brake force provided by regenerative braking and friction brakes, regenerative braking strategies (RBS) can be classified as:

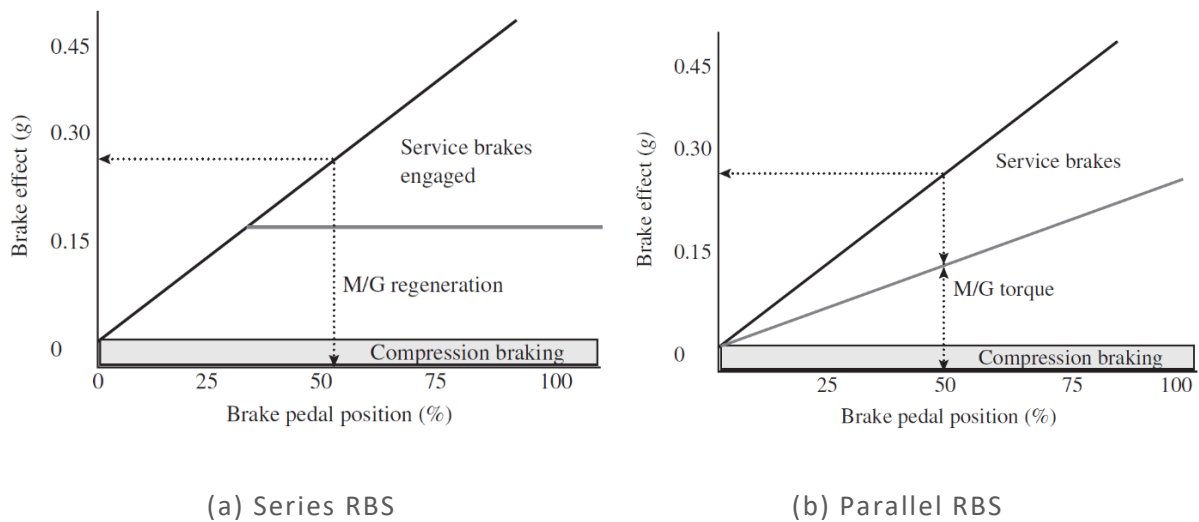


Figure 5 Regenerative Braking Strategies [11]

Series Regenerative Braking Strategy

With series RBS, as the name suggests, initially as the brake pedal is depressed, as long there is enough regenerative braking torque from electric machine, S-RBS uses only generator to brake the vehicle. Further depression of the brake pedal engages the service brakes as shown in Figure 5 (a), when the maximum generator power is reached. With S-RBS, there is always a chance of capturing kinetic energy, when the vehicle brakes.

Parallel Regenerative Braking Strategy

Parallel RBS as shown in Figure 5 (b) always engages the friction brakes together with generator brakes, whenever the brake pedal is pressed, in tandem with generator brakes. The ratio of split is determined by an algorithm which blends the two braking systems such that the braking action is smooth and seamless. Since a part of kinetic energy is always lost as heat by friction brakes, P-RBS is inferior to S-RBS in terms of fuel economy.

3 Review of HEV Control Strategies

For a hybrid vehicle to be truly beneficial over its conventional and electric counterparts, it must have a control strategy which efficiently manages all the working components involved in various hybrid modes discussed in Section 2.4. The efficient management refers to setting the working points of the HEV components, namely engine, electric machine, battery and transmission such that certain goals are achieved, commonly pertaining to fuel economy, emissions and performance.

Hybrid control strategy is usually implemented as software instructions called the Energy Management System in the hybrid supervisory controller which coordinates the operation of all other low level controllers of each individual components, namely Engine Control Unit (ECU), Battery Management System (BMS), Transmission Control Unit (TCU) and Motor Control Unit (MCU) as shown in Figure 6. The hybrid controller acts as a junction between the driver, vehicle and all other component level controllers.

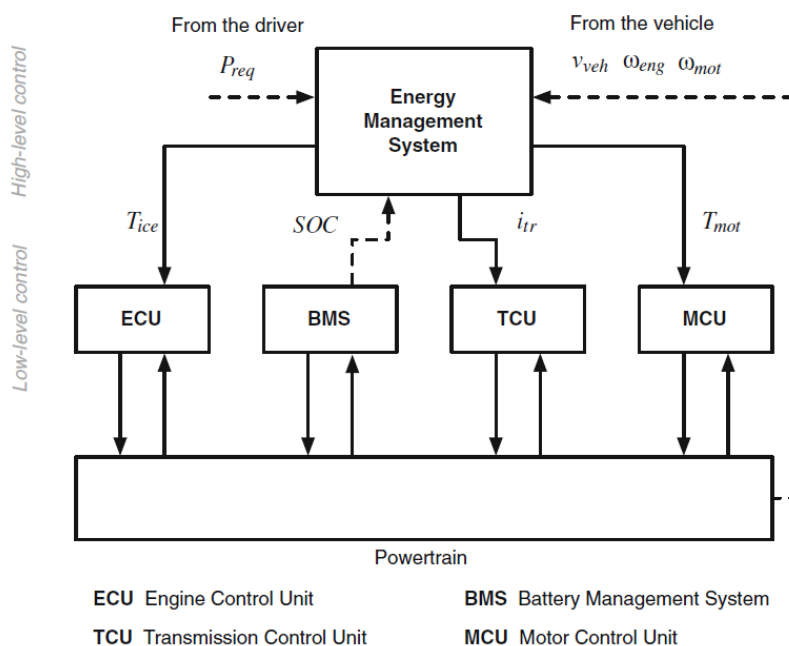


Figure 6 HEV Control Architecture [12]

The presence of multiple sources of energy and the possibility of being able to operate each source within a finite working range, say speed and load on the engine and electric machine (consequently the battery) gives rise to the challenge of searching for the optimum working point for each machine. This gives rise to the concept of Energy Management Strategy (EMS) which in a broad sense refers to the algorithm being followed by the hybrid controller designed

to optimize certain aspect of the hybrid driveline, for instance, fuel consumption minimization and emission reduction.

Because of the contrast in working principles and operating regions of the electric machine and combustion engine, it is difficult to develop an EMS in which the ideal efficiency and operation of all components is guaranteed.

Many studies have been published on control strategies for HEVs. A common goal is to select optimal driving mode and operate the active components during the selected mode in their most efficient operating regions. In a broad sense, existing EMSs can be classified as rule-based (RB), optimization-based (OB) and learning-based (LB) [13].

Since each control strategy and optimization method has its rewards and limitations, an ideal approach should use a mix of different solutions, forming an integrated EMS (iEMS) which minimizes fuel consumption and improves performance as shown in Figure 7. Past, present and future information can act as a bridge among different methods to fulfil optimization objectives.

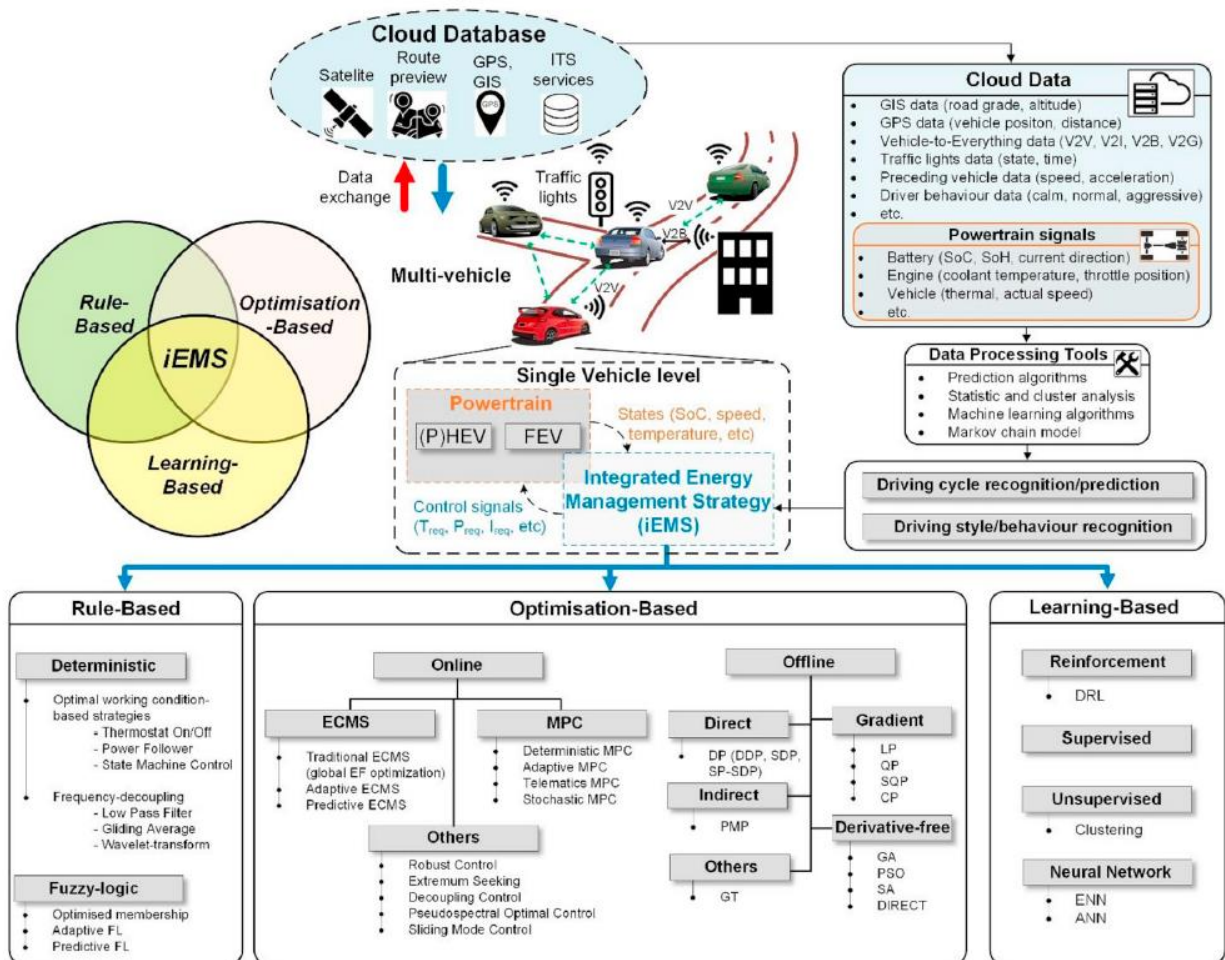


Figure 7 Classification of Energy Management Strategies [13]

3.1 Rule-Based v/s Optimization Based

3.1.1 Rule-Based Control Strategies

A rule-based (RB) strategy refers a predefined set of “if-then” rules to switch working modes and lookup tables to determine operating regions of active components, namely engine, electric machine and battery. For instance, a rule-based strategy based on SoC limits for electric drive or EV mode may have a ‘disable EV’ SoC parameter which disables pure electric drive below a set SoC, to conserve the battery. This strategy is applied to causal control problems where the drive cycle cannot be predicted.

3.1.2 Optimization Based Control Strategies

These strategies make use of one or multiple of several optimization algorithms [14] to minimize or maximize a cost function over a discrete time interval within certain static and dynamic constraints. An example of a static constraint can be a predefined engine elasticity range, i.e., the difference between the maximum and minimum engine speeds between which the engine is operated by appropriate gearing. A dynamic constraint can be dynamic limits for the SoC depending on the future information, if available, such as opportunities for regenerative braking ahead can allow a further drop in SoC. The cost function can be a linear or non-linear combination of one or more designer’s requirements of the system such as fuel consumption, emissions, mechanical losses, electrical losses or any other, depending on the application. Optimization Based strategies outperform rule-based strategies in terms of optimality when applied to acausal control problems with information about the future route and drive cycle.

ECMS converts a global optimization problem to a local one. The objective or cost function is the equivalent fuel consumption which is a combination of the actual fuel consumption in the engine and the converted fuel consumption of electrical power at ESS.

$$\dot{m}_{eq}(t) = \dot{m}_f(t) + \frac{s(t)}{Q_{LHV}} P_{batt}(t) \quad [\text{g/s}] \quad (1)$$

$\dot{m}_{eq}[\text{g/s}]$: equivalent fuel consumption of the HEV

$\dot{m}_f[\text{g/s}]$: fuel consumption in the ICE

$Q_{LHV}[\text{J/g}]$: lower heating value of fuel

$s(t)$, : equivalence factor, equivalent fuel consumption of the electrical energy being drawn from or stored to the battery, also called virtual fuel consumption in the battery

$P_{batt}[\text{W}]$: battery electrical power

The equivalence factor is sensitive to the vehicle and the drive cycle and the success of the optimization depends on its accuracy. Adaptive ECMS uses a feedback control method to dynamically tune the equivalence factor for different drive cycles. A modified form of ECMS called ECMS-CESO [15] is designed to Catch Energy Saving Opportunities across a trip, without the need for calculations used to predict vehicle velocity and horizon optimization.

3.2 Adaptive and Predictive Control Strategy

Adaptive and Predictive strategies differ from static or offline strategies in the sense that they have real-time and future information respectively to dynamically alter the states of all machines. Adaptive EMS uses information from sensors such as cameras, radars and vehicle surrounding (nearby vehicles), to adapt the control strategy to the surroundings. For example, coasting when there is a traffic jam or downhill slope ahead.

Predictive EMS uses information about the projected route including information such as terrain, traffic and anticipated driver behaviour to calculate optimal vehicle control to achieve design objectives of EMS. The information can be either relayed to the driver via driver information display and suggest the driver to take certain action for example advise the driver to release the gas pedal when a potential for coasting is detected [16], or directed to the hybrid control module which takes action based on the information.

3.3 eHorizon

The term horizon refers to the extent of human vision, which extends to a few 100 metres in front of the eyes. Hence, a human has only limited sensory prediction about the road. Electronic horizon (eHorizon) extends the horizon for the vehicle beyond human vision [4]. For example, eHorizon provides GIS data which includes road topography data such as slope, curvature, speed limits, etc. eHorizon is a map transmission technology that sends updated maps with real time information about the road terrain, traffic information, etc. to the connected vehicle. The GIS data can be downloaded via HD maps corresponding to the vehicle's longitudinal position determined by GPS. These maps differ from regular GPS maps for navigation which are two-dimensional, much less precise and less frequently updated.

If the route is known in advance, either from a planned trip, previous trips or by prediction using some prediction algorithms (artificial intelligence, machine learning), decisions that are optimal in terms of fuel consumption can be made and actions taken. The distance for which the data is

available is termed the horizon length and the maximum distance available currently is shown in Table 1.

Table 1 Attributes of eHorizon data as per ADASIS v2.x protocol [17]

	Maximal Horizon Length [m]	Nominal Resolution [m]
Static Data	8192 (13-bit)	50
Dynamic Data	4000	250

Most control strategies work on past and current data alone, with no knowledge of the future. Electronic horizon (eHorizon) [4] provides future information such as road topology, traffic and environment predictions on a future route, which can be harnessed to improve performance of an iEMS. Notable works include IMPERIUM project which works in the direction of improved efficiency of connected vehicles using eHorizon information. Some relevant works include the various proprietary predictive cruise controls by major truck manufacturers which optimise the vehicle trajectory on a hilly terrain to save fuel. [18], [19]

3.4 Meta-heuristics

Heuristic algorithms rely on underlying information about the problem to which it is applied. For example, heuristic optimization strategies for fuel consumption minimization use explicit set of rules to restrict the search area. For example, setting engine operating limits within a certain rpm range. Heuristic algorithms use readily accessible though loosely applicable information to solve a control optimization problem. Heuristics are problem-specific, i.e., an algorithm for one problem may not guarantee a solution when applied to a different problem, like the example above, which is specific to an engine in a specific vehicle.

Meta-heuristics unlike heuristic algorithms are independent of the of the problem characteristics and hence also known as black box optimization techniques. Meta-heuristic or Stochastic search methods such as Genetic Algorithm (GA), Particle Swarm Optimization (PSO), Bee Algorithm (BA), possess global optimality and robustness and are thus gaining attention [20], [21]. Despite low capability of real time implementation and no guarantee of global optimality, they possess high optimality [22]. Another advantage of meta-heuristics is the possibility to analyse the properties of the meta-heuristics itself, like the influence of metaheuristic-specific parameters on the search behaviour. [20]

3.5 Particle Swarm Optimization

PSO is based on the collective behaviour of social organisms, called particles, moving in groups, such as colony of bees, ants or flock of birds, etc. These social groups have a natural inclination to optimally perform group tasks like bees foraging for food. Members of a group interact within themselves by sharing information about their position with their local neighbours. When applied to optimization problems, the position of each particle corresponds to a discrete value of control parameter to an objective function. Figure 8 shows the sequence of finding global minima across a two-dimensional search space, the boundaries of which are set by the constraints of the optimization problem. The initial positions of the particles are randomly assigned and with successive iteration, the particles communicate among themselves and move closer to the optimal solution which minimizes or maximizes the objective function. The particles move with a velocity indicated by the length of the arrows which is proportional to the distance from the global minimum. The number of particles, number of iterations and initial positions of the particles are all tuneable parameters which define the performance and accuracy of the PSO algorithm. The communication between the particles in solving the collective task is implemented as probability functions based on evolutionary algorithm to select the fittest solution and reject the rest.

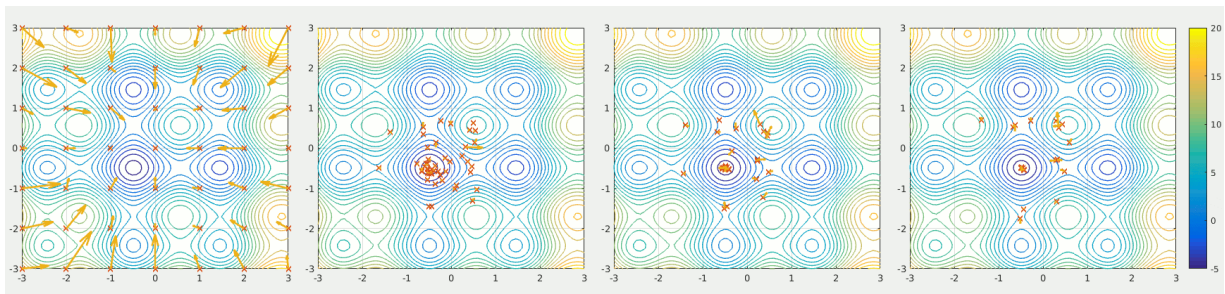


Figure 8 Simulation of a particle swarm searching for global optimum of a solution [23]

The main advantages of PSO include:

- Simple to understand and implement
- Fewer parameters need to be adjusted
- Fast convergence speed
- Strong capability of local search

In this text, a category of PSO, Artificial Bee Colony (ABC) based on the behaviour of artificial bees in a colony with the collective objective of achieving minimum fuel consumption with a variation of control parameter (in this text, motor torque), is explored. The optimization algorithm is invariably referred to as Bee Colony Optimization (BCO).

4 Vehicle Model

A hybrid electric vehicle simulation model is required to validate and analyse a control strategy or EMS, or in this context, an optimisation algorithm. Since, bee colony optimisation belongs to meta-heuristics, it requires a black box function which mimics the vehicle model for which optimisation is to be performed. The result of the optimisation is a power distribution between the engine and the electric motor across road segments for a given horizon length. The characteristic maps of engine, motor and battery were digitized [24] using Origin 2019 data analysis and graphic software [25] using the default parameters [26] from characteristic plot images of various components used in previous studies. All source images are mentioned in Appendices 11.1 – 11.5.

4.1 Vehicle Specifications

The vehicle specifications are closely based on the Ioniq Hybrid with a kerb weight of 1361 kg. A payload of 200 kg (2 passengers + luggage) was added and the total vehicle mass was rounded to 1600 kg. The dynamic tyre radius was calculated from the tyre specifications.[27]

Table 2 Vehicle Parameters: Hyundai Ioniq Hybrid [9]

Description	Symbol	Value	Unit	
Total vehicle mass	m	1600	[kg]	
Aerodynamic drag coefficient	C_x	0.24	–	
Vehicle frontal area	S_x	2.63	[m ²]	
Dynamic tyre radius	r_{dyn}	0.308	[m]	[28]

4.2 Engine

The engine is a 1.6L naturally aspirated GDi unit from the 2020 Ioniq Hybrid working on the Atkinson cycle, with a peak power of 77 kW at 5700 rpm and peak torque of 147 Nm at 4000 rpm [9]. The torque output T_e at the engine shaft is the algebraic sum of the indicated or combustion torque T_{ind} and friction torque T_{fric} for a given engine speed n_e as shown in Equation (2).

$$T_e(n_e) = T_{ind}(n_e) + T_{fric}(n_e) \quad [Nm] = f([rpm]) \quad (2)$$

$$P_e(n_e) = \frac{\pi}{30} \cdot n_e \cdot T_e(n_e) \quad [W] = [rpm] [Nm] \quad (3)$$

$$\eta_e = \frac{P_e}{P_{fuel}} = \frac{P_e}{\dot{m}_f Q_{LHV}} \quad [-] = \frac{[W]}{[g s^{-1}] [J g^{-1}]} \quad (4)$$

$$BSFC (n_e, T_e) = 3.6 \cdot 10^6 \cdot \frac{\dot{m}_f}{P_e} \quad [g kWh^{-1}] = \frac{[g s^{-1}]}{[W]} \quad (5)$$

where,

- n_e : engine shaft rotational speed
- T_e : engine output torque at shaft
- P_e : engine output power
- P_{fuel} : power of the fuel consumed to produce power P_e
- \dot{m}_f : engine fuelling rate to achieve desired power
- $Q_{LHV} = 43.4 \text{ MJ/kg}$: lower heating value of the fuel [29]
- η_e : overall engine efficiency

It is modelled as a static 2-D map with brake specific fuel consumption (BSFC) as a function of engine speed and torque as shown in Figure 9, which indicates the efficiency of the engine in converting chemical energy of the fuel to mechanical power as in Equations (4) and (5). The map was digitized from the image of a BSFC plot used in a recent control analysis study of the same vehicle [26]. The BSFC map was converted to a engine fuel map as shown in Appendix 11.1 using Equation (5), to be compatible with the IGNITE 'Basic Engine' component. The torque is a function of the engine speed and is read from a speed v/s torque 1-D lookup table. The lines of constant power indicate the power output of the engine for any given vehicle velocity and the location of the operating point on this line indicates the degree of gear selected or the gear ratio.

Engine Idling

Since the EU safety regulations do not allow the engine to be switched off during downhill driving on a highway, the fuel consumption data for the idling region needs to be estimated to extend the map. This means that at zero fuelling rate,

$$T_e (n_e) = T_{fric}(n_e) \quad (6)$$

Assuming zero fuelling rate for the friction torque line in Figure 9 and using Equation (6), the fuel map was extended to fill the missing data till the 0 Nm torque limit. For simplicity, the friction torque was assumed to be constant -15 Nm for all speeds, since the idling speed is the only point of concern.

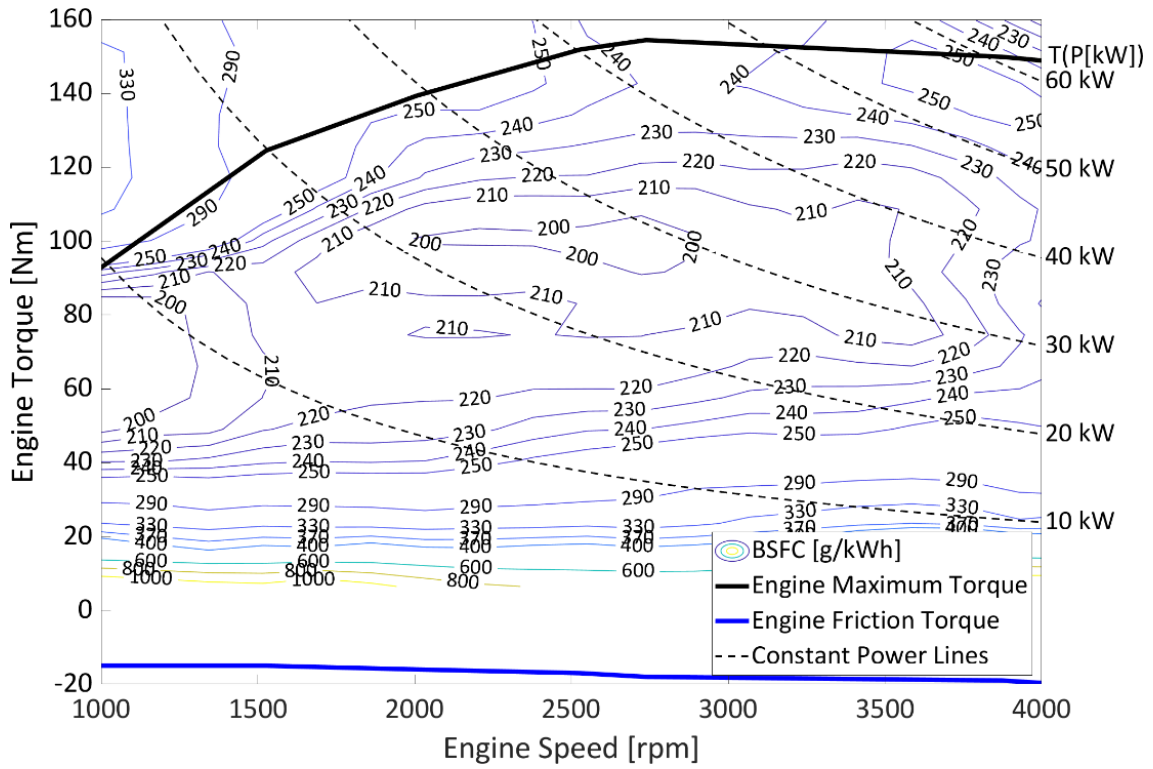


Figure 9 Digitized Engine BSFC map of Ioniq Hybrid [26]

4.3 Electric motor generator

Since the electrical data were not available for the Ioniq Hybrid, the electrical system of the 2011 Sonata Hybrid was used instead, since they are closely similar. The AC motor requires an inverter to convert the DC electric power from the battery to AC and vice-versa. The electric motor converts the electric potential of the battery to mechanical power output. It also functions as a generator during regenerative braking and engine generation, to charge the high voltage battery.

Table 3 Comparison of Electrical system of Ioniq Hybrid and Sonata Hybrid

Parameter	Ioniq Hybrid 2020 [9]	Sonata Hybrid 2011 [30]
Type	PMSM	PMSM
Peak power	32 kW	34 @ 6000 rpm
Peak torque	170	205

$$P_{mgMech} = \frac{\pi}{30} \cdot n_{mg} \cdot T_{mg}(n_{mg}) \quad [W] = [rpm][Nm] \quad (7)$$

$$\eta_{Motor} = \frac{P_{mgMech}}{P_{mgElec}} \quad (8)$$

$$\eta_{Gen} = \frac{P_{mgElec}}{P_{mgMech}} \quad (9)$$

where,

P_{mgMech} : Mechanical power at the motor generator shaft

P_{mgElec} : Electrical power at the battery terminals

Convention of T_{mg} positive (+) for motor regime and negative (-) for generator regime, is considered.

η_{Motor}, η_{Gen} : Combined inverter motor efficiency in the motor and generator regime respectively

The motor is modelled like the engine except that its efficiency means the ratio of mechanical power to electrical power during the motor phase (8) and vice-versa during the generator phase (9). The contours in Figure 10 indicate combined efficiency of the motor and inverter. The generator characteristics are assumed to be identical to the motor. The operating region is limited below the maximum torque line by the control strategy.

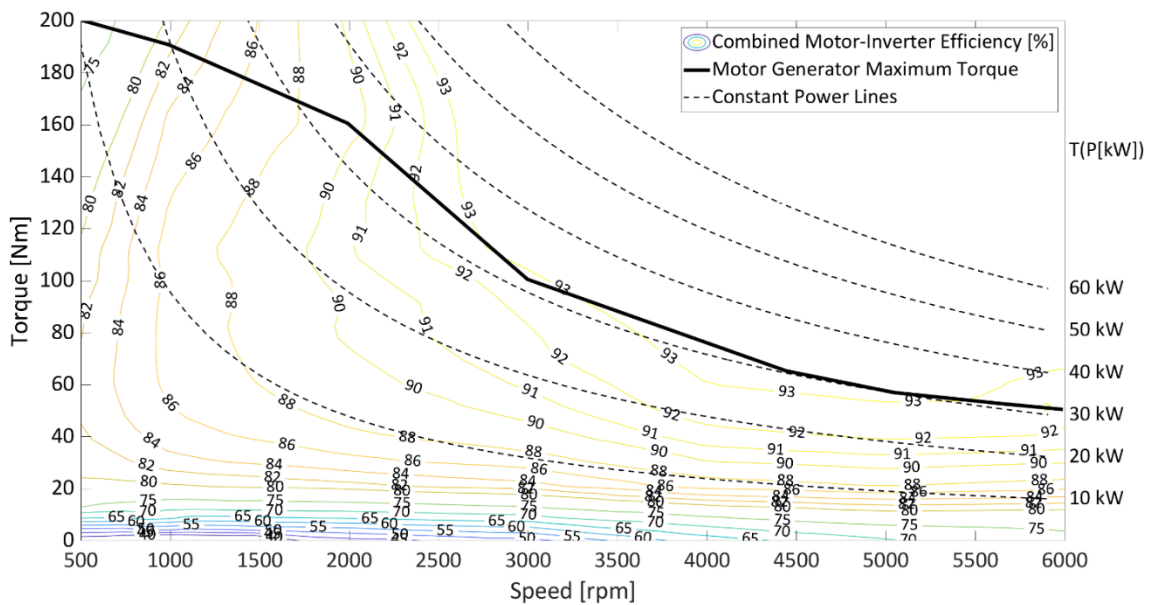


Figure 10 Combined Motor Inverter Efficiency Map (motor regime) of Sonata Hybrid [30]

4.4 Battery

The battery data correspond to that of 2011 Hyundai Sonata Hybrid in Appendix 11.5. Beginning of Test (BOT) refers to the test performed when both vehicle and battery are new while End of

Test (EOT) is the test after approximately 260,000 kms of on-road testing [31]. The test results are about a decade old and considering the development in battery technology, the battery characteristics at BOT seem to be suitable for a more recent and moderately new vehicle. The battery capacity is estimated as 1.4 kWh (5.3 Ah) with operation limited between 20 – 80% SoC, to ensure battery SoH. The battery is simplified as a single cell representing the full battery pack with a constant coulombic efficiency of 97%.

Table 4 High Voltage Lithium-ion Battery Specifications

Parameter	Symbol	Value	Units
Capacity	C_{max}	5.3	[Ah]
	E_{max}	1.4	[kWh]
Nominal voltage	V_{nom}	270	[V]
Coulombic Efficiency	$\eta_{Coulomb}$	0.97	-

4.4.1 Battery Electric Model

In this study, a 0th – order equivalent circuit model, also called *Rint* model as shown in Figure 11 is used. It comprises of a voltage source V_{OC} connected in series with an internal resistance r_{int} , the values of which are digitized form the plots in Appendix 11.5. The temperature effects on the battery characteristics are not considered.

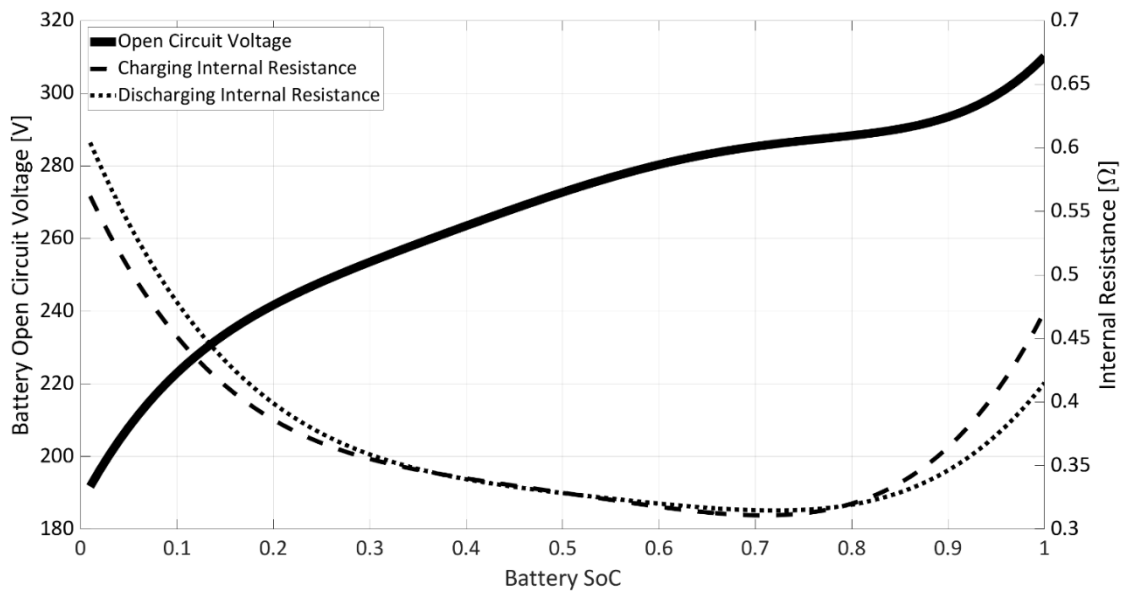


Figure 11 Battery characteristics of Hyundai Sonata Hybrid [31]

$$P_{batt} = P_{mgElec} \quad [W] \quad (10)$$

The electric power at the battery terminals P_{Batt} is equal to the electric power of the motor generator. The sign of the battery power is in accordance with the motor electric power – positive during charging and negative while discharging. Using the battery characteristics in Figure 11,

$V_{OC} = f(SoC)$: Battery open-circuit voltage, voltage at the battery terminals at no load

$R_{int} = f(SoC, sign(P_{batt}))$: Battery internal resistance

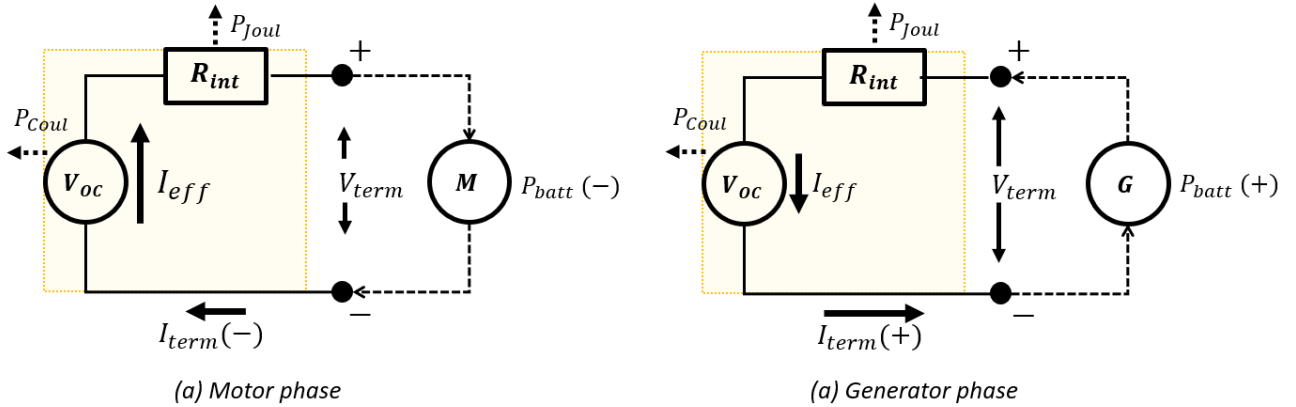


Figure 12 Equivalent Circuit diagram of battery electric model with battery losses (not to scale)

Applying Ohm's Law to the equivalent circuits shown in Figure 12, terminal voltage

$$V_{term} = V_{OC} - I_{term}R_{int} \quad [V] = [V] - [A][\Omega] \quad (11)$$

$$P_{batt} = V_{term} \cdot I_{term} \quad [W] = [V][A] \quad (12)$$

Combining equations (11) and (12)

$$I_{term}^2 + V_{OC} I_{term} - P_{batt} = 0 \quad [W] \quad (13)$$

and solving to get the battery terminal current

$$I_{term} = \frac{-V_{OC} - \sqrt{V_{OC}^2 + 4 R_{int}P_{batt}}}{2 \cdot R_{int}} \quad [A] \quad (14)$$

The sign of I_{term} corresponds to the nature of state change of the battery, positive for charging. The length of arrows in Figure 12 roughly correspond to the relative magnitude of the quantities.

4.4.2 Battery SoC Model and Losses

The change in SoC is determined by Coulomb counting method, where the change in battery capacity in Coulombs is equal to the amount of charge being moved in and out of the battery as electric current during charging and discharging respectively. This was done since Ignite uses this method for soc calculation.

The actual current inside the battery (rate of charge storage and discharge), is different from the terminal current, due to irreversibility of chemical reactions occurring inside the battery. This effective current is the rate of change of electric charge inside the battery. This means that during charging, the actual charge being stored in the cell is less than the charge being pushed into the cell at the terminals ($I_{effective} < I_{terminal}$). Similarly, during discharging, the net charge discharged from the cell is higher than the charge available at the terminals ($I_{effective} > I_{terminal}$). The rate of change of stored charge, effective current:

$$I_{eff} = I_{term} \cdot \eta_{Coul}^{\frac{I_{term}}{|I_{term}|}} \quad [A] \quad (15)$$

$$SOC_{final} = SOC_{init} + I_{eff} \cdot \frac{t_{seg}}{3600 C_{max}} \quad (16)$$

where,

I_{eff} : Effective cell current in the battery

SOC_{init} : Initial SOC at time = 0 seconds

SOC_{final} : Final SOC after time t_{seg} seconds

4.4.2.1 Coulomb Loss

Coulomb loss power P_{Coul} accounts for the energy lost due to irreversibility, determined by the change in entropy of the electro-chemical reactions, determined by coulombic efficiency. This loss is manifested as heat leading to temperature increase of the battery cells.

$$P_{Coul} = -V_{OC} * |I_{term} - I_{eff}| \quad [W] \quad (17)$$

$$P_{Joul} = -I_{term}^2 R_{int} \quad [W] \quad (18)$$

$$P_{loss} = P_{Coul} + P_{Joul} \quad [W] \quad (19)$$

$$P_{elec} = P_{batt} + P_{loss} \quad [W] \quad (20)$$

4.4.2.2 Joule Loss

Joule loss power P_{Joul} accounts for the resistive losses due to heating of the battery internal resistance when current is drawn. In addition to thermal dissipation, Joule loss also leads to a drop in battery SoC, indirectly since Joule loss causes an increase in the terminal current, which in turn increases the effective cell current hence causing drop in SoC.

Both Joule loss and Coulomb loss are always negative with respect to the battery power P_{batt} , i.e., there is a loss of power either way while charging or discharging, leading to P_{loss} being always negative.

4.5 Transmission

The gearbox of Ioniq Hybrid is a 6-speed DCT with two final drive ratios (4.188: 1st – 4th, 3.045: 5th – reverse). A single final drive is used with the 4th and 5th gears accordingly adjusted, to keep the model simple. The efficiency data was not available and are hence suitable assumptions are used.

Table 5 Transmission specifications of Hyundai Ioniq Hybrid [9]

Gear (G)	Ratio (r_G)	Efficiency (η_G)
1	3.867	0.95
2	2.217	0.95
3	1.371	0.96
4	0.930	0.96
5	0.695	0.97
6	0.558	0.97
Final Drive	4.188 (r_{FD})	0.97 (η_{FD})

4.6 Longitudinal Vehicle Dynamics

The longitudinal vehicle model governs the longitudinal position x , velocity v and acceleration a of the vehicle.

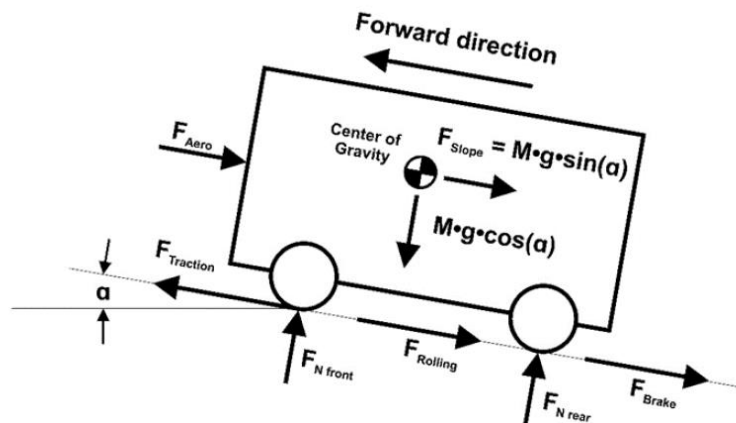


Figure 13 Longitudinal Vehicle Dynamics Model

Table 6 Environment parameters for the vehicle

Constant	Symbol	Value	Unit
Rolling resistance coefficient	c_{roll}	0.015	–
Ambient air density	ρ	1.2	[kg/m ³]
Acceleration due to gravity	g	9.81	[m/s ²]

The external longitudinal forces on a vehicle moving with velocity v are:

$$\text{Rolling resistance} \quad F_{Roll} = c_{roll} m g \cos \alpha \quad [N] \quad (21)$$

$$\text{Gradient resistance} \quad F_{Slope} = m g \sin \alpha \quad [N] \quad (22)$$

$$\text{Aerodynamic drag} \quad F_{Aero} = \frac{1}{2} \rho S_x C_x v^2 \quad [N] \quad (23)$$

Applying Newton's law to the vehicle longitudinal direction,

$$m \frac{dv}{dt} = F_{Trac} - F_{Roll}(\alpha) - F_{Aero}(v^2) - F_{Slope}(\alpha) - F_{Brake} \quad [N] \quad (24)$$

where, $a = \frac{dv}{dt}$ is the acceleration on the vehicle and $v = \frac{dx}{dt}$ is the velocity

F_{Trac} : tractive force generated by the powertrain on the wheels

F_{Brake} : brake force on the wheels

Using wheel dynamic radius r_{dyn} from Table 2, the wheel angular velocity, torque and power:

$$\omega_w = \frac{v}{r_{dyn}} \quad [rad \ s^{-1}] = \frac{[m \ s^{-1}]}{[m]} \quad (25)$$

$$T_{Trac} = F_{Trac} r_{dyn} \quad [Nm] \quad (26)$$

$$P_{Trac} = F_{Trac} v \quad [W] = [N][m \ s^{-1}] \quad (27)$$

For a hybrid vehicle with regenerative braking ability the total brake force is the sum of the mechanical brake force $F_{BrakeMech}$ and regenerative brake force $F_{BrakeRegen}$. The maximum brake force is assumed to be 10 kN.

$$F_{Brake} = F_{BrakeMech} + F_{BrakeRegen} \quad [N] \quad (28)$$

Using backward kinematics from the wheels to the traction source, the angular speed and torque required at the gearbox input:

$$\omega_{gbxInput} = \omega_w r_{FD} r_G \quad [N] \quad (29)$$

$$T_{Req} = \frac{T_{Traction}}{r_G \cdot \eta_G \cdot r_{FD} \cdot \eta_{FD}} \quad [Nm] \quad (30)$$

For a P2 HEV considered in Section 4.1, the angular velocity of the engine ω_e , motor generator ω_{MG} and gearbox input shaft $\omega_{gbxInput}$ are given as

$$\omega_e = \omega_{mg} = \omega_{gbxInput} \quad [rad\ s^{-1}] \quad (31)$$

T_e is the engine torque and T_{Motor} is the motor torque output.

During regenerative braking, the available braking torque at the generator shaft is given as

$$T_{avlRegen} = \frac{T_{Trac}}{r_{FD} \cdot r_G} \cdot \eta_{FD} \cdot \eta_G \quad [Nm] \quad (32)$$

For a Parallel HEV with multiple driving modes described in Section 2.4,

$$\text{Boost or Electric Assist:} \quad T_{Req} = T_e + T_{Motor} \quad [Nm] \quad (33)$$

$$\text{Generation while driving:} \quad T_{Req} = T_e + T_{Gen} \quad [Nm] \quad (34)$$

The total energy consumption E (s) for a distance s is given as

$$E(x) = \int_0^x F(x) \cdot dx \quad [J] \quad (35)$$

where, $F(x)$ is the net tractive force required to drive the vehicle as function of distance x from initial position 0.

4.7 IGNITE Vehicle Models

Since this thesis was part of my internship at Ricardo, the vehicle model was built in Ricardo Ignite software which is a physics-based simulation package for complete vehicle system modelling and simulation with a vast library of various powertrain components and example models. An existing model ‘*midsize p2 hybrid*’ from the examples library of Ignite software as a platform to build the vehicle model based on the characteristics described in Section 4.

4.7.1 IGNITE Model with default rule-based controller

This model simulates the longitudinal dynamics of a vehicle based on driver accelerator and brake pedal inputs. The driver is modelled as a PI controller simulating the accelerator and brake pedals to follow a given drive cycle. The ‘Parallel Hybrid Vehicle Controller’ (working described in Section 5.5) manages the various hybrid modes and generates appropriate demands for the engine and motor with distribution based on fuzzy rule-based strategies. The ‘Shift Strategy’ selects suitable gear according to a pre-defined speed and driver demand lookup table.

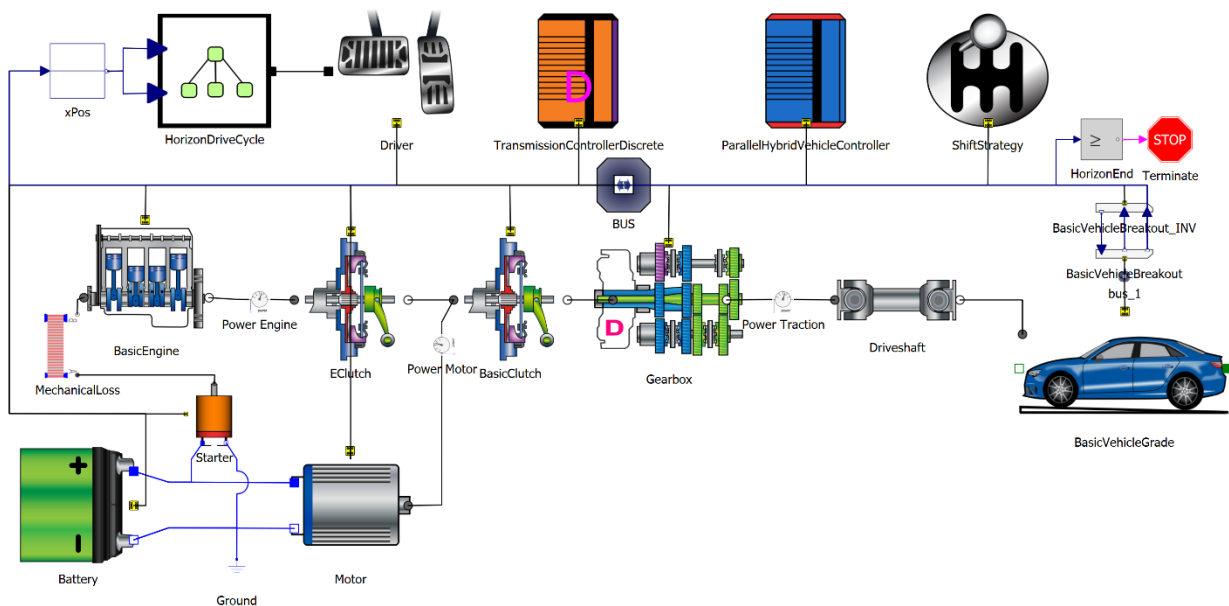


Figure 14 IGNITE Vehicle Model with Default Rule-Based Controller

4.7.2 IGNITE Model with Novel Control Strategy

This model (Appendix 11.8) lacks the hybrid controller and shift strategy from previous model and is configured to receive a velocity, motor demand and gear as a function of distance travelled in metres. The driver demand signal is bypassed to the engine as engine demand to follow the input speed profile, by providing the deficit ($P_{trac} - P_{mot}$) or excess ($P_{trac} + P_{gen}$) power.

5 Description of Control Algorithm

The control algorithm will be tested for various terrain profile scenarios with a variation of velocity and SoC parameters to find the optimum combination for each scenario. The horizon length is the extent of the horizon, i.e., the distance ahead of the vehicle till which eHorizon data is available. The horizon is divided into finite segments of equal length $xRes$ and the nodes are counted from 1 till $nSeg$. As described in Section 3.3, the maximum horizon length is estimated as 8000 m. The term *script* refers to Matlab scripts.

5.1 Terrain Scenarios

Four different hypothetical terrain scenarios are considered as shown in Figure 15, to test the algorithm. Each scenario consists of a total horizon length of 8 km with a mix of flat, uphill and downhill sections. To keep calculations simple, a constant grade is considered for each section. The maximum grade was chosen to be 8% to roughly comply with a typical highway as shown in Appendix 11.7. The script *createTerrain.m* takes the following input and creates 4 road profiles with 4 equal sections as shown in Figure 15 and saves the output as a lookup table of grade and altitude of the road against distance $\{x [m]: z [m], grade [\%]\}$ as *terrain_data.mat*. The x resolution of the terrain data is parameterized and was considered 10m.

5.2 Drive Cycles

The initial idea was to find the optimum velocity profile that minimizes fuel consumption, but that would greatly increase the complexity of the power distribution algorithm described in Section 5.4.1. Since that speed profile is not known and optimization of velocity is difficult, a quicker option is to test with different parameterized speed profiles and select the optimal velocity profile out of a set of pre-defined profiles. The drive cycles for each scenario are linearly varying with respect to time based on conventional cruise control velocity profiles across a hilly road on highways. [4], [32]

Table 7 Drive Cycle Parameters

Parameters	Symbol
Entry speed at beginning of horizon	v_{Entry}
Exit velocity at end of horizon	v_{Exit}
Minimum speed	v_{Min}
Maximum speed	v_{Max}

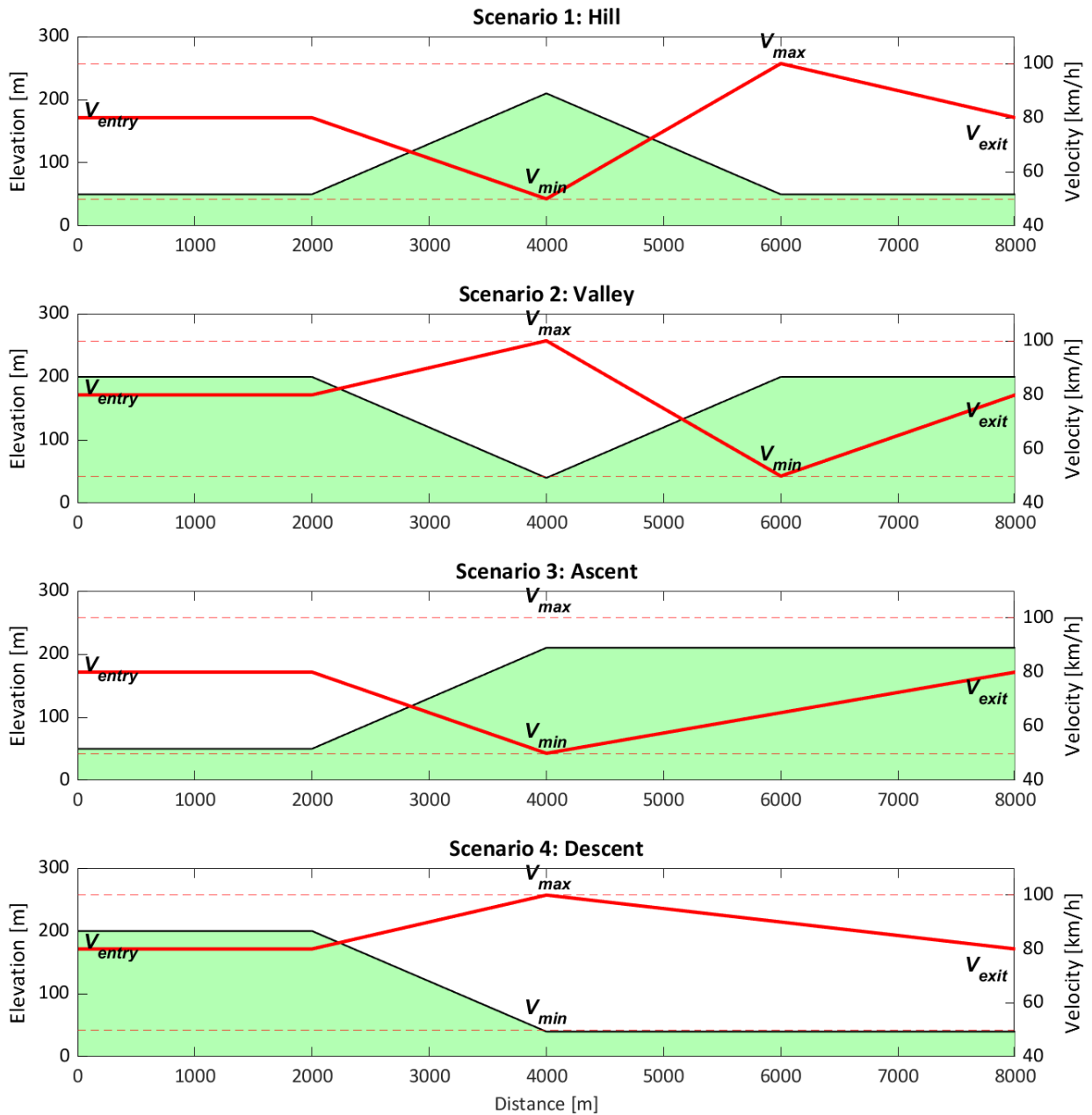


Figure 15 Velocity Profiles for Various Scenarios of Hilly Terrains

The script *createDriveCycle.m* takes the velocity parameters in Table 7 as input and creates a drive cycle for each scenario as shown in Figure 15. The pre-defined velocity profile is saved as *dc_data.mat*, as a lookup table of speed, acceleration and time against distance $\{x [m]: t [s], v [km/h], a [m/s^2]\}$.

The script *createHorizon.m* takes the following inputs and creates an input file *horizon.mat* with the necessary horizon parameters and indexes the drive cycle data against each segment node from 1 till $nSeg + 1$ segments obtained using segment resolution $xRes$, from position 0 till the end of horizon, in this case 8000 m (Section 3.3). This is done to make use of Matlab array

indexing for faster computation. There is an additional parameter *accOverride* [0 / 1], which when enabled [1], allows free coasting as described in Section 5.3.1.

Table 8 Horizon parameters

Parameters	Data file / Symbol
Vehicle parameters	<i>vehdata.mat</i>
Terrain profile	<i>terrain_data.mat</i>
Drive cycle	<i>dc_data.mat</i>
Segment resolution	<i>xRes</i> * [m]
Initial SoC	<i>SoC_{Init}</i>
Minimum SoC below which boost is disabled	<i>SoC_{Min}</i>
Maximum SoC above which generation, regeneration is disabled	<i>SoC_{Max}</i>

* *xRes* is a universal parameter used across all sub-functions using the horizon data.

5.3 Black Box Vehicle Model

Since, bee colony optimisation belongs to meta-heuristics class of optimisation, it requires multiple iterations of simulation with variable parameter combinations to search for the optimal solution. This method when applied to a physics-based real time simulation model such as IGNITE, Simulink, etc. takes hours of computation time to find an optimal solution, since these are designed to provide nearly continuous output using small discrete time intervals to simulate a given time – velocity based drive cycle such as WLTC. This limits the use of meta-heuristic algorithms to offline optimizations [33] and parameter tuning [34]–[36]. This combined with their inevitable pre-processing time overhead, bottlenecks the otherwise fast computation time of meta-heuristics, making it unsuitable for real-time predictive applications.

Thus, it is required to use a minimalistic black box model of the vehicle with all the essential stakeholders of the optimisation problem – vehicle, engine, motor, battery, gearbox, shift strategy. This model when simulated over a given discrete time or longitudinal position interval, must possess near identical dynamics characteristics to that in IGNITE. The purpose of the black box vehicle model is to act as a simple function that converts a given input (in this case, motor demand) to outputs that constitute the cost function (in this case, fuel consumption over a finite distance).

Segment	$iSeg :$	1	2	3	..	nSeg - 1	nSeg
x Position	$x_i :$	0	25	50	7975 8000
Node	$i :$	1	2	3			nSeg-1 nSeg

Figure 16 Representation of segments, nodes and x coordinates

The black box vehicle is defined as a script *Fcn.m* which takes the inputs and sequentially evaluates each sub-function as shown in Figure 15. The subscript i refers to the position at start of segment and $i + 1$ at the end of segment as shown in Figure 16.

The black box function sequentially invokes each sub-model functions beginning with the evaluation of traction power required for the given velocity v_i and road slope corresponding to segment $iSeg$. Subsequently, the corresponding power required at the gearbox input, motor power, engine power, battery electric power and SoC and the optimal gears are selected finally returning the outputs as shown in Figure 17.

Table 9 List of inputs and Outputs for black box vehicle model

Symbol	Description	Units / Range
Inputs		
$iSeg$	Segment number	[1, nSeg+1]
v_i	Velocity at start of segment	[km/h]
SoC_i	SoC at start of segment	[0, 1]
mgd_i	Motor generator torque normalized to maximum motor torque	[-1, 1]
G_i	Gear at start of segment	[1, 6]
Outputs		
v_{i+1}	Velocity at next node	[km/h]
SoC_{i+1}	SoC at next node	[0, 1]
$FC_{seg_{i+1}}$	Fuel consumed for the segment	[g]
G_{i+1}	New gear for segment $iSeg$	

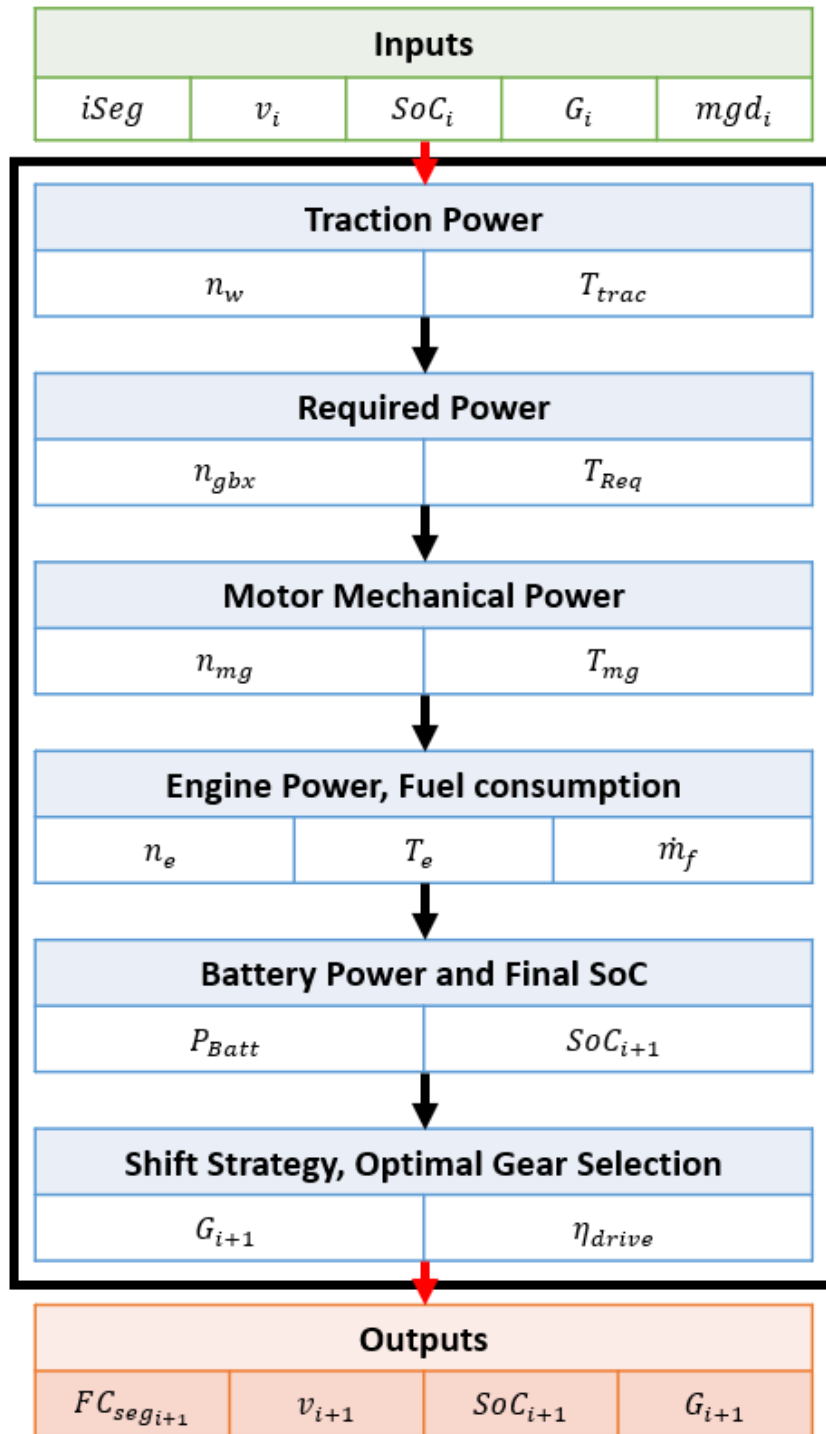


Figure 17 Overall scheme of Black Box Vehicle Function

5.3.1 Traction power

The input $iSeg$ is used as an index to find the segment boundary nodes ($i, i + 1$), corresponding to position (x_{i1}, x_{i+1}) and subsequently fetch the acceleration a_i for the segment and grades at the segment nodes. The input α_i is the mean grade of the two nodes is used to evaluate the gradient resistance F_{slope} .

To allow coasting downhill, a sub-model sets the acceleration equal to that due to the net resistance forces on the vehicle, when the gradient resistance F_{Slope} exceeds the other resistance forces $F_{Roll} + F_{Aero}$ resulting in a net forward force on the vehicle. This allows free coasting to quickly achieve the maximum speed resulting in a higher recuperation potential compared to a linear velocity profile on a descent.

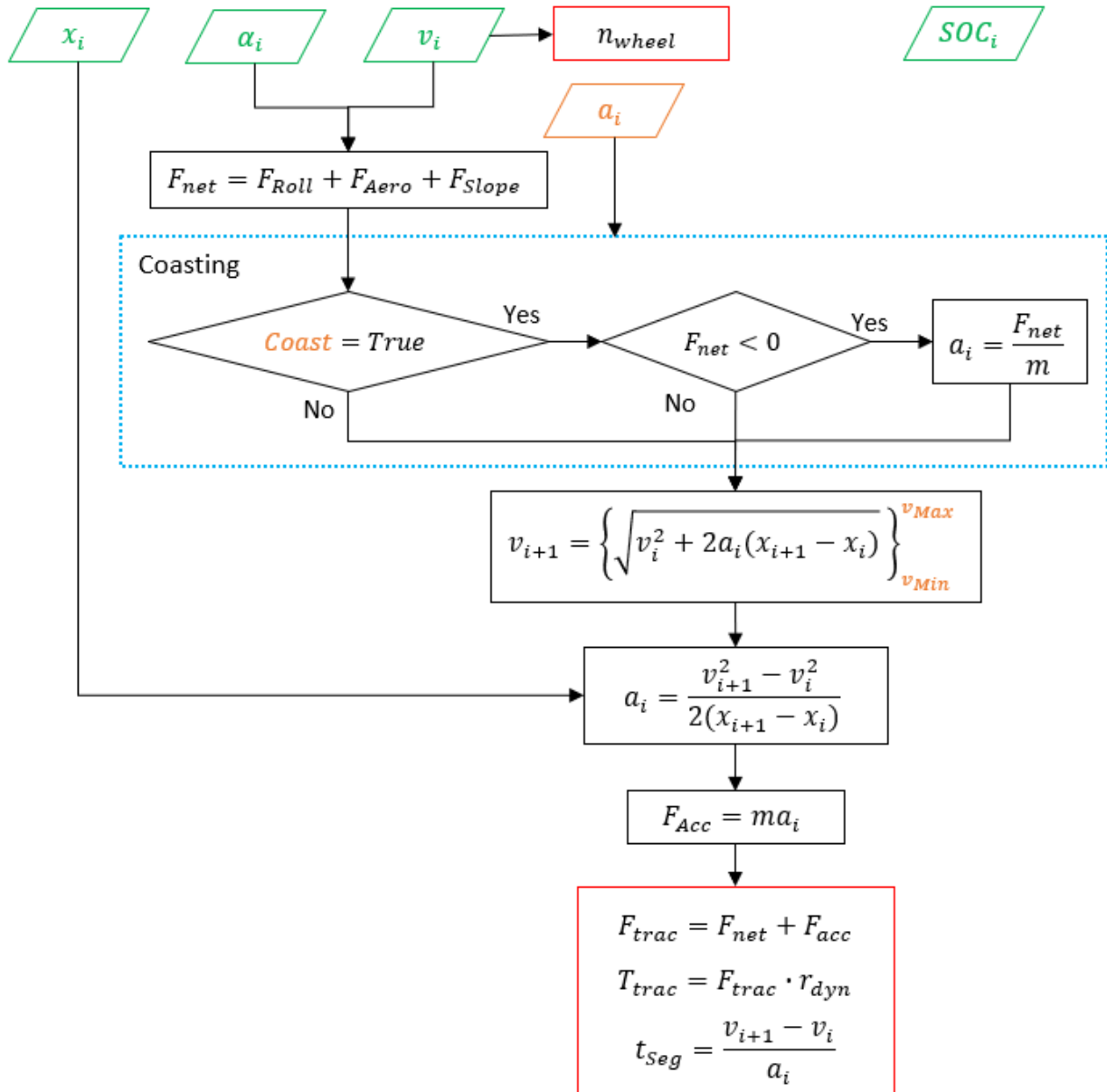


Figure 18 Traction power calculation flowchart

Acceleration at node i is currently using lookup table of drive cycle. Can be alternatively overridden as a parameter (using `accOverride` flag). The net resistance force is calculated at the wheels (excluding F_{acc}). To enable coasting downhill, a coasting sub-model which, when enabled via the `Coast` flag will override the acceleration input to allow free coasting.

The velocity at the next node (v_{i+1}) is calculated and constrained by velocity bounds (parameters v_{min} , v_{max}). If the final velocity (v_{i+1}) does not follow acceleration input, the acceleration a_i is recalculated to comply with v_{i+1} . The acceleration resistance from the final a_i is calculated. The main outputs are the wheel angular speed n_{wheel} [rpm] and traction torque T_{trac} [Nm].

5.3.2 Shift Strategy

The shift strategy consists of 3 parts – the initial pre-selection of feasible gears, finding the optimal gear and shift decision. The gear selected at node i , G_i is denoted as G_{cur} , in the context of shift.

5.3.2.1 Pre-selection of feasible gears

The power (speed, torque) at the gearbox input shaft is a function of the selected gear G_i . Since the gearbox has a discrete number of gears, it is possible to use MATLAB vectorization to evaluate important variables required to select optimal gear, for all gears and then eliminate gears based on feasibility of each individual component (i.e., motor, engine, battery). Thus, initially all gears are deemed feasible and all subsequent values are a matrix of values, with each row corresponding to a gear. The initialised values are shown in Table 10.

The set of feasible gears $\{G_{Feas}\}$ is reduced using the following constraints:

$$n_{gbxInput_{min}} < n_{gbxInput} < n_{gbxInput_{max}} \quad [\text{rpm}] \quad (36)$$

$$-T_{mg_{max}}(n_{mg}) < T_{mg} < T_{mg_{max}}(n_{mg}) \quad [\text{Nm}] \quad (37)$$

$$T_{e_{min}} (= 40 \text{ Nm}) < T_e < T_{e_{max}}(n_e) \quad [\text{Nm}] \quad (38)$$

where, $n_{gbxInput_{min}} = 1700 \text{ rpm}$, $n_{gbxInput_{max}} = 3500 \text{ rpm}$ are the minimum and maximum gearbox input shaft speeds as the boundaries for downshift and upshift respectively.

$T_{mg_{max}}$: maximum motor torque

$T_{eng_{min}}$: minimum engine torque below which engine is disconnected by the eClutch

$T_{eng_{max}}(n_e)$: maximum engine torque at the given speed n_e

The gearbox input speed limits correspond to the engine operating speed range in Section 4.2. The maximum engine and motor torques are read from the maps in Figure 9 and Figure 10 and the minimum torque for motor is set as 0 Nm while for engine it is set as 40 Nm, since operating

below this pushes the engine into regions of low efficiency and the loss in efficiency increases rapidly with decreasing torque as shown in Figure 9. The engine is thus not allowed to operate in boost mode below this torque and the deficit torque is filled by the motor.

Table 10 Optimal gear initialization table

Component	Symbol	Initial value
Transmission	G	[1 2 3 4 5 6]'
	n_{gbx}	[6 x 1]
	T_{gbx}	[6 x 1]
Motor Generator	T_{mg}	0
	η_{mg}	0
	P_{batt}	0
Engine	$eClutch$	0 [Disengaged]
	n_e	Idle [1000 rpm]
	T_e	Idle [0 Nm]
	\dot{m}_f	Idle [0.16 g/s]
Battery	SOC_{i+1}	SOC_i
	P_{coul}	0
	P_{joul}	0
	$P_{brake,mech}$	0
Optimal Gear Selection Shift Strategy	P_{fuel}	0
	P_{elec}	0
	η_{drive}	0
	G_{opt}	0
	G_{sel}	0

5.3.2.2 Finding Optimal Gear

When more than one gears are feasible, the gear with the maximum driveline throughput efficiency is the optimal gear G_{opt} as shown in Figure 19. This efficiency refers to the ratio of the total output power to the total input power, the sense of which changes according to the hybrid mode. The total power at the gearbox input is the algebraic sum of the engine power and motor generator power (sign indicates regime) and at the wheels is the traction power.

5.3.2.3 Shift Inhibit Strategy

Early simulations revealed frequent shifting, sometimes oscillations between multiple gears. The reason was location of motor operating point in regions of low torque where in the motor map in Figure 10, where efficiency changes are steep.

The shift inhibit strategy prevents shifting into the optimal gear if the optimal gear is different from the current gear. It works by checking a series of trade-offs iteratively by preferring each intermediate gear starting from the current gear, as shown in Figure 20. The trade-offs are based on the initial results and sensitivity analysis and work well for the simulations described in Section 6.3. The corresponding message is stored indicating the reason for the shift inhibit operation, shown in the blue boxes.

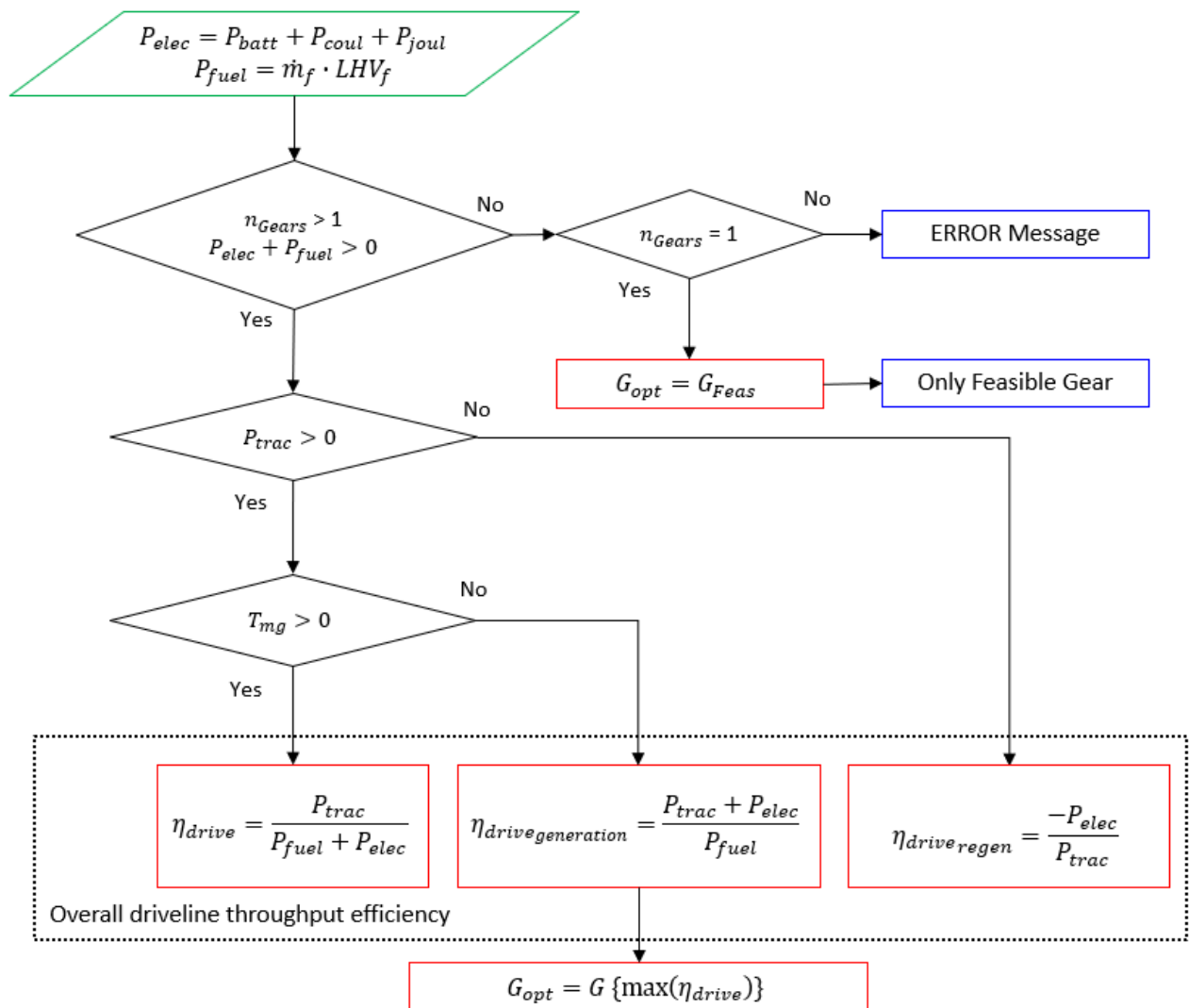


Figure 19 Optimal Gear Selection Flowchart

The algorithm in Figure 20 makes it possible to check for all intermediate gears though only following cases have been implemented in programs:

For difference in gears:

1 - check for G_{cur} only, 2 – check for $G_{cur} +/- 1$ towards G_{opt}

Cases with difference > 2 are unlikely to be encountered during any of the scenarios.

This works well to prevent unnecessary shifting in all cases. The rare cases of oscillations are because of the bee colony being unaware of the impact of shift operations on its associated cost function, i.e., instantaneous fuel consumption.

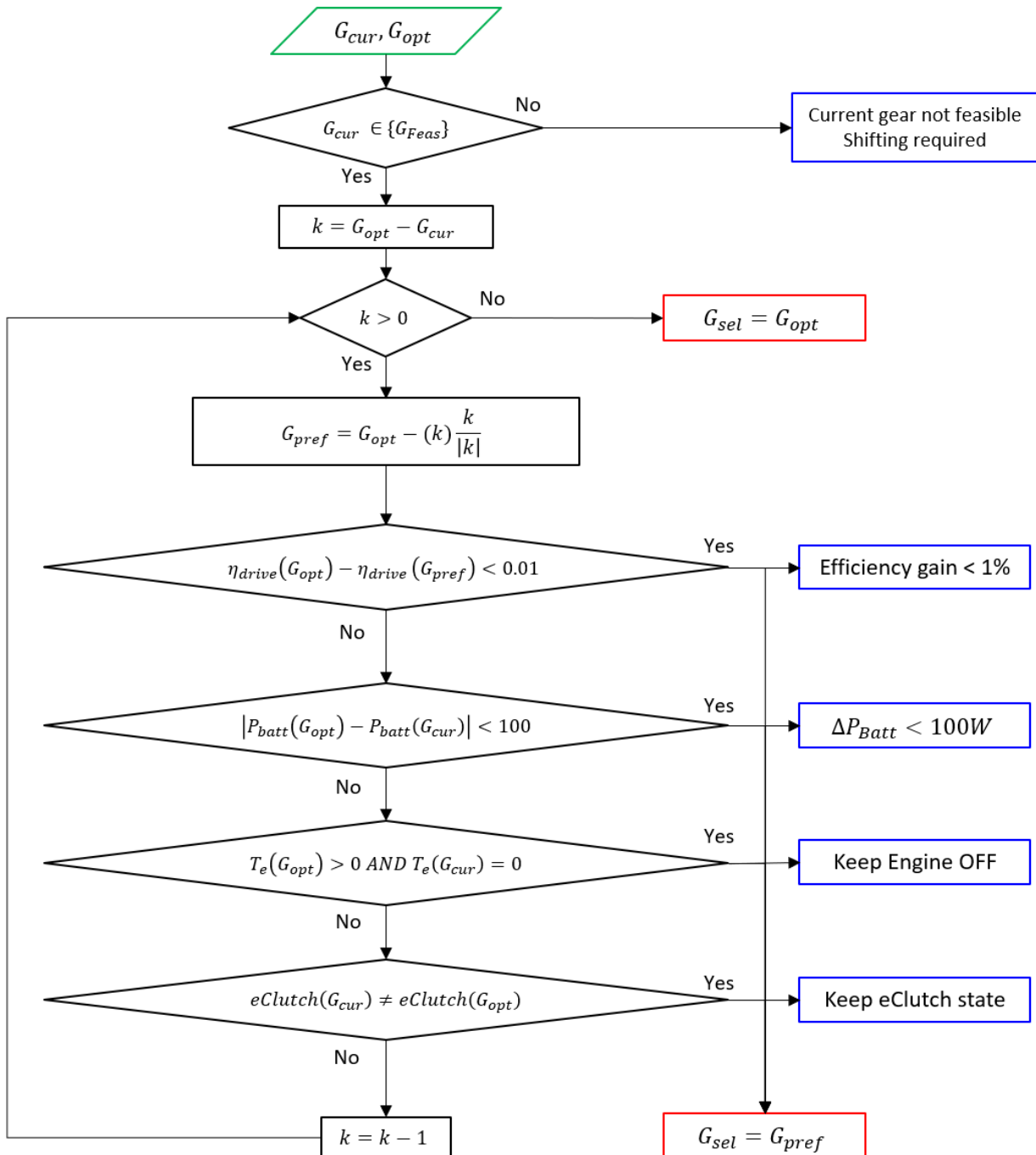


Figure 20 Optimal Gear Shift Inhibit Flowchart

5.3.3 Optimal hybrid operating mode and motor control strategy

The control strategy works with the motor being controlled explicitly by the independent variable mgd , while the engine works to fill the deficit torque $T_{Req} - T_{mg}$. The appropriate hybrid mode is chosen based on the values of the traction power and motor generator power.

This sub model represents motor generator logic to calculate the motor generator torque from the inputs to the main model function ($Fcn.m$). As shown in Figure 21 Power Distribution Flowchart for Hybrid Mode and Motor Generator Mechanical Power, the main inputs are torque request T_{Req} at the gearbox input for each feasible gear and the motor generator demand. Based on these values, the motor mechanical power is calculated which acts as an input for the next sub-model (5.3.4).

5.3.4 Engine control strategy

After the required torque and motor torque are defined, the remaining torque is provided by the engine subject to constraints of speed and torque. If the engine torque is below the limit defined in Section 4.2, the engine is set to idle and the motor torque adjusted according as shown in Figure 22.

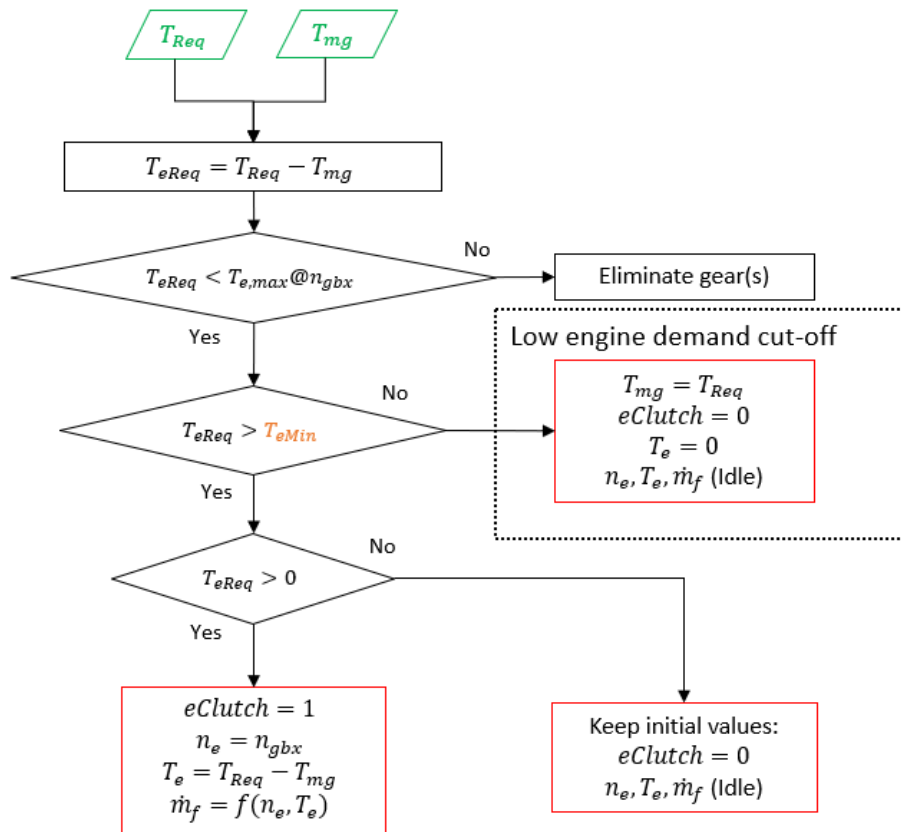


Figure 22 Power Distribution Flowchart for Engine State and Mechanical Power

5.3.5 Battery

This sub-model is constructed using equations of battery model in Section 4.4 calculating all the electrical quantities from the motor mechanical power. The main outputs are the motor efficiency, the change in battery SoC and battery power losses.

5.4 Control Algorithm for Various Scenarios

From Section 5.1 and 5.2, it is evident that the different terrain profiles and velocity trajectories demand different control strategies each specific to the characteristics of the road profile ahead. The initial section of flat road has a constant velocity till a change of slope occurs. For uphill sections, boost or EV assist is used for which the motor power follows the output of the ABC algorithm, shown as BCO Boost in Figure 23. For downhill sections, the velocity profile in Section 5.2 is overridden to accelerate the vehicle by free coasting and then regenerative braking begins once the vehicle reaches maximum velocity v_{Max} . In cases where the SoC is lower than the initial SoC at the end of the terrain journey, a generation strategy described in Section 5.4.2 is used to top up the battery to the initial capacity at the beginning of horizon.

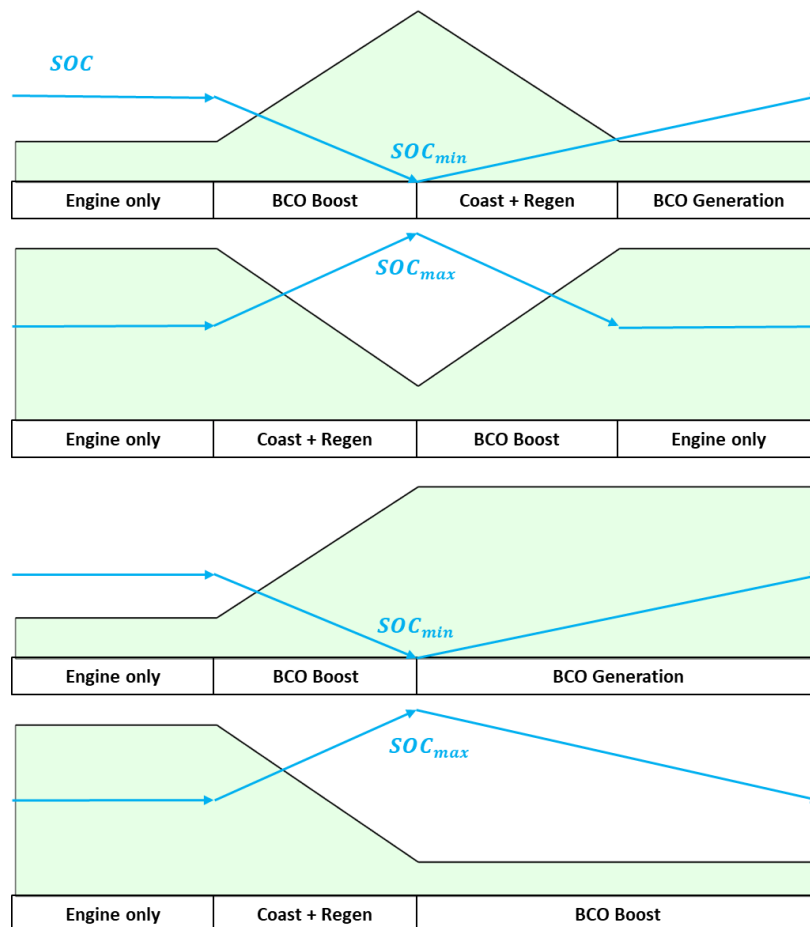


Figure 23 Control Strategies for various scenarios of hilly terrain

5.4.1 Working Principle of Artificial Bee Colony Power Algorithm for EV / Boost

The goal is to find the optimum motor demand for a section of hill climb, such that the fuel consumption for that section is minimized. The following artificial bee colony algorithm is constructed from an open-source implementation of the ABC algorithm in MATLAB [37]. Since the final SoC at the end of the horizon must be same as the initial SoC at the beginning of horizon for fuel consumption results to be directly comparable as grams.

Based on the input parameter, nPop number of bees numbered $b = 1, 2, 3, \dots, nPop$ are assigned the task of finding the optimal solution, whose job is to find the optimum trajectory by varying position Pos_b between Pos_{min} and Pos_{max} with a parameterized Step that results in a minimalization of the cost function C_b for each bee b , as shown in Figure 24. In this section the segments are denoted by the variable i , not to be confused with the node denomination in Section 5.3.

A bee has two major attributes: **Position** – represents the value of input variable of to the black box function, in this case motor demand and **Cost** – represents the output value of the black box function, in this case Cumulative Fuel Consumed after traversing through $nSeg$ segments.

The size of the solution space thus becomes:

$$\left(1 + \frac{Pos_{max} - Pos_{min}}{Step}\right)^{nSeg}$$

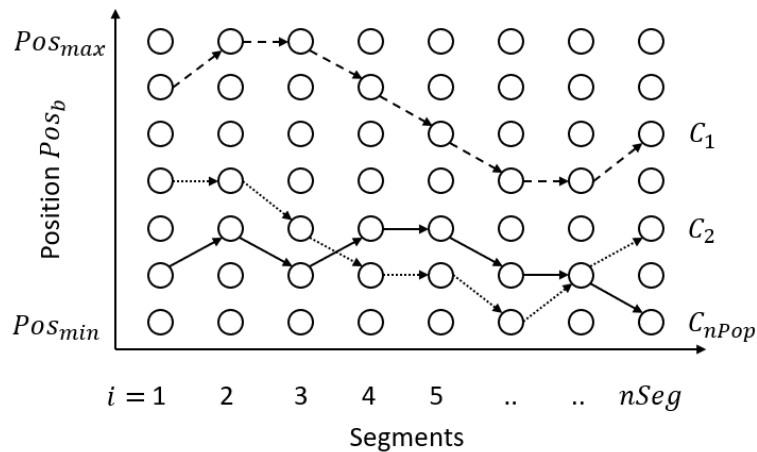


Figure 24 Representation of bees searching the solution space across segments for the global optimum

5.4.1.1 Initialization

The aim is to search for motor demand between the range [0 – 1], with parameterized step – say [0.2] iteratively for each segment of a given horizon – thus the sample size of search space is the set {0, 0.2, 0.4, 0.6, 0.8, 1}. The optimum demand is the one that results in minimum cumulative fuel consumption at the end of the horizon. For a vehicle horizon, the horizon needs to be discretized into a finite number of segments, such that the dynamics of the vehicle are respected. The position thus becomes a vector of values for each segment spanning from the segment node (beginning of segment) for a distance of $xRes$ ([m] parameter). The cost is also a vector of values for each segment, the cumulative sum of which at the end gives the cumulative fuel consumption or the aggregate cost function. Thus, the black box function described in Section 5.3, must be sequentially invoked for each subsequent segment till the end of the horizon.

As shown in Figure 24 and Figure 25, each bee is initialized with a random position for the first segment. The finite solution space shown as circles denote possible values of each bee's position Pos_b . The subsequent positions are determined by a 1/3 probability, i.e., there is an equal chance that the bee's next position relative to i :

$$Pos_{b_{i+1}} = Pos_{b_{i-1}} + \{0, +Step, -Step\} \quad [0, 1] \quad (39)$$

The Step is a parameter that defines the maximum change in position of a bee relative to previous segment. In the Figure 24, considering the position boundaries 0 and 1, the Step is 0.2.

For the first segment, each bee is initialized with a random motor demand from the set of possible solutions which for a step of 0.2 and range [0, 1] is {0, 0.2, 0.4, 0.6, 0.8, 1}. The black box vehicle function (Section 5.3) is run for one segment with this motor demand with the initial velocity and SoC values. The outputs of the first segment velocity, SoC and fuel consumption at the end of segment v_1, SoC_1, FC_{seg_1} are the main outputs of the black box function and serve as inputs for the next segment.

Using this demand, the SOC_{seg+1} is calculated. If $SOC_{seg+1} < SOC_{min}$, this means that the bee's position for this segment will cause SOC to go below limit. Thus, decrease it by one step repeatedly till a demand is achieved for which the SOC does not go below limit (implemented using a while loop in *runABC.m*).

The objective function is the cumulative cost for all the segments is calculated for each bee:

$$C_b = \sum_{i=1}^{nSeg} FC_i \quad [g] \quad (40)$$

After initialization, each bee has a vector of positions for each segment and the cost for each segment, along with Best Position and Best Cost for the population.

5.4.1.2 Iterations

As described in Section 3.5, ABC being a PSO algorithm performs a repetitive search over the solution space for a finite number of iterations or till a convergence criteria is met. The strength of PSO is the communication between the bees and their collective problem-solving approach.

5.4.1.2.1 Selection Probabilities

Each iteration begins with an analysis of the solution found by the bees, which is the normalized error of each bee's cost C_b from the worst solution C_{max} (maximum value of objective function) as in Equation (41). Then the fitness probability of each bee is calculated from its normalized error. From Equation (42), it can be seen that the fitness of a bee is exponentially proportional to its closeness to the optimum solution [38].

$$O_b = \frac{C_{max} - C_b}{C_{max} - C_{min}} \quad (41)$$

$$P_b = e^{-(O_{max}-O_b)} \quad (42)$$

5.4.1.2.2 Scout Bees

The scout bee is based on the Roulette Selection Principle of genetic algorithm where fittest individuals (with a higher fitness probability) are selected as parents [39]. For each bee in the original population, a new bee called scout bee Nb is created which inherits the position, cost and additional values such as SoC and velocity data for each segment. The scout bee selects a random segment from the parent bee's solution space and iterates from that segment till the end. The cost obtained by the new bee C_{Nb} is compared with the cost of the old bee C_b and in case the scout bee has a better solution ($C_{Nb} < C_b$), the old bee inherits the position, cost, SoC and velocity values from the new bee.

An iteration ends when all bees in the population have their values compared with the scout bees and the global best solution C_{best} is updated.

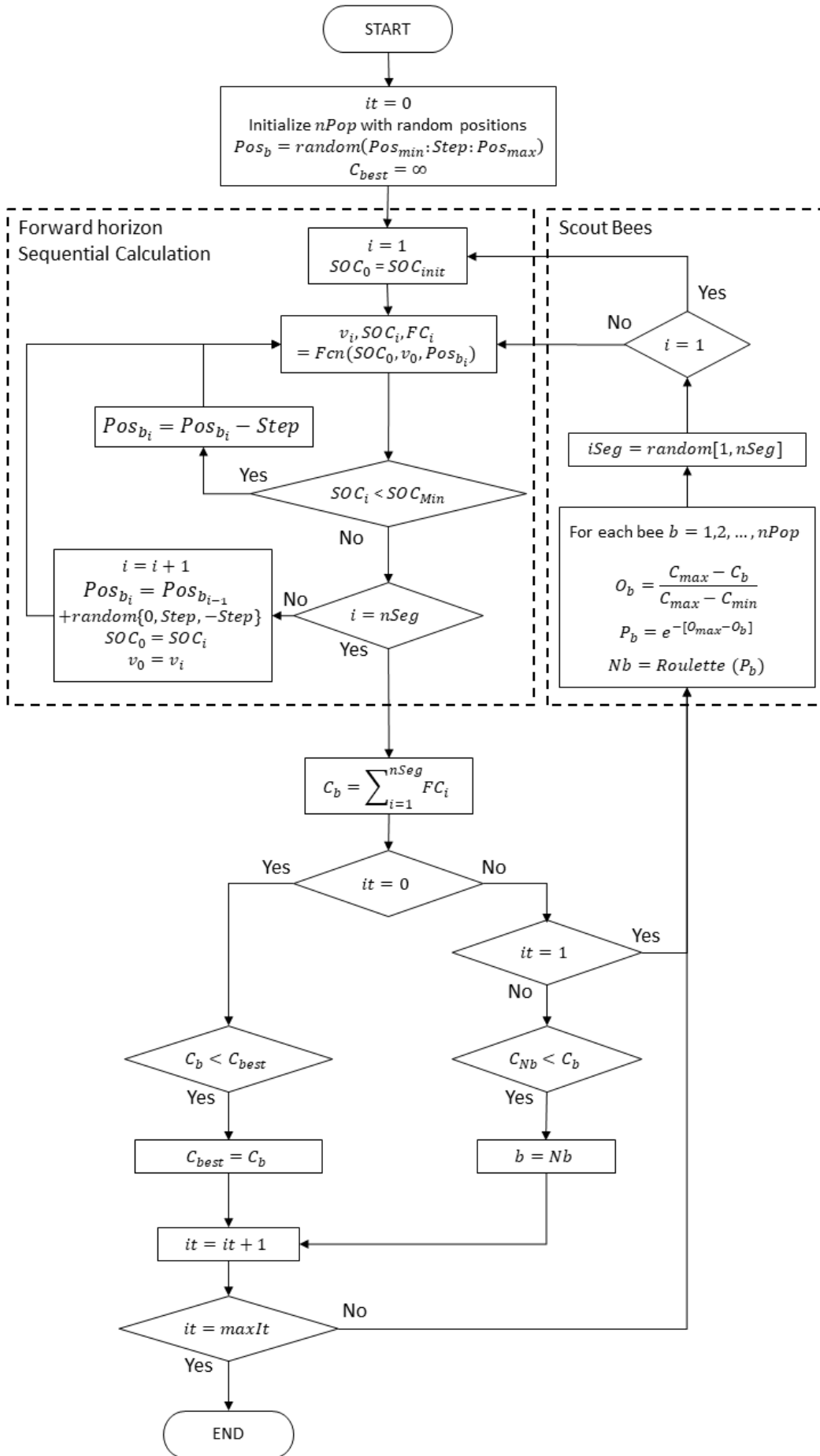


Figure 25 Artificial Bee Colony Flowchart for Optimum Power distribution in EV/Boost Mode

5.4.2 ABC for Generation

The ABC algorithm for generation is the same as that for power distribution, except for position and cost function. The position, in this case, is the generator demand, which according to the followed sign convention is motor demand with an inverted sign, i.e. within the range [-1, 0] and the cost function is the difference $SOC_{init} - SOC_{end}$, where SOC_{end} is the SoC at the end of horizon.

The Cost function does not use fuel consumption, since this would result in a multi objective optimization and suitable weights must be defined for fuel consumption and ΔSoC , since these are conflicting objectives.

5.4.3 Optimal ABC parameters

As it will be seen in this section that the performance of ABC depends on the selection of suitable parameters the most important being step size, population and maximum number of iterations.

5.4.3.1 Step Parameter

The size of the solution space increases exponentially with step size. But since the ABC is a learning-based algorithm, its performance is independent of the size of the solution space. Moreover, the step parameter limits the deviation in position between subsequent segments. It was observed that large step sizes of the order of >0.1 causes rapid oscillations of the motor demand along with inferior solutions because of a limited number of operating points to choose from. The oscillations are eliminated with a low step size of the order 0.01. Consequently, oscillations of shift are also minimized with lower step sizes. Oscillation begin to appear with step size = 0.05 and become significant at step size 0.1. Sample results with different step sizes in Attachment [].

5.4.3.2 Brute-Force Search

In this context, the BCO does not have a global optimum (minima) of fuel consumption value for reference (convergence criterion), the first task was to find the global minima using brute-force search method with a small number of segments. The vehicle was run with the following parameters, only for the BCO boost section (hill climb):

$v_{Entry} : 80 \text{ km/h}$, $v_{Min} : 50 \text{ km/h}$, $v_{Max} : 100 \text{ km/h}$, $v_{Exit} : 80 \text{ km/h}$

$SOC_{init} : 0.8$, $SOC_{Min} : 0.2$

Each possible permutation of the optimization variable (in this case, mg demand), was run on the black box vehicle with the above parameters. All solutions where the SOC dropped below SOC_{Min} , were eliminated as non-feasible solutions.

This global minimum, though available for only 8 segments, sets the benchmark for the ABC algorithm to be compared against and is enough to analyse the convergence criteria of the ABC. To ensure consistency in results, each set of permutations was run 3 times and the time in Table 11 is the mean time.

All computations and simulations were performed on a laptop with an Intel Core-i5 7200U CPU with 2 cores and 4 threads on a single core, single threaded workload. The acausal nature of black box function does not permit the use of parallel processing in MATLAB environment (using *parfor* loop and *parpool*).

Table 11 Results of brute-force search for optimum motor demand during hill climb

Step	Possible values	nSeg	Permutations	Time	minCost = FC_{min} [g]
0.2	$= 1 + \frac{1 - 0}{0.2} = 6$	6	$6^6 = 46 K$	1 min	59.07
		8	$6^8 = 1.68 M$	42 min	58.19

5.4.3.3 Population and Iterations

The same experiment was repeated, this time using ABC to search for the minimum cost (cumulative fuel consumption). To find the optimum combination of bee population $nPop$ and the corresponding iterations until convergence, a sweep was performed on the number of bees from 10 till 100 with a step of 10, with the same maximum number of iterations = 100. The cost (FC cumulative) and time were recorded for each iteration, for each bee size. Each parameter combination was run 3 times. The graph in **Error! Reference source not found.** shows the first occurrence unique cost values during the ABC search and the corresponding time. For each individual run, dots of same colour when connected with straight lines, resemble a typical stepped convergence curve. This gives an overview of the convergence speed as a function of population and iterations.

A statistical analysis was done to conclusively select the optimal ABC parameters. The results shown in Table 12 shows a comparison of two important characteristics of ABC – accuracy of convergence and time required to do so. The accuracy of the bee colony optimisation in

searching for the solution for minimum fuel consumption is calculated by FC Difference, which is the normalised error of the results of BCO to the difference of the worst exact solution (FC_{Max}) and best exact solution (FC_{min}). The calculation speed proportion of the BCO is the ratio of the time taken to compute the exact solution to the time by BCO to achieve the given solution.

Before proceeding with experiments with optimisation, it is important to analyse the performance impacts of the optimisation parameters on the solution accuracy, precision and speed. It is evident from the low standard of mean that BCO is precise enough to and in the search for optimal solution, accuracy stays within approximately 0.05% of the optimal solution and the computation speed outperforms a brute search method by at least an order.

It can be seen from Figure 26, that ABC is reliable enough to converge within 5 seconds, in most cases, and the increase of computation time with very high population sizes and iterations, provides diminishing returns.

From Figure 26, it can be inferred that a bee population of 20 – 30 converge to optimal solution within 30 iterations. So, a combination of the BCO parameters between the above values, should be selected to maintain a balanced parameter set for BCO. To provide a failsafe against missing optimal solution with very large solution space, a combination of 50 bees with 50 iterations seem to be an ideal choice for further optimizations.

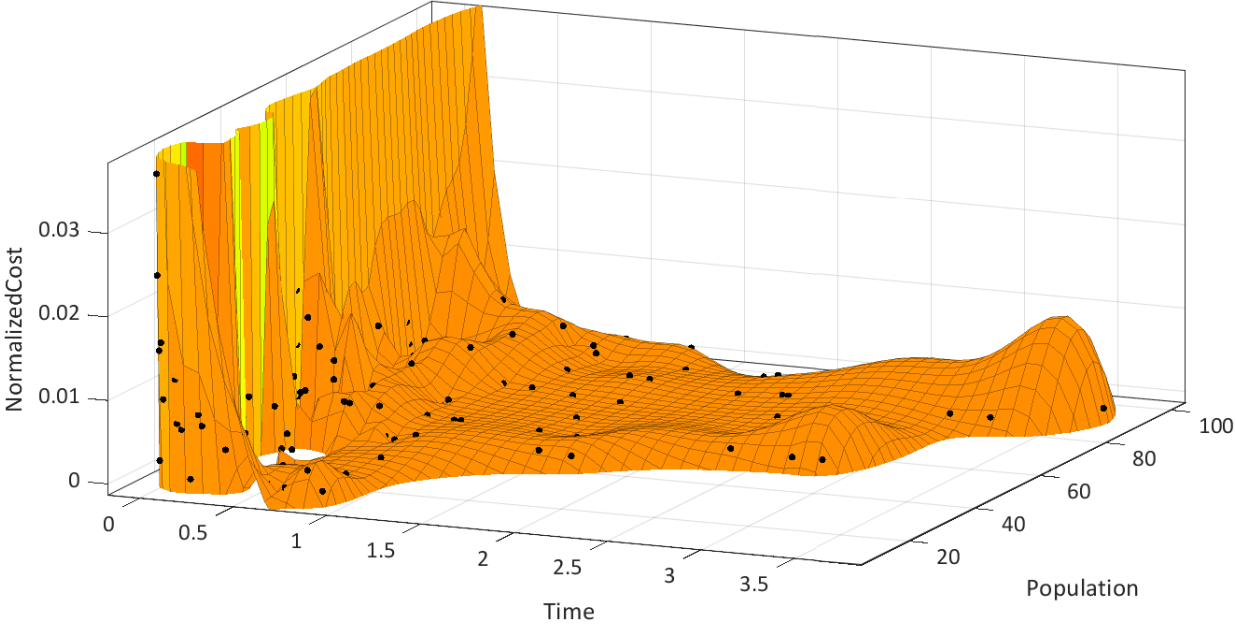


Figure 26 Convergence characteristics of ABC -REPLACE

Table 12 Comparison of Bee Colony Optimization with Brute Force Search Results

Exact solution:		Time [s]:										FC [g]:										Max:	197.56			
		2515																				Min:	58.19			
FC [g]		Iterations										FC Difference	Iterations													
		FC	5	10	20	30	40	50	60	70	80		90	100	FC	5	10	20	30	40	50	60	70	80	90	100
Population	10	59.51	59.07	58.83	58.81	58.44	58.44	58.37	58.26	58.26	58.26		10	0.95%	0.63%	0.46%	0.45%	0.18%	0.18%	0.18%	0.13%	0.05%	0.05%	0.05%	0.05%	0.05%
	20	58.58	58.49	58.29	58.27	58.26	58.26	58.26	58.26	58.26	58.26		20	0.28%	0.21%	0.07%	0.06%	0.05%	0.05%	0.05%	0.05%	0.05%	0.05%	0.05%	0.05%	0.05%
	30	58.86	58.34	58.34	58.26	58.26	58.26	58.26	58.26	58.26	58.26		30	0.48%	0.11%	0.11%	0.05%	0.05%	0.05%	0.05%	0.05%	0.05%	0.05%	0.05%	0.05%	0.05%
	40	58.99	58.84	58.29	58.26	58.26	58.26	58.26	58.26	58.26	58.26		40	0.57%	0.47%	0.07%	0.05%	0.05%	0.05%	0.05%	0.05%	0.05%	0.05%	0.05%	0.05%	0.05%
	50	58.84	58.52	58.35	58.32	58.27	58.26	58.26	58.26	58.26	58.26		50	0.47%	0.24%	0.11%	0.09%	0.06%	0.05%	0.05%	0.05%	0.05%	0.05%	0.05%	0.05%	0.05%
	60	58.58	58.30	58.27	58.26	58.26	58.26	58.26	58.26	58.26	58.26		60	0.28%	0.08%	0.06%	0.05%	0.05%	0.05%	0.05%	0.05%	0.05%	0.05%	0.05%	0.05%	0.05%
	70	58.88	58.35	58.29	58.27	58.27	58.27	58.27	58.27	58.27	58.27		70	0.50%	0.12%	0.07%	0.06%	0.06%	0.06%	0.06%	0.06%	0.06%	0.06%	0.06%	0.06%	0.06%
	80	58.63	58.38	58.29	58.26	58.26	58.26	58.26	58.26	58.26	58.26		80	0.31%	0.14%	0.07%	0.05%	0.05%	0.05%	0.05%	0.05%	0.05%	0.05%	0.05%	0.05%	0.05%
	90	58.72	58.40	58.27	58.26	58.26	58.26	58.26	58.26	58.26	58.26		90	0.38%	0.15%	0.06%	0.05%	0.05%	0.05%	0.05%	0.05%	0.05%	0.05%	0.05%	0.05%	0.05%
	100	58.51	58.32	58.29	58.26	58.26	58.26	58.26	58.26	58.26	58.26		100	0.23%	0.09%	0.07%	0.05%	0.05%	0.05%	0.05%	0.05%	0.05%	0.05%	0.05%	0.05%	0.05%
Time [s]		Iterations										Calculation speed proportional improvement	Iterations													
		Time	5	10	20	30	40	50	60	70	80		90	100	FC	5	10	20	30	40	50	60	70	80	90	100
Population	10	0.08	0.16	0.31	0.44	0.57	0.71	0.86	0.99	1.12	1.26	1.39		10	32084	15793	8175	5708	4377	3544	2939	2537	2236	1999	1804	
	20	0.13	0.26	0.55	0.82	1.08	1.35	1.62	1.90	2.17	2.44	2.72		20	20114	9616	4556	3074	2325	1857	1549	1324	1157	1029	924	
	30	0.22	0.43	0.84	1.23	1.67	2.08	2.52	2.94	3.37	3.80	4.22		30	11374	5832	3009	2039	1507	1209	999	855	745	661	596	
	40	0.27	0.55	1.13	1.73	2.29	2.88	3.43	4.05	4.64	5.22	5.79		40	9452	4603	2233	1457	1096	873	732	621	542	482	434	
	50	0.33	0.69	1.40	2.06	2.76	3.44	4.11	4.81	5.55	6.27	6.94		50	7608	3624	1802	1223	910	730	612	523	453	401	362	
	60	0.46	0.93	1.82	2.73	3.72	4.72	5.67	6.59	7.52	8.43	9.39		60	5467	2697	1385	923	675	533	443	381	335	298	268	
	70	0.64	1.27	2.46	3.63	4.82	6.03	7.26	8.51	9.76	11.03	12.29		70	3914	1974	1023	693	522	417	346	296	258	228	205	
	80	0.71	1.45	2.86	4.26	5.70	7.15	8.61	10.05	11.55	12.98	14.36		80	3522	1730	878	590	442	352	292	250	218	194	175	
	90	0.67	1.36	2.69	4.00	5.35	6.65	7.97	9.22	10.46	11.67	12.91		90	3753	1848	936	628	470	378	315	273	240	215	195	
	100	0.65	1.34	2.66	3.94	5.23	6.52	7.86	9.24	10.60	11.98	13.37		100	3896	1871	945	639	481	385	320	272	237	210	188	

5.4.3.4 Optimal Parameters with realistic solution space

The previous sub-section showed the ability of the BCO to quickly converge to the global minima, within a short time. But since the actual number of segments in a real scenario will be much > 8 and Resolution << 250m. So, the above sweep was conducted again, this time with a finer resolution of the search space and parameters close to practical values, resolution of 25 m with step: 0.01. The solution space for a 2000 m segment thus becomes 80^{101} . A bee size of 30 - 60 seems to be suitable as it consistently converges to the minimum within a reasonably short time of less than a minute. To guarantee convergence, a bee size of 50 and 50 iterations were selected as a safe option.

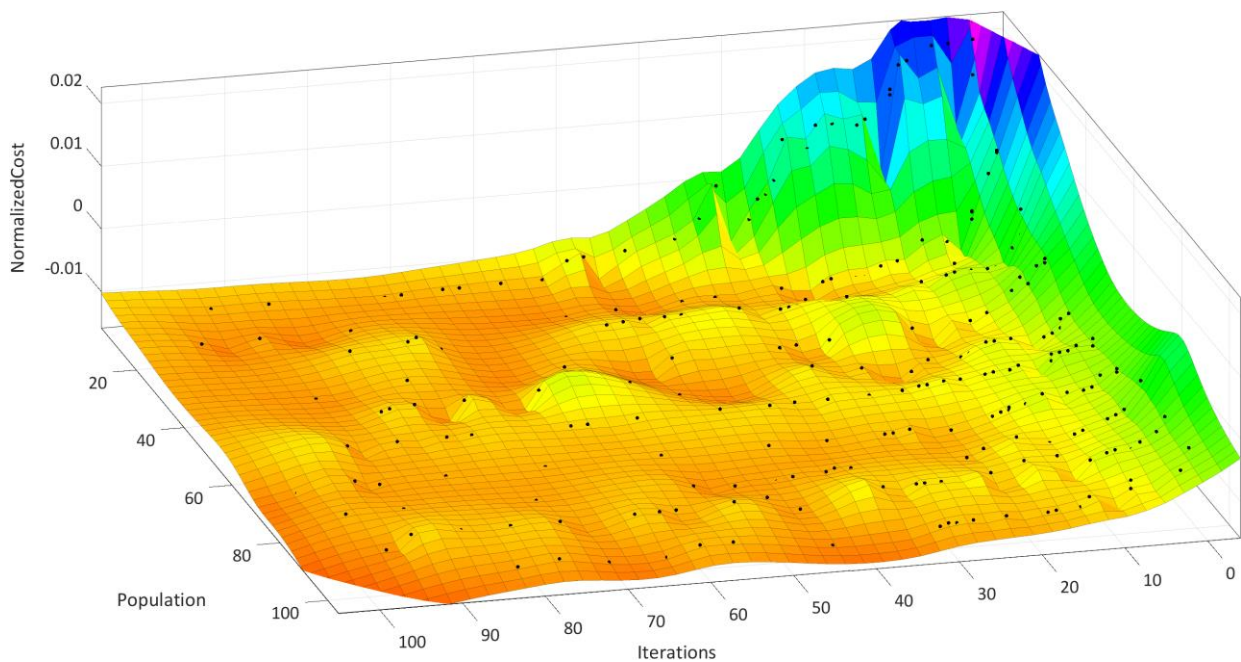


Figure 27 Convergence Characteristics of BCO with varying population sizes with 80 segments

5.5 Working of Ignite Rule-Based Parallel Hybrid Controller

The default controller from Ignite Powertrain library, called Parallel Hybrid Vehicle Controller comprises of control strategy elements which actuate the engine, electric motor and brakes depending on the driver input signals – corresponding to accelerator and brake pedal positions (0 – pedals not depressed, 1 – fully pressed pedals). The output control signals to the engine and motor correspond to the normalized power of engine ($P_e/P_{e_{max}}$) and motor ($P_{mg}/P_{mg_{max}}$) respectively. The friction brake demand is the mechanical brake force normalized to the maximum brake force (10 kN). The demand signals are quantified based on fuzzy logic strategies governing various hybrid modes (Section 2.4).

Table 13 Signals to the Ignite Rule-Based Controller

Inputs	Units	Outputs	Units
Vehicle velocity	[m/s]	Engine demand	[0 – 1]
Engine speed	[rpm]	Motor generator demand	[0 – 1]
Motor generator speed	[rpm]	Engine clutch engagement	0 or 1
Battery SoC	[0 – 1]	Friction brake demand	[0 – 1]
Driver acceleration demand	[0 – 1]		
Driver brake demand	[0 – 1]		
Maximum motor/generator torque	[Nm]		

5.5.1 Demand Split Strategy

The driver accelerator demand represents the traction power request normalised to the maximum available engine power. This strategy splits the power request between the engine and the electric motor using fuzzy logic. The input signals – battery SoC and driver accelerator demand are fuzzified as ramp functions shown in Figure 28. The resulting motor demand is limited by the product of the fuzzy outputs, each between [0 – 1].

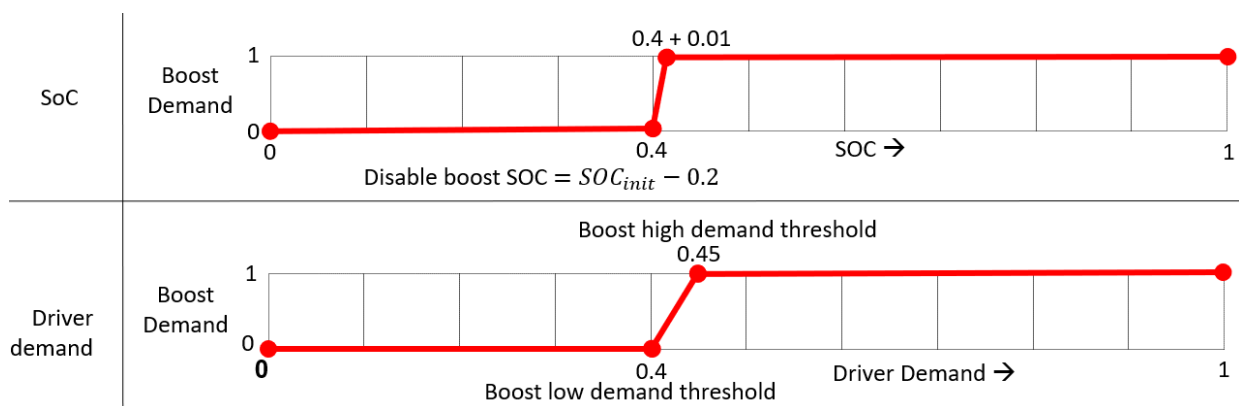


Figure 28 Demand split strategy of Ignite Rule-Based controller

5.5.2 Generation Strategy

Similar to the demand split strategy, this strategy generates a negative motor generator demand signal limited by factors of SoC, driver accelerator demand and engine speed as shown in Figure 29

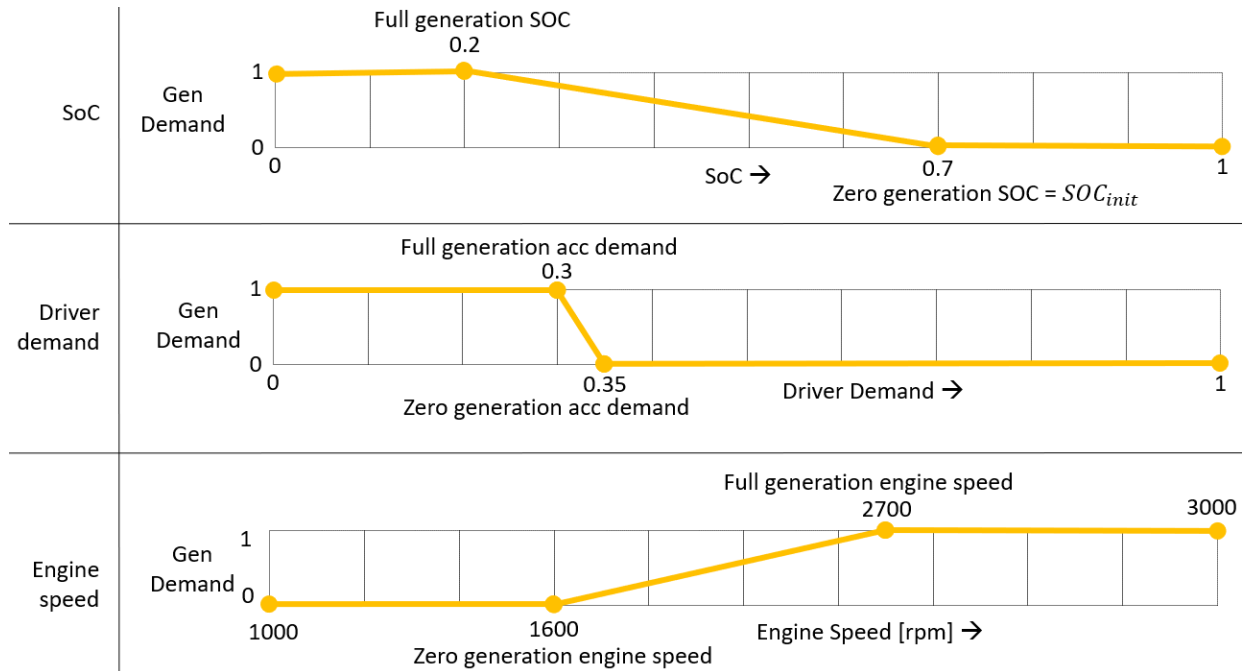


Figure 29 Generation strategy of Ignite Rule-Based controller

5.5.3 Regeneration Strategy

This follows Series regenerative braking strategy discussed in Section 2.4.1 and converts the driver brake demand to a corresponding braking torque on the generator limited by factors of SoC as shown in Figure 30. The brake power shortfall is compensated by the mechanical brakes as discussed in Section 5.3.3.

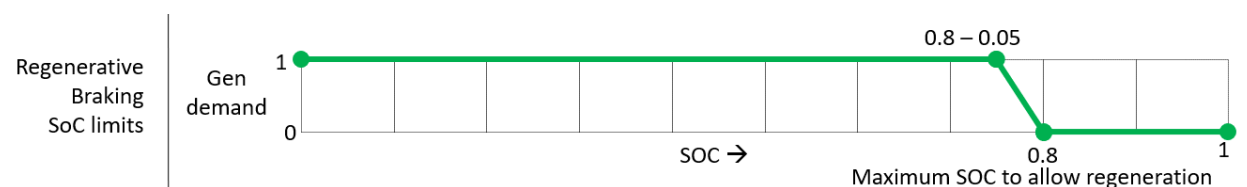


Figure 30 Regeneration strategy of Ignite Rule-Based controller

Besides the above strategies, the controller also features a Start-Stop strategy to switch off the engine in cases of low demand and stationary vehicle. And a Hybrid Clutch Control to disconnect the engine from the driveline during idling.

6 Results and Discussion

The results constitute the important characteristics of the vehicles in the MATLAB model, IGNITE model with new control strategy and IGNITE model with rule-based controller. A sweep of velocity and SoC parameters was performed as shown in Table 14, and the variant with the minimum fuel consumption is compared against rule-based controller in IGNITE. Appendix 11.9 shows a summary of the results for each variant (Plots of results in Attachments). The variant with a maximum velocity of 110 km/h was eliminated as it failed to climb a 8% grade road. The number of bees for generation was reduced to 20 since it is a simpler optimization task showing faster convergence.

Table 14 Velocity and SoC Parameter Combinations for different scenarios

Parameter	Units	Hill	Ascent	Valley	Descent
Variable Parameters					
v_{Entry}	[km/h]	70, 80, 90			
v_{Max}	[km/h]	90, 100			
SOC_{Init}	[%]	60, 70, 80		40, 50, 60	
Total combinations = $3(v_{Entry}) \times 2(v_{Max}) \times 3(SOC_{Init}) \times 4(scenarios) = 72$					
Constant / Dependent Parameters					
v_{Min}	[km/h]	50			
v_{Exit}	[km/h]	v_{Entry}			
SOC_{Min}	[%]	$SOC_{Init} - 0.2$	SOC_{Init}	$SOC_{Init} - 0.2$	$SOC_{Init} - 0.2$
SOC_{Max}	[%]	80			
Bee Colony Parameters					
$nPop$		50 – EV/Boost, 20 – Generation			
$maxIt$		50			
$Step$		0.01			

The results with the minimum fuel consumption are shown in Figure 31- Figure 34. The operating points of the engine with an indication of the gear and hybrid mode are also illustrated.

Scenario 1: Hill

Parameters summary:

xRes : 25 m
 No. of bees : 50, 20
 Iterations : 50
 Step : 0.01

V_{Entry} : 70 km/h
 V_{Max} : 90 km/h
 V_{Min} : 50 km/h
 V_{Exit} : 70 km/h

SOC_{Initial} : 70 %
 SOC_{Min} : 50 %
 SOC_{Max} : 80 %

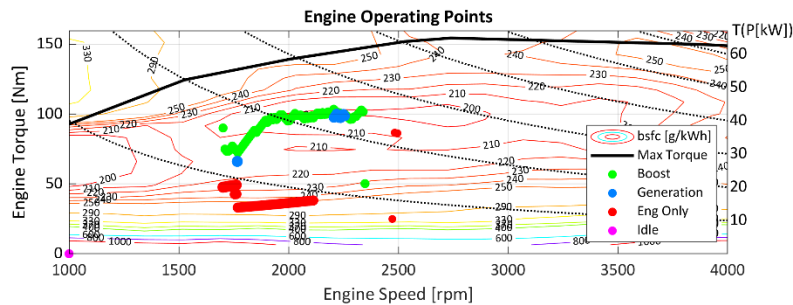
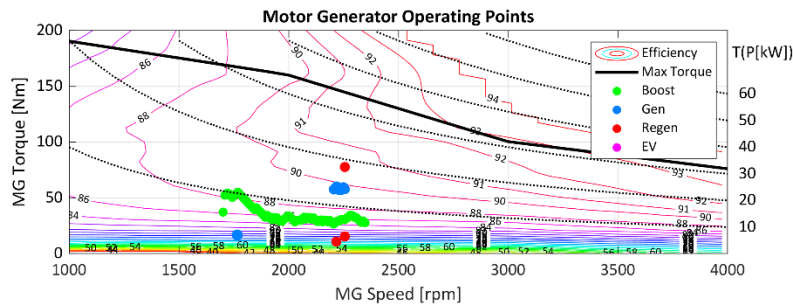
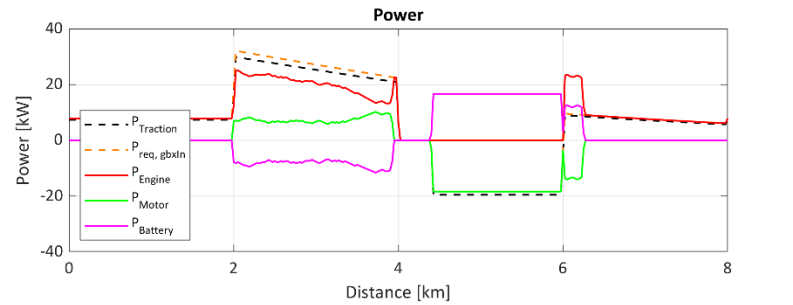
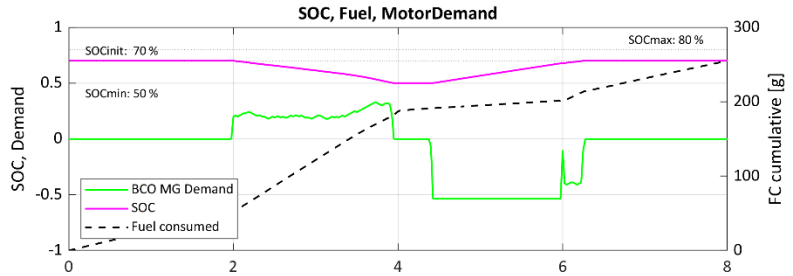
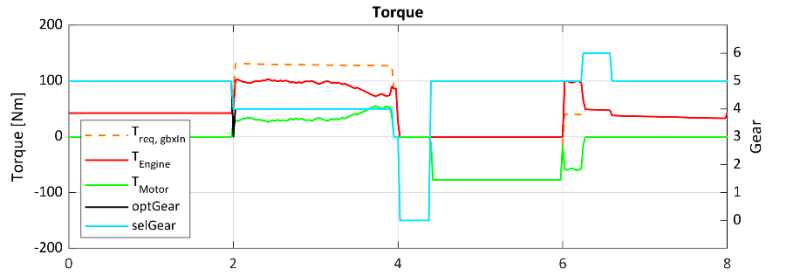
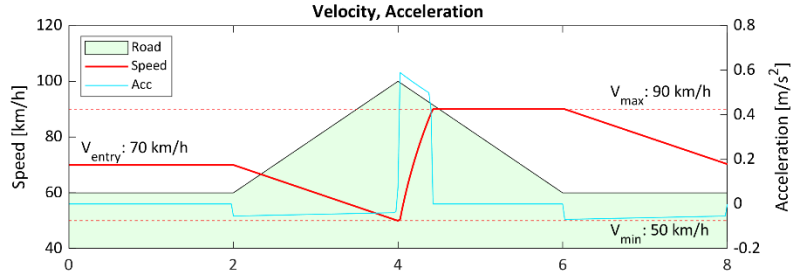
Results summary:

SOC_{endBoost} : 50 %
 SOC_{endRegen} : 67.99 %
 SOC_{exit} : 70 %
 dSOC : 0.00 %

E_{boost} : 279.9 W-h
 E_{regen} : 251.8 W-h
 E_{toGen} : 28.1 W-h
 E_{gen} : 28.1 W-h
 E_{elec,net} : 0.0 W-h

FC_{flat} : 52.43 g
 FC_{ascent} : 134.52 g
 FC_{descent} : 14.65 g
 FC_{flat} : 53.27 g
 FC_{exit} : 254.87 g

t_{end} : 399.25 s
 Simulation Time
 t_{abc-boost} : 47.8 s
 t_{abc-gen} : 15.3 s
 t_{sim,total} : 80.5 s



**Size of dots is proportional to degree of gear

Figure 31 Results of MATLAB model, Scenario 1: Hill

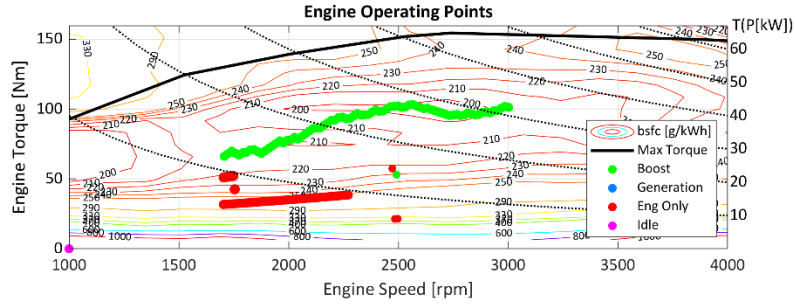
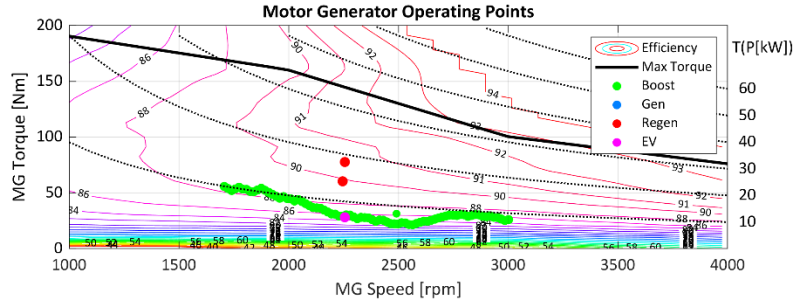
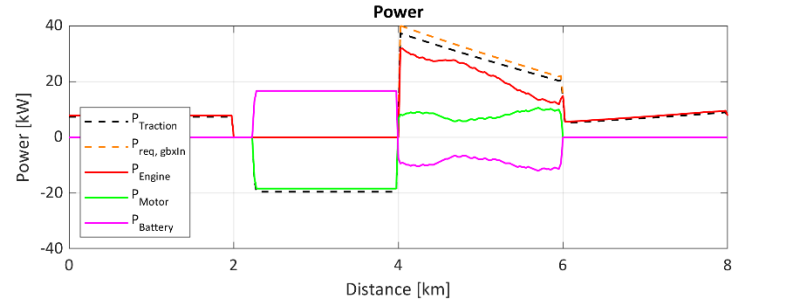
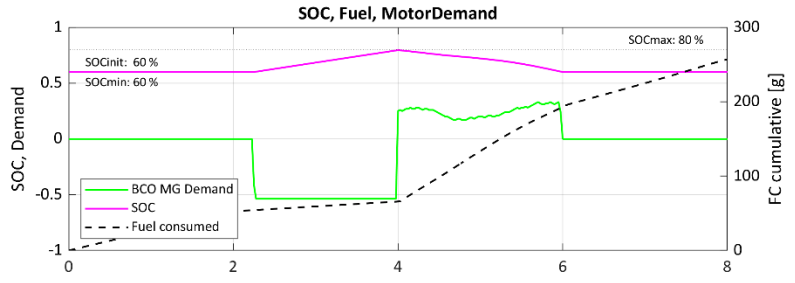
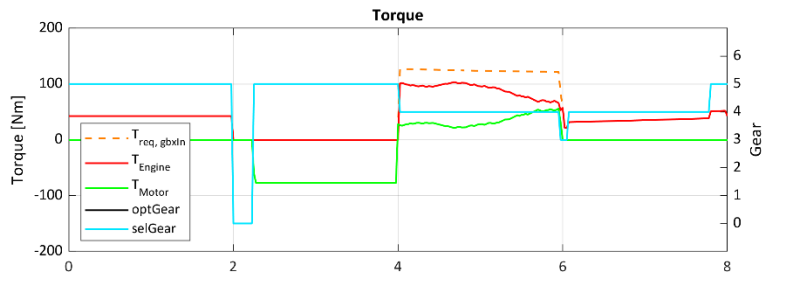
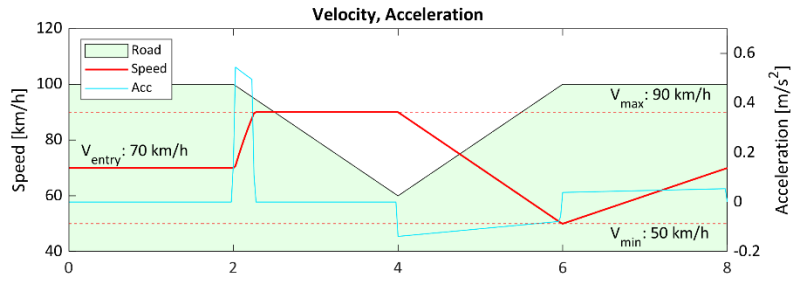
Scenario 2: Valley

Parameters summary:

xRes	: 25 m
No. of bees	: 50
Iterations	: 50
Step	: 0.01
V _{Entry}	: 70 km/h
V _{Max}	: 90 km/h
V _{Min}	: 50 km/h
V _{Exit}	: 70 km/h
SOC _{Initial}	: 60 %
SOC _{Min}	: 60 %
SOC _{Max}	: 80 %

Results summary:

SOC _{endRegen}	: 79.55 %
SOC _{endBoost}	: 60.01 %
SOC _{exit}	: 60.01 %
dSOC	: -0.01 %
E _{regen}	: 273.7 W-h
E _{boost}	: 273.6 W-h
E _{toGen}	: 0.0 W-h
E _{gen}	: 0.0 W-h
E _{elec,net}	: 0.0 W-h
FC _{flat}	: 52.43 g
FC _{descent}	: 13.34 g
FC _{ascent}	: 127.29 g
FC _{flat}	: 63.96 g
FC _{exit}	: 257.02 g
t _{end}	: 411.27 s
Simulation Time	
t _{abc-boost}	: 45.2 s
t _{abc-gen}	: 0.0 s
t _{sim,total}	: 56.6 s



**Size of dots is proportional to degree of gear

Figure 32 Results of MATLAB model, Scenario 2: Valley

Scenario 3: Ascent

Parameters summary:

xRes : 25 m
 No. of bees : 50, 20
 Iterations : 50
 Step : 0.01

 V_{Entry} : 70 km/h
 V_{Max} : 90 km/h
 V_{Min} : 50 km/h
 V_{Exit} : 70 km/h

 SOC_{Initial} : 60 %
 SOC_{Min} : 40 %
 SOC_{Max} : 80 %

Results summary:

SOC_{endBoost} : 40.01 %
 SOC_{exit} : 60 %
 dSOC : 0.00 %

 E_{boost} : 279.9 W-h
 E_{toGen} : 279.9 W-h
 E_{gen} : 279.9 W-h
 $E_{elec,net}$: 0.0 W-h

 FC_{flat} : 52.43 g
 FC_{ascent} : 135.78 g
 FC_{flat} : 176.25 g
 FC_{exit} : 364.47 g

 t_{end} : 466.30 s

 Simulation Time
 $t_{abc,boost}$: 39.6 s
 $t_{abc,gen}$: 27.8 s
 $t_{sim,total}$: 84.5 s

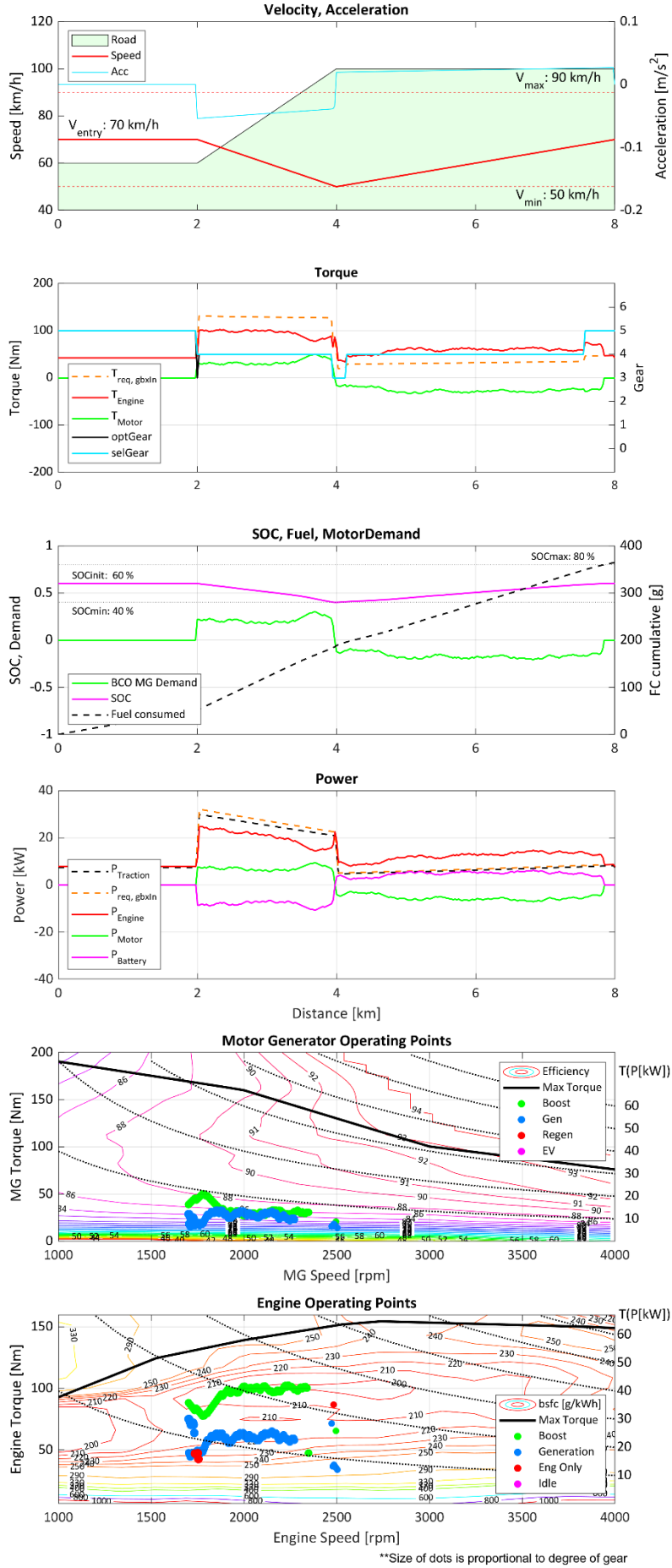


Figure 33 Results of MATLAB model, Scenario 3: Ascent only

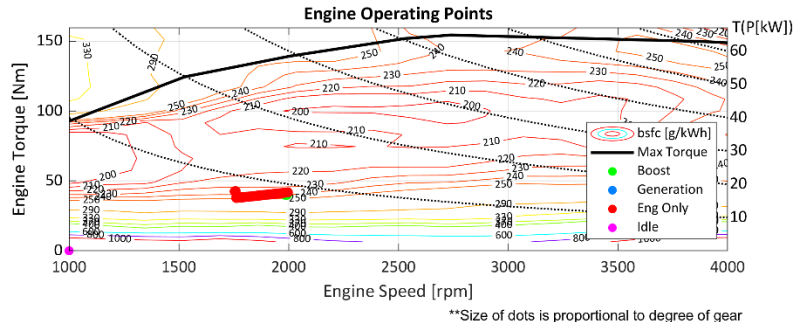
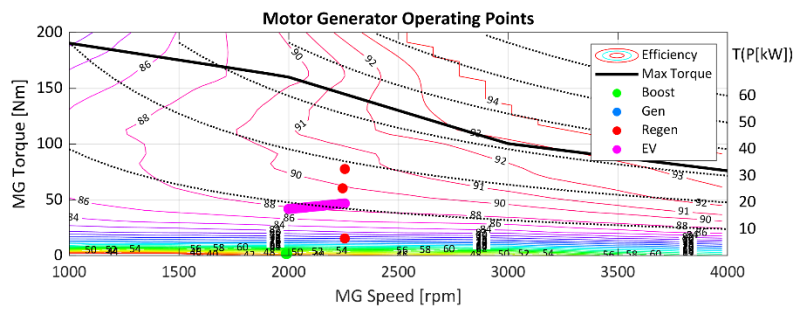
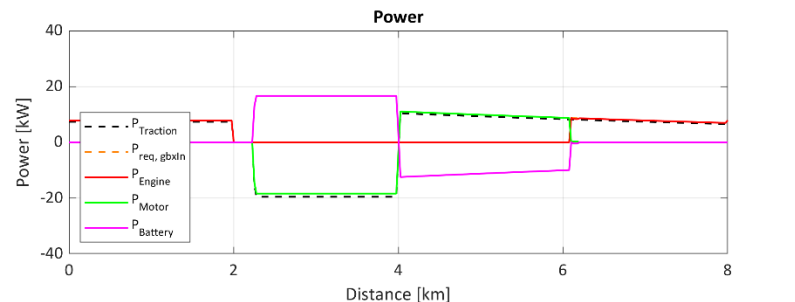
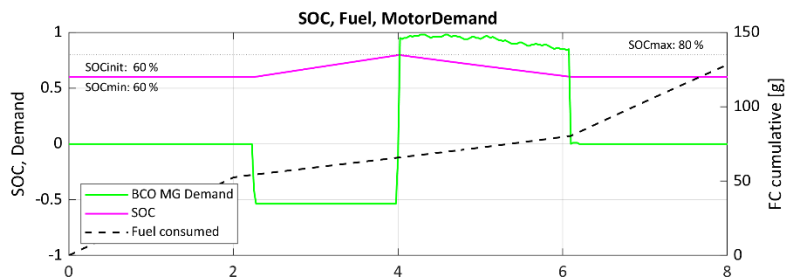
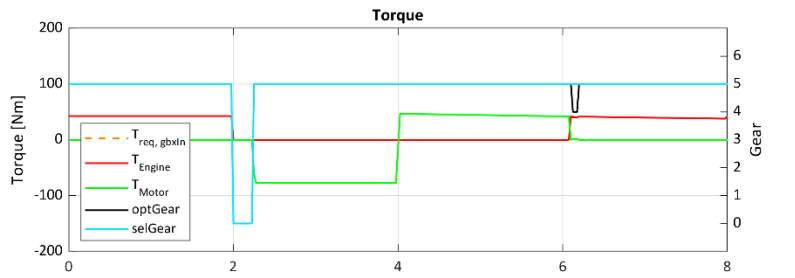
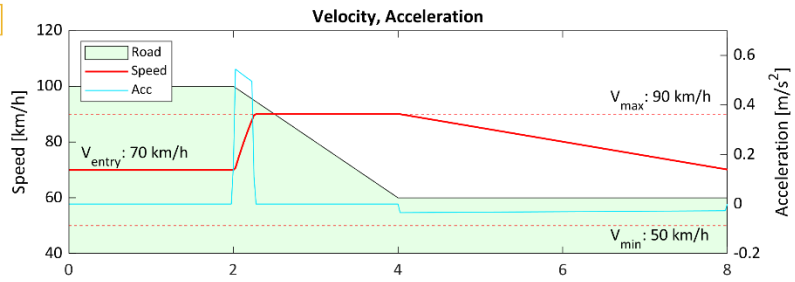
Scenario 4: Descent

Parameters summary:

xRes	: 25 m
No. of bees	: 50
Iterations	: 50
Step	: 0.01
V _{Entry}	: 70 km/h
V _{Max}	: 90 km/h
V _{Min}	: 50 km/h
V _{Exit}	: 70 km/h
SOC _{Initial}	: 60 %
SOC _{Min}	: 60 %
SOC _{Max}	: 80 %

Results summary:

SOC _{endRegen}	: 79.55 %
SOC _{exit}	: 60.09 %
dSOC	: -0.09 %
E _{regen}	: 273.7 W-h
E _{toGen}	: 0.0 W-h
E _{gen}	: 0.0 W-h
E _{elec_{net}}	: 0.0 W-h
FC _{flat}	: 52.43 g
FC _{descent}	: 13.34 g
FC _{flat}	: 62.43 g
FC _{exit}	: 128.20 g
t _{end}	: 364.86 s
Simulation Time	
t _{abc-boost}	: 80.3 s
t _{abc-gen}	: 0.0 s
t _{sim,total}	: 94.0 s



**Size of dots is proportional to degree of gear

Figure 34 Results of MATLAB model, Scenario 4: Descent only

6.1 MATLAB Model with novel control strategy

The ABC algorithm showed good response to the velocity profile with an even distribution of electric power for the entire section of the climb and increasing the EV assist towards the end of the ascent where the velocity is low, and it is a known fact that electric drive is most efficient at low speeds. The shift strategy worked well to prevent unwanted shifts and almost always selected the optimal gear.

In general, the key takeaways from the results are the following:

- The bee colony optimized power distribution algorithm effectively shifts load between the engine and the motor while responding to the velocity and terrain changes. Thus, a given pool of SoC, in this case 0.2 is always effectively distributed across an entire EV assist phase, especially in scenarios 1 and 2.
- For scenario 4, it was required to spend the SoC gained by regeneration on the downhill, by using EV assist on the flat section. This resulted in a pure electric drive till the SoC was depleted. Though the engine is in region of relatively low efficiency, the motor efficiency is reasonably good.
- Engine operating points are close to maximum efficiency region in all cases of EV assist which is a direct indicator of improved fuel consumption. This proves the effectiveness of the bee algorithm trying to minimize fuel consumption, which is a consequence of high engine efficiency.
- Generator phase is usually in high efficiency region where it is optimally applied from a heuristic standpoint. This is seen in the case of generation applied during a deceleration event after the end of a descent (Figure 31) where it pushes the engine into more efficient region. On the other hand, when applied to an acceleration event, like after the end of ascent on a flat road (Figure 33), generation led to a fall in engine efficiency.
- Motor phase is not always in region of good efficiency which is a result of the shifting strategy considering the overall system efficiency. The cost function for motor demand evaluation within the bee colony algorithm for EV assist comprises only of the engine fuel consumption. Moreover, it is impossible to have both the engine and motor operating at the region of maximum efficiency at the same time. A possible option to improve motor efficiency is addition of motor efficiency to the cost function with suitable weights to consider the trade-off between the efficiency lost on part of engine to gain efficiency on the motor side.

6.2 Validation of MATLAB vehicle model with IGNITE

The Matlab black box model (Section 5.3) was simulated along the route defined in Section 5.1 with drive cycles defined in Section 5.2 and results compared with simulation results of the IGNITE vehicle model with the new control strategy. All variables being calculated in the black box model were found to have good correlation within 1% of the IGNITE vehicle, despite using a calculation time interval of 25 m (= 1 seconds time step at 90 km/h), whereas IGNITE uses a 0.1 s time step. The small deviation in velocity (< 1km/h) can be due to various reasons, a few being response delay of the driver PI controller, inertia, stiffness and damping of the driveline components and the associated losses all of which are neglected within the MATLAB model. The deviation in SoC is due to the response delay of the motor to the controller signal and hysteresis. Besides these small deviations, the vehicle models in Ignite and Matlab are equivalent enough for a valid comparison to be made between control strategies applied to either models.

6.3 Comparison of results of new control strategy with Rule-Based controller in IGNITE

The Rule-Based controller in IGNITE was initially optimized in HEEDS MDO by my supervisor Ing. Cvetkovic to optimize equivalent fuel consumption for WLTC class 2. The rule-based controller always follows a fixed set of rules irrespective of the drive cycle and terrain. This makes it difficult to establish an ideal rule-based controller. However, even with a few forced parameters, the characteristics of a rule-based controller remain the same and can be very well compared with other control strategies. But since the scenarios being considered are much different from standard drive cycles, hence some parameters in the Rule-Based controllers had to be set accordingly for the results to be comparable. In order to directly compare the total fuel consumption values at the end of each scenario, the SoC values at the beginning and end must be equal ($\Delta SoC = 0$), indicating no net electric energy transfer.

Following changes were made to the Rule-Based controller parameters to achieve $\Delta SoC = 0$:

- Upper limit of SOC for generation was set to be the initial SoC to balance the SoC
- Engine speed limits for generation were reduced to allow generation in Scenario 3
- Driver demand limits for boost were reduced for Scenario 4 to allow boost after regeneration to reduce the SoC to initial SoC

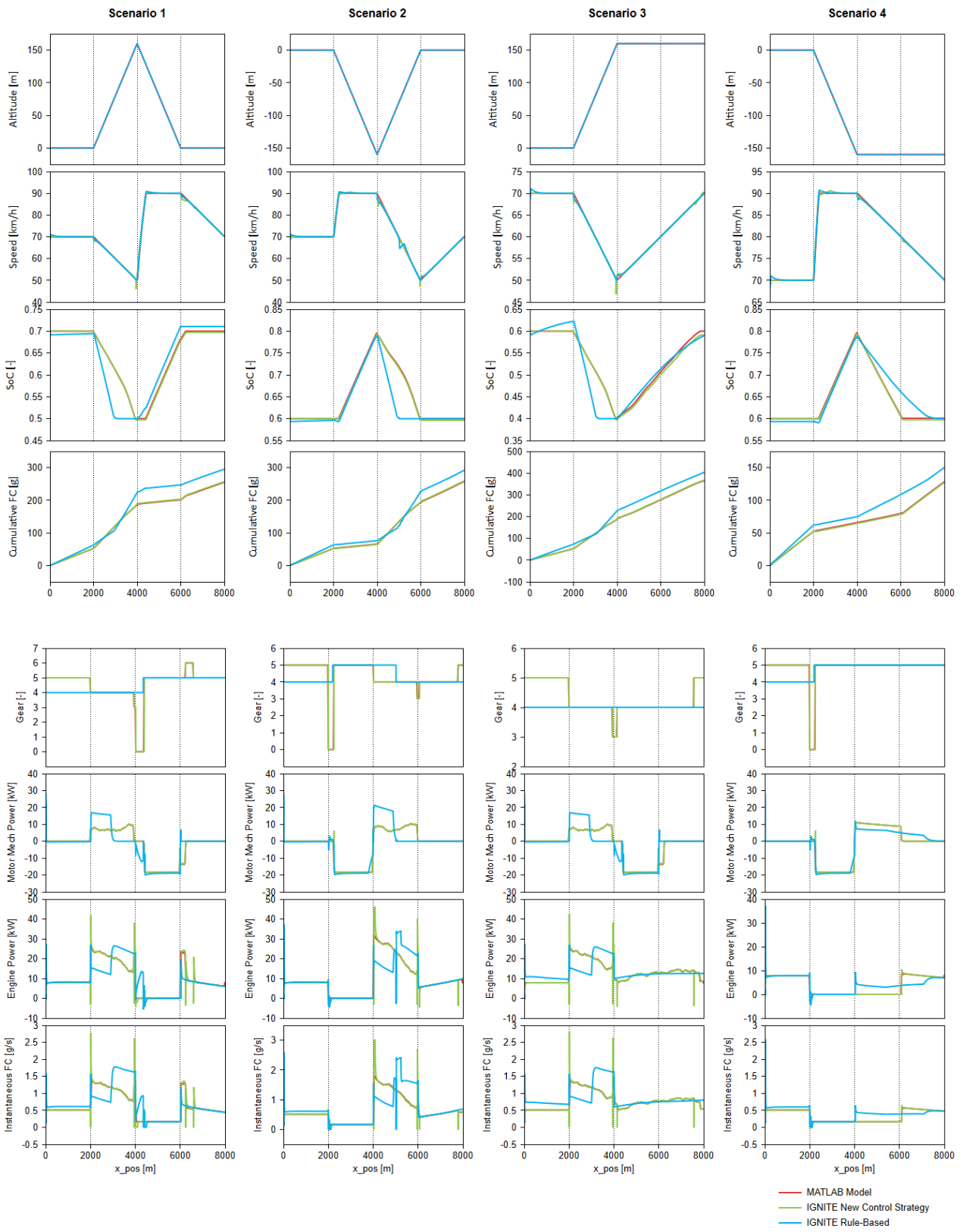


Figure 35 Comparison of results of new control strategy with IGNITE rule-based controller

Table 15 Comparison of results of fuel consumption and SoC for different models and scenarios

	MATLAB model with new controller	IGNITE model with new controller	IGNITE model with Rule-Based controller	% Difference
Scenario 1	(a)	(b)	(c)	(c-b)/c [%]
SOC_{Final}	0.7	0.697	0.706	1.27
<i>Cumulative FC</i> [g]	254.9	256.8	295	13
Scenario 2				
SOC_{Final}	0.6	0.596	0.6	0.67
<i>Cumulative FC</i> [g]	257	258.9	291.8	11.3
Scenario 3				
SOC_{Final}	0.6	0.59	0.59	0
<i>Cumulative FC</i> [g]	364.5	366.6	403.4	9.1
Scenario 4				
SOC_{Final}	0.6	0.597	0.6	0.5
<i>Cumulative FC</i> [g]	128.2	127	150	15

The rule-based controller unaware of the length of the ascent depletes the available SoC midway through the climb thus increasing the demand on the engine and hence steep rise in fuel consumption. During the descent immediately after the ascent, it generates for a short time before coasting. Generation is caused by low SoC and low engine demand. This is also visible for an ascent only scenario where it cannot avoid generation in the initial flat section.

For a descent only scenario, the rule-based controller does not boost immediately after the descent since the traction power is lower than the boost threshold. Lowering the threshold causes it to boost though with progressively decreasing demand because of the dependence on the SoC.

Compared to other scenarios, the fuel savings are meagre for scenario 3, because of aggressive generation implied during an acceleration event to increase the SoC. The fuel economy improvement in all other scenarios proves that even if not essential, if there is a requirement for boost, it is always optimal for the bee algorithm compared to the rule-based controller.

7 Conclusion

The first part of the thesis dealt with an overview of hybrid vehicles and control strategies and shortlisting of candidate hybrid vehicles, of which the 2020 Hyundai Ioniq was the most relevant as well as recent, for which I could find all the data. The second part was mostly about building the vehicle models in Ignite and Matlab from available data and theory followed by the formulation and implementation of a novel control strategy using the Matlab black box model. I created Matlab functions and scripts (Appendix 12) to implement the control strategies and scenarios (Section 5), throughout which I was guided by my supervisors Ing. Josef Morkus and Ing. Milan Cvetkovic, especially during design of the shift strategy and avoiding shift oscillations and design of scenarios. I created the flowcharts in Section 5.3 and 5.4 to represent the control flow and calculations involved in the Matlab programs, which were consistently improved with every consultation.

Another task was to explore the real-time predictive implementation potential and optimality of a custom artificial bee colony algorithm to optimize power distribution between the engine and motor during a hill climb journey using eHorizon road slope information. The Matlab code implementation of the bee algorithm, was done with the help of Ing. Cvetkovic and colleagues from TU Belgrade, Marko Stokić and Nemanja Mijovic. To equalize the initial and final SoC, I used a simple modification of the bee algorithm as generation strategy, which though not optimal in terms of fuel consumption, yet achieved the SoC target, sometimes even improving fuel consumption and engine efficiency.

The MATLAB vehicle model is capable to be used as a black box model for optimization algorithms and the key gain is its computational speed and accuracy. The artificial bee colony algorithm matches its expectations of reaching quite fast and precise global optimum. Its dependence on the cost function shows that with a well-tuned cost function, the efficiency of the overall system (Engine-Motor-Battery) can be improved.

The proposed control algorithm has better predictive abilities compared to the causal strategy of conventional rule-based controller and results in a more even distribution of power compared to the lumped distribution of the rule-based. The rule-based strategies are highly sensitive to the vehicle and control parameters and finding the optimal rule-based parameters specific to the discussed scenarios requires a research of its own. Nonetheless, the basic characteristics of any rule-based controller stay the same, thus allowing results to be compared.

The attachments (Appendix 12) also contain several autorun scripts to perform simulation, plot results and export outputs as spreadsheets for a sweep of parameters for bee colony optimization (population, iteration) and scenarios (velocity, SoC).

Overall, the goal of minimizing fuel consumption was achieved with the proposed control algorithm, though sometimes at the expense of low efficiency in other components, particularly the motor generator. This is clearly because of the single objective attribute of the optimization problem and imposition of certain hard constraints, such as forcing generation and boost to equalize the SoC.

7.1 Possible continuation of the thesis

A possible continuation of work would be a simultaneous optimization of the vehicle trajectory together with optimum power distribution, which would require trade-off calculation between speed and time [40], since trip time and fuel consumption are conflicting objectives.

It would be also possible to improve the generation strategy to minimize fuel consumption together with achieving target SoC. The shift strategy can be further optimized by its addition to the bee colony cost function.

Addition of variables to the cost function translates to addition of dimensions to the bee colony search space, which will test the performance of the bee colony optimization over multiple dimensions and objectives.

The Matlab black box model can be parameterized to represent any parallel hybrid vehicle and prove a useful tool for testing other optimization algorithms.

8 Bibliography

- [1] European Commission, “Statistical Pocketbook 2019: EU transport,” 2019. .
- [2] “EV, Hybrid and Traditional Car | NewMotion | NewMotion.”
<https://newmotion.com/en/knowledge-center/news-and-updates/comparisons-between-an-electric-car-a-hybrid-car-and-a-traditional-car> (accessed Dec. 26, 2020).
- [3] “Five trends transforming the Automotive Industry.” [Online]. Available:
www.pwc.com/auto.
- [4] R. Varnhagen, “Electronic Horizon: A Map as a Sensor and Predictive Control,” in *SAE Technical Papers*, Aug. 2017, vol. 2017-Augus, no. August, doi: 10.4271/2017-01-1945.
- [5] “Hybrid vehicle drivetrain.” https://en.wikipedia.org/wiki/Hybrid_vehicle_drivetrain (accessed Jul. 19, 2020).
- [6] “Graphical description of the five hybridization schemes from P0 to P5,... | Download Scientific Diagram.” https://www.researchgate.net/figure/Graphical-description-of-the-five-hybridization-schemes-from-P0-to-P5-considering-the_fig1_329788832 (accessed Dec. 31, 2020).
- [7] S. Onori, L. Serrao, and G. Rizzoni, *Hybrid electric vehicles: Energy management strategies*, no. 9781447167792. 2016.
- [8] *Cost, effectiveness, and deployment of fuel economy technologies for light-duty vehicles*. National Academies Press, 2015.
- [9] “2020 Hyundai Ioniq Hybrid (104 kW / 141 PS / 139 hp) (for Europe) specs review.” https://www.automobile-catalog.com/car/2020/2909180/hyundai_ioniq_hybrid.html (accessed Dec. 27, 2020).
- [10] “Hybrid Electric Vehicle P2 Reference Application.”
<https://www.mathworks.com/help/autoblks/ug/explore-the-hybrid-electric-vehicle-p2-reference-application.html>.
- [11] J. M. Miller, *Propulsion systems for hybrid vehicles, 2nd edition*. 2010.
- [12] “Developing HEV Control Systems - YouTube.”
<https://www.youtube.com/watch?v=IAFeCqhal3o> (accessed Dec. 31, 2020).
- [13] D.-D. D. Tran, M. Vafaeipour, M. el Baghdadi, R. Barrero, J. van Mierlo, and O. Hegazy, “Thorough state-of-the-art analysis of electric and hybrid vehicle powertrains: Topologies and integrated energy management strategies,” *Renewable and Sustainable Energy Reviews*, vol. 119, p. 109596, 2020, doi: 10.1016/j.rser.2019.109596.
- [14] T. J. Bohme and B. Frank, *Hybrid Systems, Optimal Control and Hybrid Vehicles, Advances in Industrial Control*. 2017.
- [15] A. Rezaei, J. B. Burl, B. Zhou, and M. Rezaei, “A New Real-Time Optimal Energy Management Strategy for Parallel Hybrid Electric Vehicles,” *IEEE Transactions on Control Systems Technology*, vol. 27, no. 2, pp. 830–837, 2019, doi: 10.1109/TCST.2017.2775184.

- [16] M. Cvetković and I. Dmitry Rozhdestvenskiy Doc Cristina Olaverri Monreal, "CZECH TECHNICAL UNIVERSITY IN PRAGUE FACULTY OF TRANSPORTATION SCIENCES DEPARTMENT OF TRANSPORT TELEMATICS Real-Time Driver Advisory System for Fuel Economy based on the ADASIS data," *České vysoké učení technické v Praze. Vypočetní a informační centrum.*, Jan. 2018. Accessed: Dec. 31, 2020. [Online]. Available: <https://dspace.cvut.cz/handle/10467/74399>.
- [17] "Final report on Fuel Consumption and Emission reduction evaluation D6.2 Final report on Fuel Consumption and Emission reduction evaluation," 2019. Accessed: Dec. 31, 2020. [Online]. Available: www.imperium-project.eu.
- [18] G. Milton, "Prediction of potential benefits with IMPERIUM technology; Prediction of potential benefits with IMPERIUM technology," 2018. [Online]. Available: www.imperium-project.eu.
- [19] E. Armengaud *et al.*, "IMPERIUM-Implementation of Powertrain Control for Economic and Clean Real driving emLssion and fuel ConsUMption," 2018. [Online]. Available: <https://www.researchgate.net/publication/332719555>.
- [20] C. Bacher, "Metaheuristic optimization of electro-hybrid powertrains using machine learning techniques," *Ads.Tuwien.Ac.At*, vol. 2013, 2013, [Online]. Available: https://www.ads.tuwien.ac.at/publications/bib/pdf/bacher_13.pdf%5Cnhttp://publik.tuwien.ac.at/files/PubDat_221212.pdf.
- [21] T. Apitzsch, C. Klöffler, P. Jochem, M. Doppelbauer, and W. Fichtner, "Metaheuristics for online drive train efficiency optimization in electric vehicles," *Working Paper Series in Production and Energy*, 2016, doi: 10.5445/IR/1000063608.
- [22] P. Zhang, F. Yan, and C. Du, "A comprehensive analysis of energy management strategies for hybrid electric vehicles based on bibliometrics," *Renewable and Sustainable Energy Reviews*, vol. 48, pp. 88–104, 2015, doi: <https://doi.org/10.1016/j.rser.2015.03.093>.
- [23] "File:ParticleSwarmArrowsAnimation.gif - Wikipedia." <https://en.wikipedia.org/wiki/File:ParticleSwarmArrowsAnimation.gif> (accessed Dec. 31, 2020).
- [24] "Origin: Data Analysis and Graphing Software." <https://www.originlab.com/index.aspx?go=PRODUCTS/Origin> (accessed Dec. 27, 2020).
- [25] "Help Online - Origin Help - XYZ Gridding Methods." <https://www.originlab.com/doc/Origin-Help/XYZGridding-Method> (accessed Dec. 27, 2020).
- [26] W. Lee *et al.*, "Control analysis of a real-world P2 hybrid electric vehicle based on test data," *Energies*, vol. 13, no. 15, pp. 1–14, 2020, doi: 10.3390/en13164092.
- [27] "Help Online - Origin Help - Digitizer." <https://www.originlab.com/doc/Origin-Help/Tool-Digitizer> (accessed Dec. 27, 2020).
- [28] "Tyre overall rolling diameter." <https://www.errolstyres.co.za/content/tyre-overall-rolling-diameter> (accessed Dec. 27, 2020).

- [29] "Fuels - Higher and Lower Calorific Values."
https://www.engineeringtoolbox.com/fuels-higher-calorific-values-d_169.html
 (accessed Jan. 01, 2021).
- [30] T. Burress, "Benchmarking of Competitive Technologies," 2012. Accessed: Dec. 27, 2020. [Online].
- [31] T. Gray, M. Shirk, and J. Wishart, "2011 Hyundai Sonata 3539-Hybrid Electric Vehicle Battery Test Results," 2010. Accessed: Dec. 27, 2020. [Online].
- [32] "Optimal Driving Strategies for Minimizing Fuel Consumption and Travelling Time."
 Accessed: Dec. 29, 2020. [Online]. Available: www.kth.se/sci.
- [33] H. Y. Hwang and J. S. Chen, "Optimized fuel economy control of power-split hybrid electric vehicle with particle swarm optimization," *Energies*, vol. 13, no. 9, 2020, doi: 10.3390/en13092278.
- [34] C. Desai and S. S. Williamson, "Particle swarm optimization for efficient selection of hybrid electric vehicle design parameters," in *2010 IEEE Energy Conversion Congress and Exposition, ECCE 2010 - Proceedings*, 2010, pp. 1623–1628, doi: 10.1109/ECCE.2010.5618098.
- [35] Y. H. Cheng, C. M. Lai, and J. Teh, "Application of particle swarm optimization to design control strategy parameters of parallel hybrid electric vehicle with fuel economy and low emission," *Proceedings - 2018 International Symposium on Computer, Consumer and Control, IS3C 2018*, pp. 342–345, 2019, doi: 10.1109/IS3C.2018.00093.
- [36] Z. Chen, R. Xiong, and J. Cao, "Particle swarm optimization-based optimal power management of plug-in hybrid electric vehicles considering uncertain driving conditions," *Energy*, vol. 96, pp. 197–208, Feb. 2016, doi: 10.1016/j.energy.2015.12.071.
- [37] "Artificial Bee Colony Optimization - File Exchange - MATLAB Central."
<https://www.mathworks.com/matlabcentral/fileexchange/74122-artificial-bee-colony-optimization>
 (accessed Jul. 19, 2020).
- [38] D. Teodorović, "Bee colony optimization (BCO)," in *Studies in Computational Intelligence*, vol. 248, Springer, Berlin, Heidelberg, 2009, pp. 39–60.
- [39] "Genetic Algorithms - Parent Selection - Tutorialspoint."
https://www.tutorialspoint.com/genetic_algorithms/genetic_algorithms_parent_selection.htm
 (accessed Jan. 01, 2021).
- [40] M. Held, *Optimal Speed and Powertrain Control of a Heavy-Duty Vehicle in Urban Driving*. .
- [41] P. Holcner, "VYSOKÉ UENÍ TECHNICKÉ V BRN FAKULTA STAVEBNÍ POZEMNÍ KOMUNIKACE I. MODUL BM01-M01 TRASA POZEMNÍCH KOMUNIKACÍ STUDIJNÍ OPORY PRO STUDIJNÍ PROGRAMY S KOMBINOVANOU FORMOU STUDIA." Accessed: Jan. 06, 2021. [Online].

9 List of Figures

- Figure 1 Topology of various HEV architectures [5] 6
- Figure 2 Topology and features of Parallel HEV configurations based on position of electric machine [6]..... 8
- Figure 3 Various hybridization degrees with increasing electrification [7] 9
- Figure 4 Topology of a P2 Parallel Hybrid Electric Vehicle [10]..... 9
- Figure 5 Regenerative Braking Strategies [11]..... 11
- Figure 6 HEV Control Architecture [12] 12
- Figure 7 Classification of Energy Management Strategies [13] 13
- Figure 8 Simulation of a particle swarm searching for global optimum of a solution [23]..... 17
- Figure 9 Digitized Engine BSFC map of Ioniq Hybrid [26]..... 20
- Figure 10 Combined Motor Inverter Efficiency Map (motor regime) of Sonata Hybrid [30]..... 21
- Figure 11 Battery characteristics of Hyundai Sonata Hybrid [31] 22
- Figure 12 Equivalent Circuit diagram of battery electric model with battery losses (not to scale)..... 23
- Figure 13 Longitudinal Vehicle Dynamics Model 25
- Figure 14 IGNITE Vehicle Model with Default Rule-Based Controller..... 28
- Figure 15 Velocity Profiles for Various Scenarios of Hilly Terrains 30
- Figure 16 Representation of segments, nodes and x coordinates..... 32
- Figure 17 Overall scheme of Black Box Vehicle Function 33
- Figure 18 Traction power calculation flowchart 34
- Figure 19 Optimal Gear Selection Flowchart..... 37
- Figure 20 Optimal Gear Shift Inhibit Flowchart..... 38
- Figure 21 Power Distribution Flowchart for Hybrid Mode and Motor Generator Mechanical Power 39
- Figure 22 Power Distribution Flowchart for Engine State and Mechanical Power 40
- Figure 23 Control Strategies for various scenarios of hilly terrain 41
- Figure 24 Representation of bees searching the solution space across segments for the global optimum..... 42
- Figure 25 Artificial Bee Colony Flowchart for Optimum Power distribution in EV/Boost Mode 45
- Figure 26 Convergence characteristics of ABC -REPLACE..... 48
- Figure 27 Convergence Characteristics of BCO with varying population sizes with 80 segments..... 49
- Figure 28 Demand split strategy of Ignite Rule-Based controller..... 50
- Figure 29 Generation strategy of Ignite Rule-Based controller..... 51
- Figure 30 Regeneration strategy of Ignite Rule-Based controller 51
- Figure 31 Results of MATLAB model, Scenario 1: Hill..... 53
- Figure 32 Results of MATLAB model, Scenario 2: Valley 54
- Figure 33 Results of MATLAB model, Scenario 3: Ascent only 55
- Figure 34 Results of MATLAB model, Scenario 4: Descent only 56
- Figure 35 Comparison of results of new control strategy with IGNITE rule-based controller 59
- Figure 36 Source Image of 2020 Ioniq Hybrid Engine BSFC Map [26]..... 68
- Figure 37 Fuelling Rate Map of 2020 Ioniq Hybrid extended till friction torque 68
- Figure 38 Source Image of 2011 Hyundai Sonata Combined Motor Inverter Efficiency Map [30]..... 69
- Figure 39 Open Circuit Voltage v/s SOC Characteristics of 2011 Hyundai Sonata Hybrid Battery [31]..... 70
- Figure 40 Charging Internal Resistance v/s SOC of 2011 Hyundai Sonata Hybrid Battery [31] 70
- Figure 41 Charging Internal Resistance v/s SOC of 2011 Hyundai Sonata Hybrid Battery [31] 70
- Figure 42 Ignite Vehicle Model with new controller..... 72

10 List of Tables

<i>Table 1 Attributes of eHorizon data as per ADASIS v2.x protocol [17]</i>	16
<i>Table 2 Vehicle Parameters: Hyundai Ioniq Hybrid [9]</i>	18
<i>Table 3 Comparison of Electrical system of Ioniq Hybrid and Sonata Hybrid</i>	20
<i>Table 4 High Voltage Lithium-ion Battery Specifications</i>	22
<i>Table 5 Transmission specifications of Hyundai Ioniq Hybrid [9]</i>	25
<i>Table 6 Environment parameters for the vehicle</i>	26
<i>Table 7 Drive Cycle Parameters</i>	29
<i>Table 8 Horizon parameters</i>	31
<i>Table 9 List of inputs and Outputs for black box vehicle model</i>	32
<i>Table 10 Optimal gear initialization table</i>	36
<i>Table 11 Results of brute-force search for optimum motor demand during hill climb</i>	47
<i>Table 12 Comparison of Bee Colony Optimization with Brute Force Search Results</i>	49
<i>Table 13 Signals to the Ignite Rule-Based Controller</i>	50
<i>Table 14 Velocity and SoC Parameter Combinations for different scenarios</i>	52
<i>Table 15 Comparison of results of fuel consumption and SoC for different models and scenarios</i>	60
<i>Table 16 Comparison of battery parameters of Ioniq and Sonata Hybrid</i>	69
<i>Table 17 Test Results of 2011 Hyundai Sonata Hybrid Battery [31]</i>	69
<i>Table 18 Design speeds and grade for various road classes in the Czech Republic [41]</i>	71
<i>Table 19 Results: Scenario 1: New control strategy with different velocity and SoC parameters</i>	73
<i>Table 20 Results: Scenario 2: New control strategy with different velocity and SoC parameters</i>	74
<i>Table 21 Results: Scenario 3: New control strategy with different velocity and SoC parameters</i>	75
<i>Table 22 Results: Scenario 4: New control strategy with different velocity and SoC parameters</i>	76

11 Appendix

11.1 2020 Ioniq Hybrid Engine BSFC Map

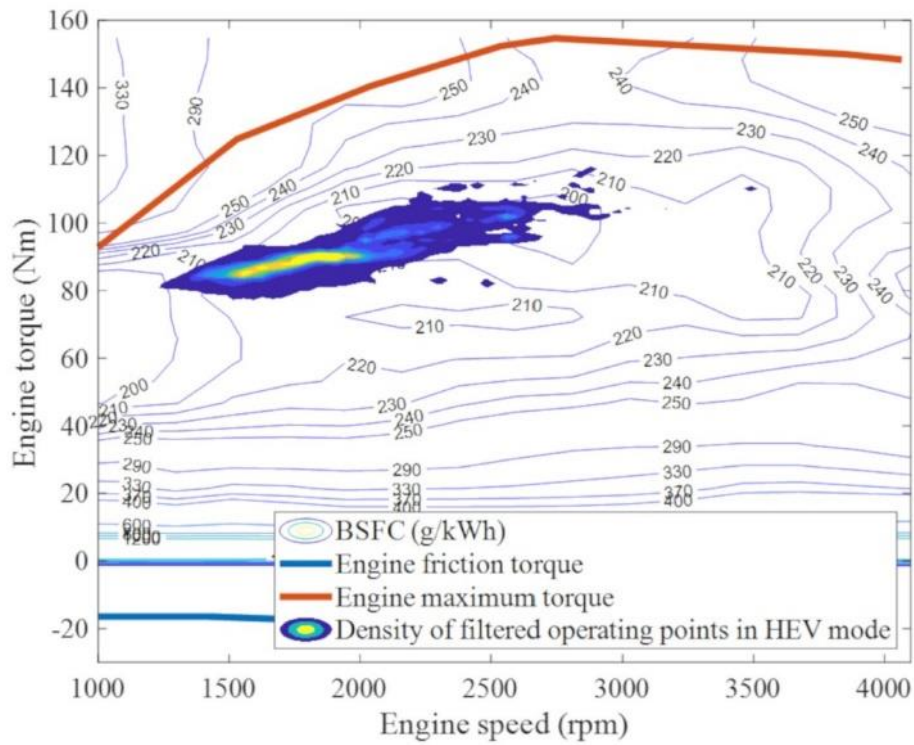


Figure 36 Source Image of 2020 Ioniq Hybrid Engine BSFC Map [26]

11.2 Engine Fuel Consumption Map extended till engine friction torque

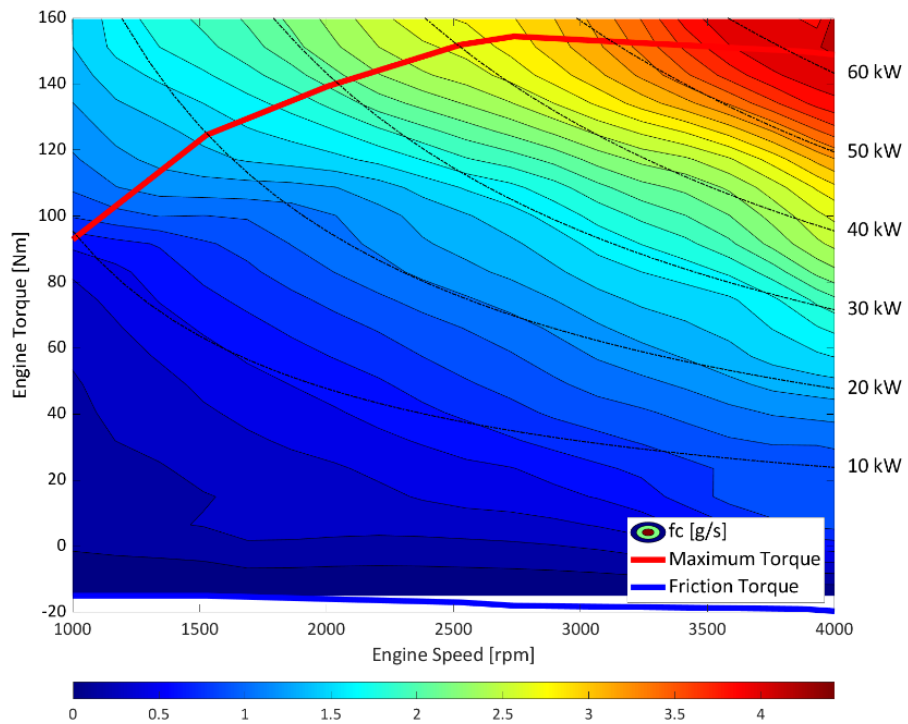


Figure 37 Fuelling Rate Map of 2020 Ioniq Hybrid extended till friction torque

11.3 2011 Hyundai Sonata Hybrid Combined Motor Inverter Map

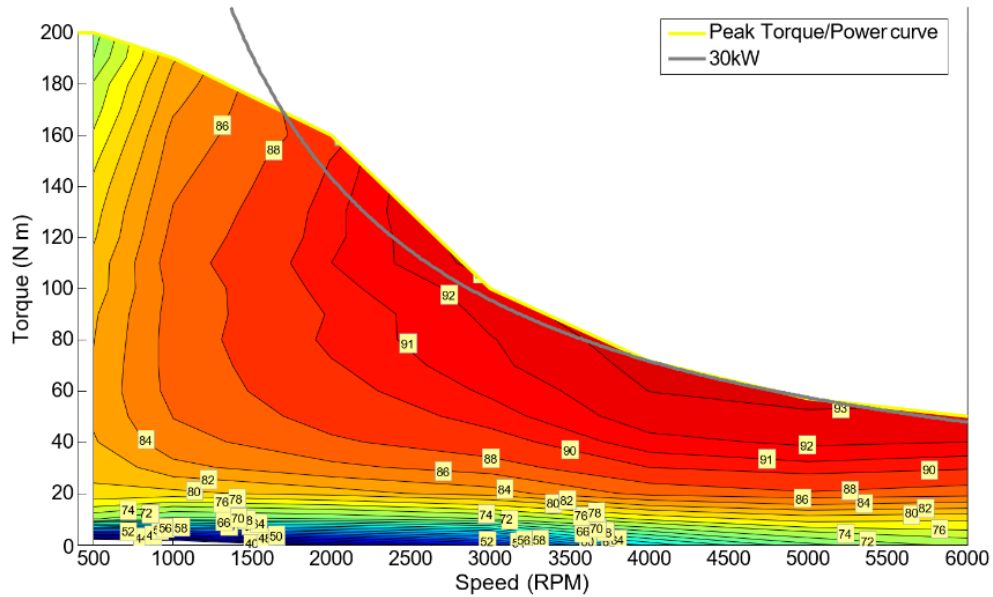


Figure 38 Source Image of 2011 Hyundai Sonata Combined Motor Inverter Efficiency Map [30]

11.4 Battery specifications of 2020 Hyundai Ioniq and 2011 Sonata Hybrid

Table 16 Comparison of battery parameters of Ioniq and Sonata Hybrid

	2020 Ioniq Hybrid [9]	2011 Sonata Hybrid [31]	Units
Type	Lithium-ion Polymer	Lithium-ion	
Capacity	5.3	5.3	[Ah]
	1.56	1.4	[kWh]
Nominal cell voltage	-	3.75	[V]
Nominal pack voltage	240	270	[V]
Number of cells	72	72	-

11.5 Original Battery Test Results of 2011 Hyundai Sonata Hybrid

Table 17 Test Results of 2011 Hyundai Sonata Hybrid Battery [31]

	Test Date	Odometer (mi)	Rated Capacity (Ah)	Measured Capacity (Ah)	Measured Energy (Wh)
BOT	July 22, 2011	5,730	5.30	5.29	1,394
EOT	May 29, 2013	160,116	5.30	4.15	1,060
Difference	—	154,386	—	1.14 (22%)	334 (24%)

11.6 2011 Hyundai Sonata Hybrid Battery Characteristics

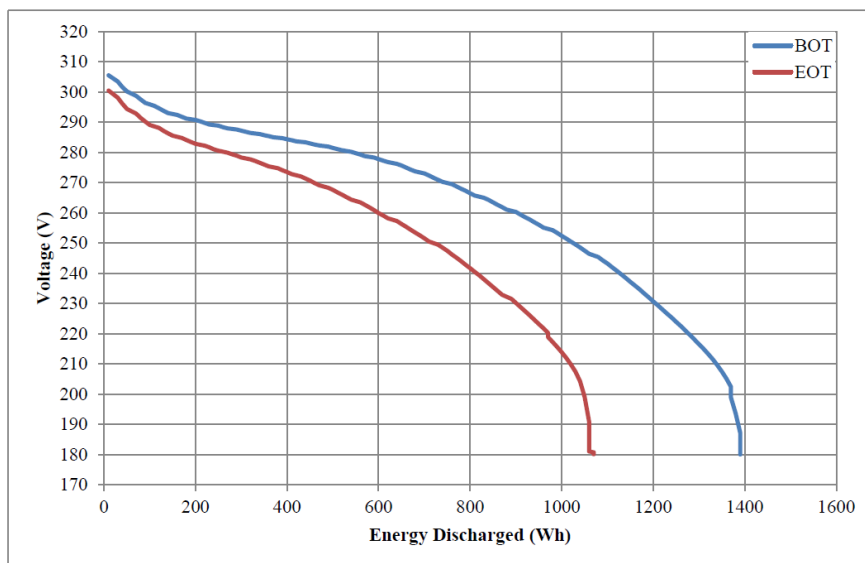


Figure 39 Open Circuit Voltage v/s SOC Characteristics of 2011 Hyundai Sonata Hybrid Battery [31]

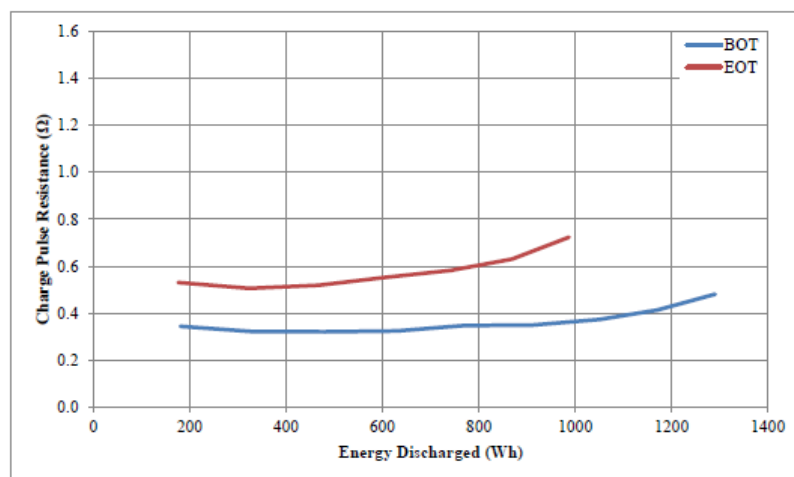


Figure 40 Charging Internal Resistance v/s SOC of 2011 Hyundai Sonata Hybrid Battery [31]

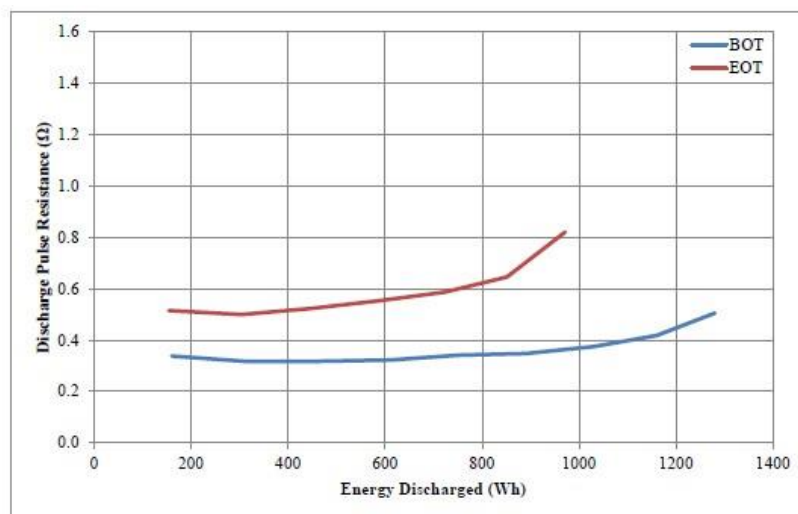


Figure 41 Discharge Internal Resistance v/s SOC of 2011 Hyundai Sonata Hybrid Battery [31]

11.7 Design speeds and road grade data for motorways in the Czech Republic

Table 18 Design speeds and grade for various road classes in the Czech Republic [41]

Tabulka 9 – Návrhové rychlosti podle druhu území a největší dovolené podélné sklony (s) návrhových kategorií silnic a dálnic¹⁾

Kategorijní typ silnice nebo dálnice	Návrhová rychlost v km/h pro území			
	rovinaté nebo mírně zvlněné	pahorkovité	horské	
	podélný sklon (s) v %			
D 33,5	120	120	100 ^{****)}	80 ^{****)}
D 27,5	3	4 ^{**)}	4,5 ^{**)}	4,5 ^{**)}
R 33,5; R 27,5	120	100	80	
R 25,5	3,5	4,5	5 ^{**)}	
S 24,5	100	80	70	
	3,5	4,5 (až 6 ^{****)})	6	
S 20,75	90	80	70	
	4	4,5 (až 6 ^{****)})	6	
S 11,5	90	80	70	
	4,5	6	7,5	
S 9,5	80	70	60	
	4,5	6	8	
S 7,5	70	60	50	
	4,5	7	9	
S 6,5	60	60	50	
	7	8	9	
S 4,0	40	40	30	
	10	11	12	

¹⁾ Hodnoty pro větve křižovatek jsou uvedeny v ČSN 73 6102.

^{**)} Překročení hodnoty je třeba doložit rozbořem zvýšení spotřeby pohonných hmot a je vázáno na souhlas příslušného ústředního orgánu státní správy ve věcech dopravy.

^{****)} Vyšších hodnot lze použít v případech, kdy neobvyklé zvýšení objemu zemních prací nadměrně zvýší ekonomickou náročnost řešení nebo by se nadměrně zvětšilo trvalé odnětí kvalitní nebo chráněné zemědělské půdy. Současně je však nutné při použití větších sklonů posoudit zvýšenou spotřebu pohonných hmot a bezpečnost dopravy.

^{****)} Rozhodnutí o návrhové rychlosti závisí na možnostech daných především konfigurací terénu.

11.9 Summary of Results with new Control Strategy

Results Plot (Appendix 12) File Name Identifier: plotFileName.png:

[Scenario]_[Comb]of[18]_socInit[socInit]_Min[socMin]_Max[socMax]_vEntry[vEntry]_vMax[vMax]_vMin[vMin]_Rep.png

A. Scenario 1 – Hill

Table 19 Results: Scenario 1: New control strategy with different velocity and SoC parameters

Scenario 1: Hill											
Comb	Rep	vEntry	vMax	socInit	socMin	tEnd	tN	fcEnd	fcN	fcN*tN	fcN*tN
2	2	70	90	70	50	400.53	1.00	254.87	0.00	0.00	1.00
1	2	70	90	60	40	400.53	1.00	254.89	0.00	0.00	1.00
2	1	70	90	70	50	400.53	1.00	255.10	0.01	0.01	1.01
1	1	70	90	60	40	400.53	1.00	255.25	0.02	0.02	1.02
3	1	70	90	80	60	400.53	1.00	255.37	0.02	0.02	1.02
3	2	70	90	80	60	400.53	1.00	255.54	0.03	0.03	1.03
4	2	70	100	60	40	389.48	0.81	259.63	0.21	0.17	1.02
5	1	70	100	70	50	389.48	0.81	260.11	0.23	0.18	1.04
8	2	80	90	70	50	373.73	0.54	261.18	0.27	0.15	0.82
7	1	80	90	60	40	373.73	0.54	261.21	0.27	0.15	0.82
7	2	80	90	60	40	373.73	0.54	261.37	0.28	0.15	0.83
9	1	80	90	80	60	373.73	0.54	261.55	0.29	0.16	0.83
4	1	70	100	60	40	389.48	0.81	261.57	0.29	0.24	1.10
6	2	70	100	80	60	389.48	0.81	261.68	0.29	0.24	1.11
8	1	80	90	70	50	373.73	0.54	261.84	0.30	0.16	0.85
5	2	70	100	70	50	389.48	0.81	261.91	0.30	0.25	1.12
6	1	70	100	80	60	389.48	0.81	262.78	0.34	0.28	1.15
9	2	80	90	80	60	373.73	0.54	264.69	0.43	0.23	0.97
11	1	80	100	70	50	363.09	0.36	267.08	0.53	0.19	0.89
12	2	80	100	80	60	363.09	0.36	267.19	0.53	0.19	0.90
10	2	80	100	60	40	363.09	0.36	267.22	0.53	0.19	0.90
11	2	80	100	70	50	363.09	0.36	267.55	0.55	0.20	0.91
14	2	90	90	70	50	351.97	0.17	267.75	0.56	0.10	0.73
13	2	90	90	60	40	351.97	0.17	268.51	0.59	0.10	0.77
15	2	90	90	80	60	351.97	0.17	268.61	0.59	0.10	0.77
14	1	90	90	70	50	351.97	0.17	268.64	0.60	0.10	0.77
15	1	90	90	80	60	351.97	0.17	268.79	0.60	0.11	0.78
10	1	80	100	60	40	363.09	0.36	269.01	0.61	0.22	0.98
13	1	90	90	60	40	351.97	0.17	269.15	0.62	0.11	0.79
12	1	80	100	80	60	363.09	0.36	271.01	0.70	0.25	1.06
17	1	90	100	70	50	341.67	0.00	274.32	0.84	0.00	0.84
16	1	90	100	60	40	341.67	0.00	274.63	0.85	0.00	0.85
16	2	90	100	60	40	341.67	0.00	274.94	0.87	0.00	0.87
18	1	90	100	80	60	341.67	0.00	275.49	0.89	0.00	0.89
17	2	90	100	70	50	341.67	0.00	275.78	0.90	0.00	0.90
18	2	90	100	80	60	341.67	0.00	277.98	1.00	0.00	1.00

B. Scenario 2 – Valley

Table 20 Results: Scenario 2: New control strategy with different velocity and SoC parameters

Scenario 2: Valley											
Comb	Rep	vEntry	vMax	socInit	socMin	tEnd	tN	fcEnd	fcN	fcN*tN	fcN+tN
3	1	70	90	60	60	412.56	1.00	257.02	0.00	0.00	1.00
3	2	70	90	60	60	412.56	1.00	257.44	0.03	0.03	1.03
2	1	70	90	50	50	412.56	1.00	257.48	0.03	0.03	1.03
2	2	70	90	50	50	412.56	1.00	257.54	0.03	0.03	1.03
1	2	70	90	40	40	412.56	1.00	257.56	0.03	0.03	1.03
1	1	70	90	40	40	412.56	1.00	257.83	0.05	0.05	1.05
6	2	70	100	60	60	399.92	0.76	259.12	0.13	0.10	0.90
6	1	70	100	60	60	399.92	0.76	259.16	0.14	0.10	0.90
5	2	70	100	50	50	399.92	0.76	259.39	0.15	0.11	0.91
5	1	70	100	50	50	399.92	0.76	259.52	0.16	0.12	0.92
4	1	70	100	40	40	399.92	0.76	259.84	0.18	0.14	0.94
4	2	70	100	40	40	399.92	0.76	259.94	0.19	0.14	0.95
8	2	80	90	50	50	390.25	0.58	262.40	0.34	0.20	0.92
8	1	80	90	50	50	390.25	0.58	262.43	0.34	0.20	0.93
7	2	80	90	40	40	390.25	0.58	262.64	0.36	0.21	0.94
7	1	80	90	40	40	390.25	0.58	262.80	0.37	0.21	0.95
9	1	80	90	60	60	390.25	0.58	263.58	0.42	0.24	1.00
9	2	80	90	60	60	390.25	0.58	263.69	0.42	0.25	1.01
12	2	80	100	60	60	377.19	0.34	263.98	0.44	0.15	0.78
12	1	80	100	60	60	377.19	0.34	263.98	0.44	0.15	0.78
11	1	80	100	50	50	377.19	0.34	264.28	0.46	0.16	0.80
11	2	80	100	50	50	377.19	0.34	264.42	0.47	0.16	0.81
10	2	80	100	40	40	377.19	0.34	264.76	0.49	0.17	0.83
10	1	80	100	40	40	377.19	0.34	264.79	0.49	0.17	0.83
14	2	90	90	50	50	372.75	0.25	268.21	0.71	0.18	0.96
14	1	90	90	50	50	372.75	0.25	268.25	0.71	0.18	0.97
13	1	90	90	40	40	372.75	0.25	268.79	0.75	0.19	1.00
13	2	90	90	40	40	372.75	0.25	268.82	0.75	0.19	1.00
18	2	90	100	60	60	359.17	0.00	269.74	0.81	0.00	0.81
18	1	90	100	60	60	359.17	0.00	269.98	0.82	0.00	0.82
17	1	90	100	50	50	359.17	0.00	270.01	0.82	0.00	0.82
17	2	90	100	50	50	359.17	0.00	270.02	0.82	0.00	0.82
16	1	90	100	40	40	359.17	0.00	270.64	0.86	0.00	0.86
16	2	90	100	40	40	359.17	0.00	270.70	0.87	0.00	0.87
15	2	90	90	60	60	372.75	0.25	272.78	1.00	0.25	1.25
15	1	90	90	60	60	372.75	0.25	272.86	1.01	0.26	1.26

C. Scenario 3 – Ascent only

Table 21 Results: Scenario 3: New control strategy with different velocity and SoC parameters

Scenario 3: Ascent											
Comb	Rep	vEntry	vMax	socInit	socMin	tEnd	tN	fcEnd	fcN	fcN*tN	fcN*tN
1	1	70	90	60	40	467.59	1.00	364.47	0.00	0.00	1.00
2	1	70	90	70	50	467.59	1.00	367.54	0.08	0.08	1.08
1	2	70	90	60	40	467.59	1.00	369.30	0.12	0.12	1.12
2	2	70	90	70	50	467.59	1.00	369.86	0.13	0.13	1.13
4	2	70	100	60	40	467.59	1.00	372.93	0.21	0.21	1.21
11	1	80	100	70	50	429.62	0.45	374.59	0.25	0.11	0.70
7	2	80	90	60	40	429.62	0.45	375.46	0.27	0.12	0.72
10	2	80	100	60	40	429.62	0.45	375.92	0.28	0.13	0.73
10	1	80	100	60	40	429.62	0.45	377.28	0.32	0.14	0.77
6	1	70	100	80	60	467.59	1.00	377.50	0.32	0.32	1.32
12	2	80	100	80	60	429.62	0.45	378.18	0.34	0.15	0.79
12	1	80	100	80	60	429.62	0.45	379.30	0.37	0.17	0.82
5	1	70	100	70	50	467.59	1.00	380.06	0.39	0.39	1.39
5	2	70	100	70	50	467.59	1.00	380.94	0.41	0.41	1.41
8	2	80	90	70	50	429.62	0.45	381.76	0.43	0.19	0.88
14	2	90	90	70	50	398.55	0.00	381.82	0.43	0.00	0.43
13	2	90	90	60	40	398.55	0.00	383.13	0.46	0.00	0.46
16	1	90	100	60	40	398.55	0.00	383.76	0.48	0.00	0.48
6	2	70	100	80	60	467.59	1.00	383.99	0.48	0.48	1.48
7	1	80	90	60	40	429.62	0.45	384.11	0.49	0.22	0.94
14	1	90	90	70	50	398.55	0.00	384.18	0.49	0.00	0.49
17	2	90	100	70	50	398.55	0.00	384.64	0.50	0.00	0.50
16	2	90	100	60	40	398.55	0.00	384.98	0.51	0.00	0.51
17	1	90	100	70	50	398.55	0.00	385.53	0.52	0.00	0.52
9	2	80	90	80	60	429.62	0.45	386.00	0.53	0.24	0.98
18	1	90	100	80	60	398.55	0.00	386.29	0.54	0.00	0.54
3	2	70	90	80	60	467.59	1.00	388.72	0.60	0.60	1.60
3	1	70	90	80	60	467.59	1.00	392.91	0.71	0.71	1.71
4	1	70	100	60	40	467.59	1.00	393.17	0.71	0.71	1.71
8	1	80	90	70	50	429.62	0.45	394.20	0.74	0.33	1.19
11	2	80	100	70	50	429.62	0.45	395.75	0.78	0.35	1.23
9	1	80	90	80	60	429.62	0.45	398.02	0.83	0.37	1.28
15	1	90	90	80	60	398.55	0.00	398.79	0.85	0.00	0.85
13	1	90	90	60	40	398.55	0.00	401.94	0.93	0.00	0.93
18	2	90	100	80	60	398.55	0.00	403.28	0.96	0.00	0.96
15	2	90	90	80	60	398.55	0.00	404.77	1.00	0.00	1.00

D. Scenario 4 – Descent only

Table 22 Results: Scenario 4: New control strategy with different velocity and SoC parameters

Scenario 4: Descent											
Comb	Rep	vEntry	vMax	socInit	socMin	tEnd	tN	fcEnd	fcN	fcN*tN	fcN+tN
3	1	70	90	60	60	366.14	1.00	128.20	0.00	0.00	1.00
3	2	70	90	60	60	366.14	1.00	128.20	0.00	0.00	1.00
2	1	70	90	50	50	366.14	1.00	128.23	0.00	0.00	1.00
2	2	70	90	50	50	366.14	1.00	128.23	0.00	0.00	1.00
1	1	70	90	40	40	366.14	1.00	128.65	0.02	0.02	1.02
1	2	70	90	40	40	366.14	1.00	128.65	0.02	0.02	1.02
6	1	70	100	60	60	349.58	0.73	131.45	0.15	0.11	0.88
6	2	70	100	60	60	349.58	0.73	131.50	0.15	0.11	0.88
5	1	70	100	50	50	349.58	0.73	131.60	0.15	0.11	0.88
5	2	70	100	50	50	349.58	0.73	131.67	0.16	0.11	0.89
4	2	70	100	40	40	349.58	0.73	131.97	0.17	0.12	0.90
4	1	70	100	40	40	349.58	0.73	131.97	0.17	0.12	0.90
9	2	80	90	60	60	341.00	0.59	136.59	0.38	0.22	0.97
9	1	80	90	60	60	341.00	0.59	136.72	0.38	0.23	0.97
8	2	80	90	50	50	341.00	0.59	137.82	0.43	0.25	1.02
8	1	80	90	50	50	341.00	0.59	137.82	0.43	0.25	1.02
7	1	80	90	40	40	341.00	0.59	138.20	0.45	0.27	1.04
7	2	80	90	40	40	341.00	0.59	138.21	0.45	0.27	1.04
12	1	80	100	60	60	324.82	0.32	140.26	0.54	0.18	0.87
12	2	80	100	60	60	324.82	0.32	140.26	0.54	0.18	0.87
11	2	80	100	50	50	324.82	0.32	140.64	0.56	0.18	0.88
11	1	80	100	50	50	324.82	0.32	140.73	0.56	0.18	0.89
10	2	80	100	40	40	324.82	0.32	140.82	0.57	0.18	0.89
10	1	80	100	40	40	324.82	0.32	140.82	0.57	0.18	0.89
14	1	90	90	50	50	321.00	0.26	144.13	0.72	0.19	0.98
14	2	90	90	50	50	321.00	0.26	144.21	0.72	0.19	0.98
13	1	90	90	40	40	321.00	0.26	144.48	0.73	0.19	0.99
13	2	90	90	40	40	321.00	0.26	144.49	0.73	0.19	1.00
15	1	90	90	60	60	321.00	0.26	147.92	0.89	0.23	1.15
15	2	90	90	60	60	321.00	0.26	147.96	0.89	0.23	1.15
18	2	90	100	60	60	304.98	0.00	149.72	0.97	0.00	0.97
18	1	90	100	60	60	304.98	0.00	149.72	0.97	0.00	0.97
17	2	90	100	50	50	304.98	0.00	150.07	0.98	0.00	0.98
17	1	90	100	50	50	304.98	0.00	150.29	0.99	0.00	0.99
16	1	90	100	40	40	304.98	0.00	150.42	1.00	0.00	1.00
16	2	90	100	40	40	304.98	0.00	150.42	1.00	0.00	1.00

12 Attachments

	Description	Filename
IGNITE Models		CD\ignite\
	Ignite Model with new controller	: BCO.ignx
	Ignite Model with Rule-Based controller	: RB.ignx
	Results	: All_BCO_RB.rpostx

MATLAB Functions		CD\main\
	Battery	: Batt.m
	Traction Power	: calcTraction.m
	Vehicle Black Box Function	: Fcn.m
	ABC for Boost	: runABC.m ¹
	ABC for Generation	: runABCgen.m

MATLAB Scripts		CD\main\
	Simulate full horizon	: calcFullHorizon.m
	Sweep of ABC parameters	: ABCsweep.m
	Sweep of Velocity, SoC	: autorunAllSce.m
		CD\main\createHorizon\
	Create Terrain Profiles	: createTerrain.m
	Create Velocity Profiles	: createDriveCycle.m
	Create Horizon Data File	: createHorizon.m
	Main data file with all vehicle data	: vehdata.mat

Results of new control strategy for different velocity and soc combinations

	Plots	: CD\results\plots\plotFileName.png
	Summary excel spreadsheet	: CD\results\Summary_Scenarios.xlsx

Master's Thesis PDF:

CD\Hill Climbing Algorithm for Fuel Consumption Optimization of HEV vehicles.pdf

¹ This function was developed with the help of my thesis supervisor Ing. Cvetkovic and colleagues from TU Belgrade, Marko Stokić and Nemanja Mijovic.